



University of
Nottingham
UK | CHINA | MALAYSIA

**The Chemistry of First Row
Transition Metal-oxo Clusters**

Name: Margaret Smith

**Thesis Submitted to the University of Nottingham for
the Degree of Master of Research**

Contents

Abstract.....	1
Acknowledgements.....	2
1 Introduction	3
1.1 Introduction to Magnetism	4
1.1.1 Double Exchange Phenomena	6
1.1.2 Single Molecular Magnetism	11
1.2 The Metal-Oxo Bond	13
1.3 Transition Metal Bonding Models	15
1.4 Terminal Oxo Groups.....	16
1.5 The Oxo Wall Theory	21
1.6 Polyoxometalates	25
2 Aims.....	20
3 Discussion.....	22

3.1 Scandium.....	22
3.2 Titanium	24
3.3 Vanadium	33
3.4 Chromium	42
3.5 Manganese.....	50
3.6 Iron.....	61
3.7 Cobalt.....	72
3.8 Nickel.....	76
3.9 Copper.....	79
3.10 Zinc.....	85
4 Second and Third Row Transition Metals	90
5 Conclusions	92
7 References	96

Abstract

Transition metal-oxo clusters have been widely studied in recent years due, in part, to their varied redox behaviour and magnetic properties. In particular, the design and fabrication of new first-row transition metal-oxo clusters is a significant target in the fields of catalysis and molecular magnetism. The properties of the systems change significantly across the periodic table, with high stability and relative inertness associated with early transition metal-oxo compounds contrasting with the highly reactive oxidizing chemistry of compounds based on later transition metals. This critical review outlines the chemistry of the oxo-clusters of the first-row transition metals, illustrating the synthetic pathways, structural features and fundamental chemistry of these systems.

Acknowledgements

The following thesis would not have been completed successfully without the individuals mentioned below.

Firstly, I would like to thank my Master of Research supervisor and mentor Dr G. Newton for the opportunity to undertake and learn in depth about research conducted in this field, expanding both my knowledge and understanding. Furthermore, I would like to express my gratitude for his continued incredible support and guidance throughout my entire year of study as well as his continuous encouragement and willingness to help wherever he can.

I would like to show my appreciation to postdoc Dr J. Cameron for his guidance and sharing both his knowledge and experience which were a huge help in completing this review to a high standard. Moreover, I would also like to thank him for his support and enthusiasm to always assist me whenever possible throughout the year and his patience in answering my questions.

I am grateful and fortunate to have had the opportunity to work with and learn from two experienced chemists who have both helped in developing my chemistry knowledge and skills.

Many thanks to the other members of the Newton group, including Masters students, PhD students and postdocs, for also advising me and sharing their experience both in and out of the lab, as well as providing me with day-to-day help where needed and for making this year a wonderful experience.

On a more personal note, special regards to my family who have constantly encouraged me to do the best I possibly can and supported me unconditionally. Also, I would like to thank my friends for always being there for me and making my time even more enjoyable.

1 Introduction

Transition metal-oxide clusters are broadly defined as polynuclear species where an ensemble of two or more metal atoms with a partially filled d-sub shell are bonded and stabilised by oxo ligands, such as OH^- , O^{2-} or H_2O .¹ The chemistry of the complexes of first-row transition metals is highly diverse with a multitude of different reactivity and property patterns emerging across the series. Their physical properties can broadly be attributed to their partially-filled d-electron shells, the nature of their coordinating ligand, and their coordination geometry.² In general, the d-electrons are responsible for the most noteworthy properties of these elements in both free atoms and bulk phase materials.³ Transition metal clusters have attracted enormous attention because their structural, electronic, and magnetic properties can be unique and very different from those of their bulk phase.⁴

1																	18
1	2																2
H	Li	Be															He
Hydrogen	Lithium	Beryllium															Helium
3	4																10
Na	Mg																Ne
Sodium	Magnesium																Neon
11	12	3	4	5	6	7	8	9	10	11	12	13	14	15	16	17	18
K	Ca	Sc	Ti	V	Cr	Mn	Fe	Co	Ni	Cu	Zn	Al	Si	P	S	Cl	Ar
Potassium	Calcium	Scandium	Titanium	Vanadium	Chromium	Manganese	Iron	Cobalt	Nickel	Copper	Zinc	Aluminum	Silicon	Phosphorus	Sulfur	Chlorine	Argon
19	20	21	22	23	24	25	26	27	28	29	30	31	32	33	34	35	36
K	Ca	Sc	Ti	V	Cr	Mn	Fe	Co	Ni	Cu	Zn	Ga	Ge	As	Se	Br	Kr
Potassium	Calcium	Scandium	Titanium	Vanadium	Chromium	Manganese	Iron	Cobalt	Nickel	Copper	Zinc	Gallium	Germanium	Arsenic	Selenium	Bromine	Krypton

Figure 1. A section of periodic table illustrating first row transition metals.⁵

Oxide (O^{2-}) groups are a particularly interesting class of ligands for transition metal clusters, because they offer the potential to act as capping ligands and as multiply-bridging nodes within polynuclear clusters. Their lack of organic substituents means that they are particularly stable to highly oxidising conditions, and their small size and negative charge mediate strong coupling interactions between neighbouring metal centres.⁶

Metal-oxo clusters epitomise an intermediate class of systems, falling between monomeric molecular precursors and the infinite lattice of the bulk, however, the isolation of discrete metal-oxo clusters via utilisation of simple ligands derived from water has been relatively limited. Notably, while

there are many reports of isolated metal–oxo complexes of group 3–8 transition metals,^{7,8,9} and in particular Fe-O and Mn-O clusters, isolation of analogous oxo-complexes of the late first-row transition metals (groups IX–XI) has rarely been achieved. If an oxo group is to stabilise a cluster as a terminal ligand, it will form multiple bonds to the transition metal ion, resulting in, for example, a M=O group. In order for a transition metal to stabilise such an interaction it must be high valent (with a maximum of two d_{π} electrons), leading to the proposal of the ‘oxo wall’ concept that states that the transition metals to the left of group 8 can stabilise multiple-bonded (terminal) oxo groups, while those to the right cannot.^{10,11} Despite this, metal-oxo species to the right of group 8, which are broadly considered to be reactive intermediates, have been synthesised, manipulated and characterised.¹² Such examples do, however, remain rare.¹³ Spin, postulated for the first time by Uhlen Beck and Goudsmit,¹⁴ is a fundamental property of all elementary particles. In transition-metal complexes, the electronic spin is determined by the number of unpaired electrons at the metal centre. When transition metal ions are combined in a polynuclear cluster, the spins of neighbouring centres can couple, causing them to align and leading to phenomena such as ferromagnetism and antiferromagnetism.¹⁵ While the spins of paramagnetic systems are randomly aligned, those of ferromagnetic materials are aligned in parallel, and those in antiferromagnets are antiparallel.¹⁶

1.1 Introduction to Magnetism

The principles of Magnetism were first established by Ampeère, Oersted, Faraday, Maxwell and Pierre Curie before the field of magnetochemistry was launched in the 1950s. The area of Molecular Magnetism, however, did not materialise until the early 1980s.¹⁷ Thereafter, much of the early effort was directed towards the pursuit of molecule-based magnetic solids that order at high temperatures.

Molecular Magnetism is a rapidly expanding interdisciplinary research area which deals with the design, synthesis and study of magnetic molecules and materials. Chemists, physicists, material scientists, and chemical engineers, both experimentalists and theoreticians, all actively contribute to

this field.¹⁸ The development of Molecular Magnetism since the NATO ASI in Italy in 1983, which is considered by many to be the beginning of the Molecular Magnetism era, has been tremendous.¹⁹ Breakthrough achievements include synthesising both molecular ferrimagnets and ferromagnets, organic ferromagnets, single molecule magnets (SMMs), single chain magnets, room temperature magnetic switches and molecular photomagnets.^{20,18,21}

It can be considered that the modern era of molecular magnetism began with the magnetic characterisation of $[\text{Mn}^{\text{III}}_8\text{Mn}^{\text{IV}}_4\text{O}_{12}(\text{O}_2\text{CMe})_{16}(\text{H}_2\text{O})_4]$.^{22,23} The molecule contains a Mn-O core, and is stabilised by the coordination of acetate ligands. Of the 12 Mn ions, the eight d^4 Mn^{III} centres have upward spins and the four d^3 Mn^{IV} have downward spins. The combination of the anisotropy of the Mn^{III} centres and the residual ferrimagnetic (i.e. non-cancelling antiparallel) spin ground state led to slow relaxation of magnetisation up to 4K and the first identification of single molecule magnetism.²⁴

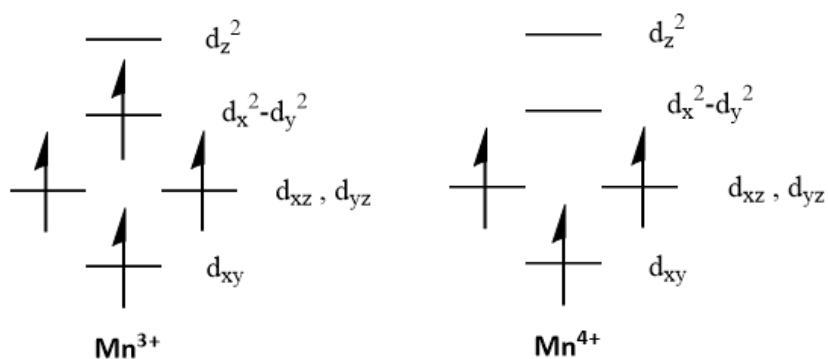


Figure 2. Schematic of the two common Mn oxidation states discussed herein.

Following the discovery of magnetic hysteresis in a single molecule, extensive effort was devoted to the understanding of SMM behaviour.²⁵ The research motivation stemmed from the potential these molecules offer in the future, including applications in areas such as information storage, quantum computing and spin-based molecular electronics.^{26,27} While most SMMs depend

upon the superexchange of spins between metal centres, the majority of permanent magnets with high ordering temperatures tend to depend on the delocalisation of itinerant electrons.²⁸

1.1.1 Double Exchange Phenomena

Mixed-valence complexes, as illustrated by the Creutz–Taube ion $[(\text{NH}_3)_5\text{Ru}(\text{m-pyz})\text{Ru}(\text{NH}_3)_5]^{5+}$ (pyz = pyrazine),²⁹ are clusters containing two or more metal ions with different formal oxidation states, opening the possibility of intervalence charge transfer (IVCT) between metal centres.³⁰ These clusters were recognised by chemists over a century ago,³¹ and classifications of the systems occurred according to the extent of electron delocalisation. The most widely accepted classification scheme was originally proposed by Robin and Day and concentrates on the degree of electronic interaction present between sites of varying valence and the subsequent charge delocalization.³² Three levels of delocalization proposed were categorised as Class I; localised, Class II; weakly localised and Class III; fully delocalised.³² Class II compounds are of particular interest since they are excellent models for investigating the mechanisms of electron transfer. Therefore, by altering the factors affecting the transition, such as temperature, solvent, ligand sphere, transition metal ion and others, detailed information on the extent of the impact on IVCT can be obtained.³³

Furthermore, mixed-valence complexes can exhibit a phenomenon known as double exchange. This spin-dependent phenomenon was first proposed by Clarence Zener in 1951 to rationalise the properties of mixed-valence manganite's with the perovskite structure.³⁴ In molecular systems, magnetic coupling in general is governed by super-exchange interactions³⁵ which often leads to antiferromagnetic order.³⁶ However, recent theoretical and experimental results show that ferromagnetic ground states can be achieved via double-exchange³⁴ interactions in di-nuclear transition metal complexes by charge transfer and/or charge disproportionation between the transition metal atoms.^{37,38,39} Unlike the direct-exchange interaction, the double-exchange interaction

involves spin-dependent electron delocalisation through nonmagnetic atoms, which was originally suggested for three-dimensional transition metal oxides.²⁴

Metal-oxo clusters, and specifically mixed-valent metal-oxo species such as $\text{Mn}^{\text{III}}\text{O}^{2-}\text{Mn}^{\text{IV}}$, are prime candidates to exhibit double exchange (Figure 3).⁴⁰ Figure 4 illustrates the movement of $d\sigma$ (e_g) electrons between the octahedral manganese centres and bridging oxo anions.⁴¹ The concurrent movement of the two electrons occur when the electron originating on the O anion is transferred to the Mn metal centre and vice versa to ensure that the single spin in the Mn^{III} e_g orbitals is effectively delocalised between the metal centres and the spin orientation is retained, resulting in the effective parallel alignment of spins on neighbouring metal centres.^{42,43} Despite a considerable number of theoretical investigations have been carried out on this phenomenon, limited experimental investigations have been reported.^{44,37}

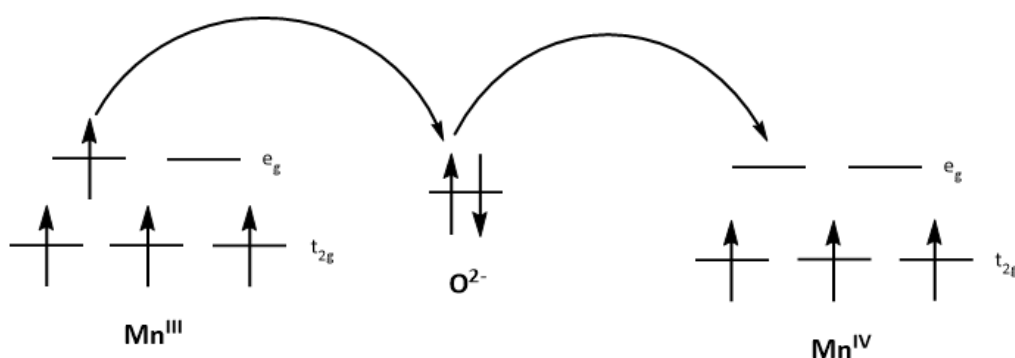


Figure 3. Schematic demonstrating the movement of electrons during the double exchange phenomena. One electron is transferred from a bridging O^{2-} anion to the Mn^{IV} centre and one from a Mn^{III} centre to the O^{2-} anion, retaining their spin.⁴⁵

This class III mixed-valence system requires the delocalization of electrons between the metal centres. In order to achieve this successfully, the integration of symmetric bridging ligands with suitable frontier orbitals is necessary to facilitate electron transfer between the metals. Even when

Heisenberg exchange favours antiferromagnetic coupling, double exchange still induces a parallel spin alignment as a result of the peripatetic electron retaining its spin during the transfer.⁴⁶ This highlights the importance of utilising the double-exchange phenomenon to create and design clusters with high-spin ground states, therefore, emphasising the encouraging potential of transition metal-oxo clusters in this field.⁴⁵

1.1.2 Single Molecular Magnetism

SMMs are zero-dimensional systems displaying slow magnetisation relaxation resulting from a combination of a significant non-zero ground state spin (S), together with easy-axis-type magnetic anisotropy (D), creating a large energy barrier to the magnetization reversal.⁴⁷ Large S values can arise from ferromagnetic or non-cancelling antiferromagnetic exchange between neighbouring spins. The nature of the magnetic interactions between neighbouring spins and the geometric alignment of anisotropy axes within a cluster are effectively determined by the nature of the bridging and capping ligands.⁴⁸ Throughout the past decade robust evidence has been found to suggest that the most critical parameter to be considered during SMM design is the single-ion anisotropy.⁴⁹ In order for the SMM to be robust this parameter needs to be large, therefore, the emphasis has been shifted to lanthanides (Ln) and actinides (An) which can exhibit large anisotropies due to spin-orbit coupling.⁵⁰ Such systems have been found to exhibit, in some cases, very high blocking temperatures (TB, the highest temperature at which an SMM displays hysteresis), hinting at future applications at relatively high temperatures (above the boiling point of liquid nitrogen).⁵¹

First-row transition-metals are commonly used in the preparation of SMMs. In particular Mn^{III} has been widely used due to its high spin value ($S = 2$) and anisotropy resulting from its Jahn-Teller distortion. Broadly speaking the preparation of such systems has been done by simple 'one-pot' reactions, relying on self-assembly.⁵² After the discovery of the archetypal manganese complex,^{22,23} many studies were reported into the synthesis and characterisation of dinuclear and polynuclear 3d-

metal coordination clusters with desirable SMM properties.⁵³ The general premise throughout the reported synthesis involved reacting a 3d-metal salt, commonly including halides, nitrates, sulphates and perchlorates, with a chelating polydentate organic ligand. This includes Schiff bases molecules, such as hydroxyprodines, amino diol-type ligands, and carboxylic acid-based ligands.¹⁹ The isolated clusters usually incorporate further auxiliary bridging ligands that have been captured in-situ. The preparation of coordination clusters without strictly designing the product has been termed serendipitous assembly and it is a productive means of preparing SMMs.⁵⁴

1.2 The Metal-Oxo Bond

In 1962, Carl Ballhausen and Harry B. Gray established a bonding model defining the structural criteria for metal-oxo complexes based on experimental and theoretical investigations of the vanadyl ion (VO^{2+}) (Figure 6).⁵⁵ This was followed by Jorgensen⁵⁶ and Furlani⁵⁷ who applied a crystal field model to develop an energy level scheme for the vanadyl cation. Furlani considered the VO^{2+} ion alone, therefore, failed to account for all of the observed energy levels. However, by studying the VO^{2+} ion in aqueous solution as the octahedral $[\text{VO}(\text{H}_2\text{O})_5]^{2+}$ complex, Jorgensen was able to obtain a scheme which qualitatively accounted for the correct crystal field energies. In this case, the importance of ligand to metal-bonding in the oxo cations was emphasised, as π -bonding was found to account for the drastic reduction of the free ion value, the resistance of VO^{2+} to protonation and the charge transfer bands of the electronic spectrum of $\text{VOSO}_4 \cdot 5\text{H}_2\text{O}$. The main feature of this model is the significant destabilisation of the degenerate d_{xy}, d_{xz} orbitals due to π -bonding with the oxo ligand.⁵⁸

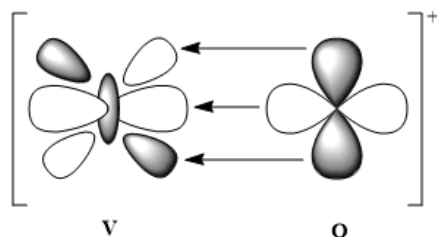


Figure 6. Schematic illustrating the orbital representation of bonding in the VO^{2+} ion.⁵⁹

The π -bonding interaction between transition metal d-orbitals and the 2p orbitals of the oxo-ligand is a result of the overlap between the filled π -symmetry ligand orbital and the typically unoccupied metal d-orbital (Figure 7). In order for this to be successful, the vacant orbitals residing on the metal must be at the correct orientation and symmetry for the oxo-ligand to donate electrons to the metal centre. A terminal oxo ligand is a doubly or triply bonded oxygen atom which acts as a multi-electron π -donor to an early, electrophilic transition metal.⁶⁰ Therefore, terminal oxo ligands are usually favoured by early transition metals as these have few d-electrons, high oxidation states and fewer ligands on the metal centres. Following the molecular orbital model of electronic structure, as illustrated in Figure 6, early transition metals with an electronic configuration of d^0 , d^1 and d^2 are able to form triple bonds with terminal oxo ligands to produce tetragonal mono metal-oxo complexes due to the strong π -donor character of the oxo group. In this case, two electrons occupy the sigma-bonding orbital, four electrons reside in the doubly degenerate pair of π -bonding orbitals and the lone electron is non-bonding with respect to the MO interaction.

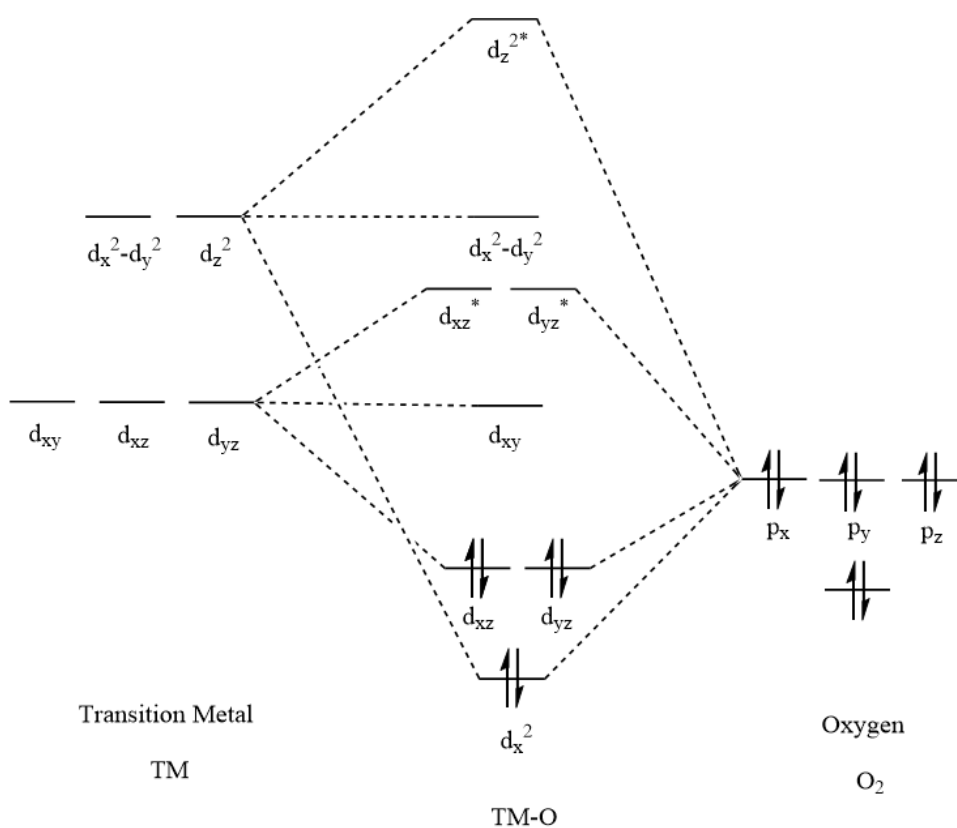


Figure 7. MO diagram representing the bonding between a transition metal and oxygen.⁶¹

Various ligands are employed when it comes to synthesising and stabilising transition metal clusters, depending on the metal present and the intended function of the ligand. Ligands such as OH^- and NH_3 , are strong σ -donors whereas ligands such as O^{2-} and alkoxides are strong π -donors. O^{2-} is a particularly good ligand for high-valence transition metal clusters due to the strong electron donating capabilities of oxygen, with two or more electron pairs available for donation into the vacant metal d-orbitals. These occur in both terminal and bridging positions. Note that the oxide ligand is a much stronger donor than, for example, hydroxo-ligands. Therefore, the net stabilisation gained by forming two π -bonds to one O^{2-} ligand is considerably greater than from forming two σ -bonds to two distinct HO^- ligands. However, this stabilisation effect significantly diminishes on moving from left to right across the periodic table. Beyond group 9, terminal metal oxo-complexes with $\text{M}=\text{O}$ units are

extremely rare (and do not exist for complexes with a coordination number of 6). This concept is explained by the oxo wall. The MO diagram shown in Figure 7, illustrates that both σ -donating (e.g. OH^-) and π -donating (e.g. O^{2-}) orbitals are present. When considering the π -orbitals of the oxygen ligand specifically, two electrons enter the σ -donor molecular orbital leaving two electrons to share across the two π -donor orbitals. If one electron in each MO is used to bond with the metal, a strongly covalent bond is formed.⁵⁵

1.3 Transition Metal Bonding Models

Various models describing the bonding in transition metal compounds have been developed over the years. Crystal Field Theory (CFT), developed by Hans Bethe and John Hasbrouck van Vleck⁶¹ characterises the strength of metal-ligand bonding in transition metal complexes by describing the breaking of the orbital degeneracy in the presence of ligands. Overall, the energy of the system shifts according to the strength of the metal-ligand bonds. The interaction of ligands with the metal cation causes splitting of the d-orbitals energies to occur, therefore, breaking their degeneracy. This results from electrostatic repulsion between the d-orbital electrons on the metal and those residing on the ligand, however, the magnitude of this effect varies according to the geometric structure of the complex, the oxidation state of the metal and the strength of the ligand field.

The most widely used bonding model for transition metal compounds chemistry^{62,63} and chemical bonding theory^{64,65} is now ligand field theory (LFT).^{66,67,68} This theory was developed relatively more recently, incorporating aspects of both crystal field theory and MO theory and therefore, providing a more complete overview of bonding within metal complexes.⁶⁹ LFT can be considered a simplified version of MO theory which focuses on the valence d orbitals of the TM and the frontier orbitals of the ligands. Alternatively, it can also be considered as a more sophisticated version of CFT, which considers only electrostatic interactions between the metal and the ligands. The concept attempts to integrate the overlap of the ligand p-orbitals with the d-orbitals of the metal with

suitable symmetry, demonstrating the effect of different ligands on the splitting parameter, Δ_o (the difference in energy between the t_{2g} and e_g orbitals in an octahedral complex).⁷⁰ This powerful model helps to explain trends in geometries, magnetic properties, bond energies, excitation energies, and other physical properties of TM compounds.

1.4 Terminal-Oxo Groups

Ballhausen and Gray demonstrated that there were no stable tetragonal transition metal-oxo species beyond the iron-ruthenium-osmium group of the periodic table.⁵⁸ Ligand field energy diagrams indicate that strongly bonded metal-oxo groups cannot exist if there are more than two π -antibonding electrons. Therefore, the criteria for stable terminal metal-oxo bonds can be derived from simple ligand-field theory considerations.¹⁰ The formation of terminal-oxo ligands on metal complexes typically arises due to a number of factors relating to d-electron configuration and oxidation-state stabilities.⁷¹ The oxidation state of the metal and the coordination number become increasingly important, moving from left to right across the periodic table,⁷² with the stability of the highest oxidation state decreasing from Ti^{IV} to Mn^{VII} . After manganese, high oxidation states are progressively difficult to attain because the 3d-electrons are more tightly bound due to increasing nuclear charge.⁷³

The oxide ligand is particularly versatile with the ability to form multiple bonds to metal atoms which can also be referred to as multiple bridging modes. The p-orbitals of oxo ligands are energetically readily accessible, however, the oxo ligand is too reactive for the formation of stable complexes with a single bound oxo-species.⁷⁴ According to the M-O bond character, it is possible to partition the terminal transition metal oxides into three groups: the early transition metals (group III-V), the chromium and manganese triads and the group VIII metals. The first have empty d-orbitals and are therefore capable of forming M-O triple bonds where all four oxygen electrons are paired with an electron on the metal ion, hence rendering the oxygen ions inert.⁵⁹

The scarcity of terminal oxo groups present in late transition metal complexes is a direct result of the electron-rich character of these elements, because terminal oxo groups require π -bond donation to vacant metal d-orbitals.⁷⁵ The Cr^+ and Mn^+ triads have no empty d-orbitals and no doubly occupied d-orbitals, therefore, tend to form conventional π -bonds and are expected to be moderate in their reactivity, as has been demonstrated experimentally.⁷⁶ The group VIII metals are unable to readily form triple bonds since there are no empty d-orbitals to overlap the oxygen lone pair. However, these are capable of producing the very reactive oxo double bonds since they have doubly occupied d-orbitals available for π -resonance. The reactivity of metal-oxo systems can be understood by considering how the d-orbital filling on the metal dictates the type of metal-oxygen bond formed. Early transition metals form strong, inert triple bonds and later transition metals form weak, reactive biradical double bonds.⁵⁹

1.5 The Oxo Wall Theory

The concept of the 'oxo-wall' was first proposed in 1962 by Carl Ballhausen and Harry Gray based on their studies of the vanadyl ion (as discussed previously).⁵⁵ The theory states that elements to the right of the Fe-Ru-Os group on the periodic table (see Figure 8) cannot support a terminal oxo ligand in a tetragonal geometry as the electrons begin to populate the antibonding orbitals of the $\text{M}=\text{O}$ unit.⁶⁰ More commonly, it also states that no terminal oxo complexes should be formed by metal centres with an octahedral symmetry and a d-electron count beyond 5.⁷⁷ The energy of the metal d-orbitals decreases on moving to the right of the d-block metals and past the oxo-wall, thereby increasing the oxo character in the π^* level of metal-oxo complexes. In order to form oxo-clusters with first-row transition metal elements beyond the wall, a reduction in the coordination number of the cluster is required in order to liberate orbitals which can accommodate non-bonding or weakly antibonding electrons.⁷⁸ The absence of effective π -bonding to the metal (i.e. from a strongly π -donating ligand like O^{2-}) results in an especially basic and therefore, unstable oxo group, particularly

with regards to protonation or attack by other electrophiles. The early transition metals generally form stable metal–oxo $[M=O]_n$ cores containing high oxidation state metal ions and dianionic O_2 ligands. On the other hand, late transition metals are expected to stabilise metal–oxyl $[M-O\cdot]_n$ species involving lower-valent metals (M^{n+1}) and the oxygen-centred radical ($O\cdot-$) anion.¹²

Sc	Ti	V	Cr	Mn	Fe	Co	Ni	Cu	Zn
Y	Zr	Nb	Mo	Tc	Ru	Rh	Pd	Ag	Cd
La	Hf	Ta	W	Re	Os	Ir	Pt	Au	Hg

Figure 8. Transition metal section of the periodic table highlighting the early (blue), mid (orange) and late (red) transition metals and illustrating the location of the oxo wall.⁶⁰

It is worth noting that in some instances, terminal oxo compounds with well-characterised electronic structures⁷⁹ have been formed, comprising of transition metals existing to the right of the oxo wall⁸⁰ without violating the oxo wall theory. This is because they do not assume a tetragonal symmetry. The isolation of terminal oxo clusters comprising of late transition metals residing in group 10 or beyond remains difficult to achieve as they are considered too unstable. This is because of the repulsion between the oxygen electrons and the metal d-orbitals. However, terminal oxo palladium compounds have been successfully synthesised. The relative stability of these complexes was investigated and it was found that the ancillary ligands are vital in taming the clusters by preventing the formation of highly reactive terminal oxo intermediates. Strong donor ligands were the best suited to high-valent, terminal oxo palladium(IV) compounds.⁷⁹ Prior claims were made stating exceptions to the theory had been found. For example, a platinum(IV)-oxo complex, namely $K_7Na_9[O=Pt^{IV}(H_2O)L_2]$, $L = [PW_9O_{34}]^{9-}$, had been synthesised and isolated at room temperature. Hill et al. explored the synthesis

and characterisation of platinum, palladium, and gold-oxo clusters where one ligand in each was a single oxygen atom multiply bonded to the metal centre.⁸¹ This was an exciting find due to it being the first late-transition metal-oxo cluster with the potential to be an important species in catalytic technologies such as fuel cells and industrial oxidative reactions, among other applications. However, it was later discovered that this was incorrect due to inaccurate structural interpretation and was later withdrawn.⁸²

The vertical boundary believed to exist between groups VIII and IX of the periodic table because metals residing in groups X and XI can only bind oxygen atoms *via* bridging between two metal centres.⁷² In late transition metal polynuclear complexes, the metal cations are often linked together by bridging ligands, such as oxo- or hydroxo-groups. Taken together, this allows a useful observation to be made: complexes with terminal oxo bonds 0–2 d-electrons are ubiquitous, while in complexes with more than 2 d-electrons or oxidation states greater than 4⁺, oxo ligands are usually found in bridging positions between two or more metal centres. Consequently, only a few stable d⁴ M=O complexes exist.⁸³

Metal oxo-hydroxo clusters are primarily assembled in water with organic ligands present. The formation of such open-shell transition metal un-ligated clusters cannot be readily isolated. However, when these are successfully synthesised, the clusters form the building blocks for many natural and synthetic metal oxides, including homogeneous catalysts as well as environmental, energy and biomedical applications.⁸⁴ Interestingly, of the first-row transition metals, vanadium(V/VI) is readily isolated in stable configurations without supporting organic or inorganic ligands.^{85,86} Organic ligands are usually included in clusters as they provide a stabilisation mechanism, allowing complexes to form and be isolated in water. These have been used to isolate single-molecule magnet clusters that possess unique magnetic behaviour.^{87,88} Inorganic ligands, such as polyoxometalate fragments and oxo-anions are also useful in capturing fragments of transient polynuclear forms^{89,90} or creating water-soluble species for catalysis. Inorganic oxo-anion ligands link clusters in various ways to form functional open

frameworks. However, despite the increased stability, ligands often hinder molecules for certain applications, such as in medicine⁹¹ and technology.^{92,93}

Terminal inorganic or organic capping ligands are employed to prevent aggregation, coalescence and possible polymerisation of metal clusters and can therefore have a major influence on the nuclearity and structure of the complex obtained.^{94,95} Capping ligands can also act as surface modifiers by forming a well-controlled passivation layer and improving the catalytic performance via steric and electronic effects.⁹⁶ These are often denoted as stabilising agents or capping ligands because they are typically used to stabilise metal-oxo clusters that are too unstable to exist on their own. Numerous polynuclear metal-oxo species have been isolated and characterised where oxo ligands are responsible for their formation. However, bridging species are themselves unable to stabilise the cluster because of their susceptibility to both hydrolysis and oligomerisation. Polyoxometalates (POMs) are an interesting subclass of metal-oxo compounds because their chemistry is not dictated by organic capping ligands and instead it is the terminal oxo ligands that limit the nuclearity of the POM.⁹⁷

1.6 Polyoxometalates

Holm has previously proposed that terminal M=O groups are stabilised at metal centres with a minimum oxidation state of 4⁺.⁹⁸ As a result, oxo-anions formed by the early first-row transition metals (comprising elements in groups III-VI) are especially stable and abundant.⁶⁰ The stability of the terminal metal-oxo moiety is largely determined by the d-electron count.⁷⁷

POMs are unique in that they are molecular analogues of solid-state metal oxide clusters comprising of early transition metals, commonly Mo, W, V or Nb in their highest oxidation states with various different structural configurations (Figure 9). POMs are distinguishable from other coordination complexes due to their high nuclearities, reaching values of up to 368 metal atoms in a

given cluster.^{99,100} The first synthesized POM was reported by Berzelius in the early 19th century,¹⁰¹ with the characterization and systematic study of their structure and properties beginning in the early 20th century with Rosenheim.¹⁰² In 1991, Pope and Müller¹⁰³ stated in a review that ‘POMs form a class of inorganic compounds that is unmatched in terms of molecular and electronic, structural versatility, reactivity, and relevance to analytical chemistry, catalysis, biology, medicine, geochemistry, material science and topology.⁸⁶ Another prominent characteristic of POMs is their tremendous redox behaviour and in particular their ability to accept or release a large number of electrons without decomposition or structural modification. POMs typically have empty nd orbitals, therefore, it is easy to put an electron into the empty frontier orbitals which is a crucial characteristic as this the reason for their high redox activity.¹⁰⁴ Since then, there has been an exponential growth in research and publications regarding these structures, including the bottom-up assembly of organic-inorganic hybrids.¹⁰⁵

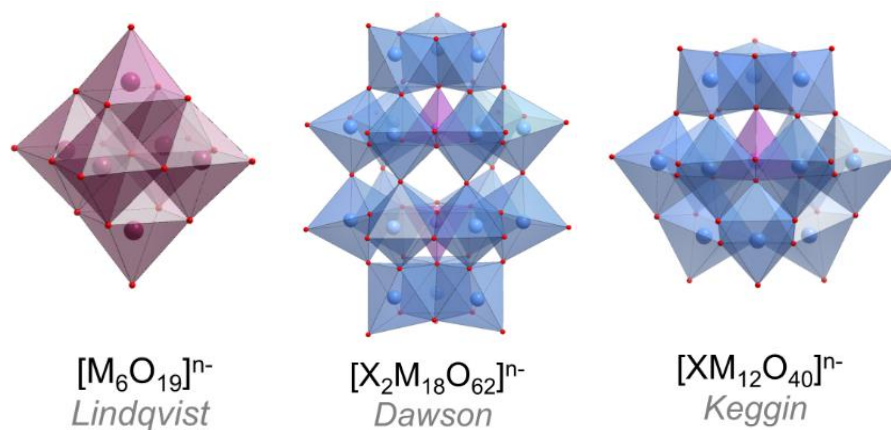


Figure 9. Polyhedral representation of the three main polyoxometalate structures: Lindqvist $[M_6O_{19}]^{n-}$ and Dawson $[X_2M_{18}O_{62}]^{n-}$ ($M = V, Mo, W$) ($X = P$) and Keggin $[XM_{12}O_{40}]^{n-}$. The metal centres in plum/blue, the O centres in red, and X centres in purple.¹⁰⁶

The surface of POMs are almost exclusively composed of terminal-oxo ligands providing access to the formation of hydrogen bonding (Figure 10). Bridging M-O-M units may also be present, however, these are prone to protonation, leading to the formation of hydroxyl groups. These molecular clusters can be regarded as soft Lewis bases due to the abundance of surface-bound oxygen atoms able to donate electrons to suitable electron acceptors.¹⁰⁶ The inert oxo groups act as a capping ligand on the surface of the cluster, protecting it from further reactions which would lead to the precipitation of the bulk metal oxide.¹⁰⁷ POMs are classified into two subfamilies regarding the presence or absence of an internal heteroatom (X). These are (i) isopolyanions (IPAs, with the general formula $[M_xO_y]^{n-}$) and (ii) heteropolyanions (HPAs, with the general formula $[X_zM_xO_y]^{n-}$). Keggin structures are common arrangements of POM-type clusters, where twelve $\{MO_6\}$ octahedra collectively form three $\{M_3O_{15}\}$ triads surrounding a single central $\{XO_4\}$ unit to create an overall tetrahedral species.¹⁰⁸

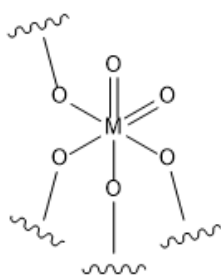


Figure 10. Schematic representation of the bonding present in POMs and other metal oxide clusters, illustrating both terminal and bridging-oxo bonds.

In 1972, Pope¹⁰⁹ divided all POMs into three types. Type I, which comprises of polyanions in which each addendum atom (transition metal atoms that make up the main framework of the POM) has one unshared terminal-oxo ligand. Type II, is characterized by two unshared terminal-oxo ligands per addendum atom and type III, is a combination of the two former.¹¹⁰ Pope predicted that only type

I and III polyanions can be reversibly reduced. According to the molecular orbital theory of oxo-type octahedral complexes, species with one terminal oxygen (type I) have one non-bonding t_{2g} orbital which can accommodate one or two electrons by reduction. However, anions with two unshared oxygens (type II) lack the non-bonding t_{2g} orbital because the orbitals are able to participate in π -bonding.¹¹¹

2 Aims

Many studies have illustrated the great importance of transition metal oxo-clusters and there is considerable interest in these compounds for their distinctive catalytic, magnetic and electrochemical properties. However, much of this research has been concentrated on a limited range of cluster types and compositions, with a particular focus on early, heavy transition metals. This includes elements such as tungsten and molybdenum because of their ability to form stable oxo bonds when assembling their molecular metal-oxo clusters. Exploration into Mn-based oxo-complexes has also been a focus of research activity, primarily because of their unique magnetic properties. Herein, this review will aim to provide a comprehensive overview of a range of first-row transition metal-oxo clusters, spanning each metal from scandium to zinc. This report will describe the metal-oxygen bonding model for oxo-clusters and the effect of the electronic structure of the metal, discussing their unique syntheses, structures and chemistry. Furthermore, an explanation for why the physical and chemical properties of each cluster as well as their potential application in a wider field varies between each metal ion due to their different electronic structures.

Based on the understanding of oxo-ligands and POMs, the potential of first-row transition metals in forming polynuclear oxo-complexes is explored by summarising previous research conducted in this area. This includes looking in detail at the impact structure and bonding has on enhancing desirable properties and why this is important in magnetism. More specifically, examining a cluster's magnetic properties and why this changes moving across the periodic table from left to right. Oxo-bonding is addressed in terms of its role in the double exchange process and single molecular magnetism by exploring why these phenomena are prominent in clusters comprising of certain metals in particular and how these properties emerge in mid- to late-transition metal oxo-clusters. For example, metal-oxo bonding plays an important role in double exchange where the paramagnetic metal sites are separated by bridging ligands, inducing electron delocalisation at the metal centre. Electrons are transferred simultaneously between metal centres via an O^{2-} anion while retaining their spin. This is a significant process in designing complexes with a high-spin ground state.

Also, this overview will explain why other structural features result in fascinating properties that develop across the first-row d-block elements, such as photo reactivity and multi-redox chemistry.

By describing the fundamentals of metal-oxo bonding in first-row transition metal clusters and the implications of this on their physical properties, this review aims to provide a framework through which we can better understand and predict the properties of such systems. Moreover, the hope is to demonstrate how these clusters are linked both structurally and chemically moving across the periodic table. Overall, the aim of this review is to provide a summary of exciting, state of the art metal-oxo clusters in this field and illustrate how controlled synthesis of these species can allow the tuning of their physical properties. Increasing our understanding of metal-oxo clusters will allow the bespoke development of a new generation of materials for applications in energy storage, catalysis and molecular magnetism.

3 Discussion

3.1 Scandium

In 1879, Scandium was the first transition metal to be isolated as an oxide by Lars Fredrik Nilson in Sweden.¹¹² Sc can exist in its metallic state although it is more commonly found in complexes as Sc^{III} and predominantly has an octahedral geometry.¹¹³ Typically, this element forms mononuclear, dinuclear or trinuclear species, varying depending on the pH of the reaction solution and the concentration of scandium present. Polynuclear clusters tend to only occur at high concentrations and high nuclearity scandium clusters are extremely rare.¹¹⁴ Polynuclear complexes feature a variety of unusual symmetries and structural patterns¹¹⁵ and it is anticipated that Sc clusters have applications in magnetic, optical, electronic and catalytic processes.¹¹⁶ Scandium is the first transition metal in the periodic table, therefore, is often used as a model to study complex phenomena associated with d-shell electrons.¹¹⁷

Prior to this study, it has been demonstrated that Sc-oxide nanostructures are effective catalysts for certain reactions, such as the selective reduction of nitric oxides with methane while others scandium clusters have also been encapsulated into closed carbon cages, such as fullerenes, to form novel composite nanostructures.¹¹⁸ Clusters such as Sc₃O₆ have previously been synthesised and studies have investigated their electronic and magnetic properties, explaining trends in metal–oxygen bonding and in the stability of the M–O–M bridge.⁴ The present study focuses exclusively on the various types of bonding displayed by the scandium oxygen system, which also has a prominent position in the studies of Bauschlicher and Andrews.¹¹⁹

The bond length measured indicated a triple bond, which can be understood in terms of Sc 3d² O 2p⁰ donations and O 2p⁴ Sc 3d⁰ back-donation. Hence, the unpaired electron is largely localised in the non-bonding Sc 4s orbital. Only minor structural changes in the cluster are seen upon adding or removing electrons, since this involves the weakly-bonding half-filled valence orbitals.¹²⁰ This

robustness towards oxidation or reduction is a general signature of transition metal oxide chemistry. It is directly related to the availability of near-degenerate, non-bonding states which is a signature of the early d- and f-elements.¹²¹

In 1995, an article was published reporting the synthesis, characterisation and structure of a new polynuclear scandium picrate complex with the molecular formula $[\text{Sc}_3(\text{pic})_3(\text{TDTD})_{1.5}(\text{OH})_5(\text{H}_2\text{O})](\text{pic})(\text{H}_2\text{O})_5$ (**1**). This cluster was obtained by reacting scandium picrate and trans-1,4-dithiane-1,4-dioxide (TDTD), (dithiane is a heterocyclic compound composed of a cyclohexane core structure wherein two methylene bridges are replaced by sulphur atoms), in water. This consists of polymeric chains of centrosymmetric scandium clusters, connected via TDTD bridges. The Sc^{III} ions present in the structure have different coordination numbers, with two being six-coordinate and the other seven-coordinate. The monodentate or bidentate picrates, water molecules, monodentate or bridging TDTD ligands and bridging hydroxo-groups provide the backbone of the scandium coordination polyhedrons. Uncoordinated water molecules and picrate ions complete the crystal structure.¹²² This provided a starting point in terms of researching Scandium oxo-clusters.

High-nuclearity scandium clusters are unusual, as illustrated by the fact only two pentanuclear scandium oxo-alkoxide clusters¹²³ and one hexanuclear hydroxo-picrate cluster¹²² are reported. A paper published in 2011 elaborates on previous work, exploring behaviour of Sc^{III} under hydro/solvothermal synthesis conditions. The authors explored the hydrothermal reaction of $\text{Sc}(\text{CH}_3\text{CO}_2)_3 \cdot 3\text{H}_2\text{O}$ with croconic acid ligands ($\text{C}_5\text{O}_5\text{H}_2$, H_2croc) in a mixture of ethanol and distilled water when heated at 200°C. A unique Sc^{III} -croconate polynuclear complex, of general formula $[\text{Sc}_7(\text{croc})_6(\text{H}_2\text{O})_6(\text{OH})_7\text{O}] \cdot 4\text{H}_2\text{O}$ was reported as the first example of a discrete heptanuclear hydroxo-oxo scandium cluster (Figure 11).¹²⁴

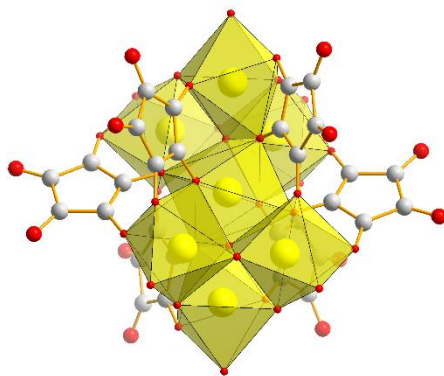


Figure 11. Polyhedral structural representation of the heptanuclear complex $[\text{Sc}_7(\text{croc})_6(\text{H}_2\text{O})_6(\text{OH})_7\text{O}] \cdot 4\text{H}_2\text{O}$. The Sc^{III} polyhedra in yellow, the O centres in red, C centres in grey, and N centres in blue. The hydrogen atoms have been omitted for clarity.¹²⁴

Overall, the asymmetric unit comprises of two Sc^{III} ions, a croconate ligand, a coordinated water molecule, a coordinated oxygen atom and two water molecules. The first central Sc^{III} ion is surrounded by eight oxygen atoms: six from the six equivalent croconate ligands, one from the oxide anion and one from the hydroxo group, thus forming a distorted rhombohedral geometry. The second Sc^{III} coordination environment is surrounded by seven oxygen atoms: two from equivalent croconate ligands, two from μ_2 -OH groups, two from μ_4 -OH anions and one from μ_4 -O or μ_4 -OH anion, so that a mono-capped distorted octahedron is formed around the Sc ions. Interestingly, charge from the doubly negatively charged croconate ligands extends throughout the empty scandium d-orbitals, creating an extended π -system as a result of the d^0 electron configuration of Sc^{III} .¹²⁴

3.2 Titanium

Titanium is particularly suited to forming higher nuclearity oxo-cluster, not dissimilar to polyoxometalates commonly formed by V, Mo and W (see section 1.8)¹²⁵ where titanium centres are either five or six coordinate.¹²⁶ Due to the rich structural chemistry of titanium oxo-clusters, in addition

to their attractive photochemical properties and low toxicity, these species are commonly used as a photocatalysts for solar energy conversion.¹²⁷ Additionally, these clusters have also been used in order to gain a better understanding of the properties of bulk titanium oxides by using the molecular analogues as easily tuneable model compounds.¹²⁸ While the first crystal structure of a Ti oxo-cluster was reported in 1966, numerous titanium-oxo-clusters have since been prepared, with nuclearities ranging from 2 to 34.¹²⁹ Polyoxotitanates (POT) are cage-type clusters of general formulae $[\text{Ti}_x\text{O}_y(\text{OR})_{4z-2y}]$ and can be synthesized in a nucleophilic reaction of metal-alkoxides. In the case of polyoxotitanates, this involves the reaction of $[\text{Ti}(\text{OR})_4]$ (R = alkyl) with water, where the degree of polymerization depends crucially on the $[\text{H}_2\text{O}]/[\text{Ti}(\text{OR})_4]$ ratio in the initial hydrolysis reaction. These represent a unique family of titanium oxide species with versatile but synthetically controllable structural features. POTs have received special interest, not only for their catalytic properties¹³⁰ but also for their potential optical properties resulting from their bonding nature.¹³¹

A new neutral lacunary super-Keggin titanium cluster with the molecular formula, $[\text{Ti}_{17}\text{O}_{24}(\text{OPr}^i)_{20}]$ (**1**) (Figure 12), was reported in 1999. The super-Keggin can be described as a $[\text{Ti}_{13}\text{O}_{40}]_{28}$ Keggin complex which is capped by four five-coordinate titanium centres..¹³⁰ The neutral lacunary complex (a lacunary structure being a derivative of a POM structure where one or more addenda atoms and their attendant oxide ions are removed) was synthesised via a reaction between titanium isopropoxide and acetic acid in the molar ratio 1:1.3 at 150 °C. The formation of the cluster was driven by the production of water, thus the reaction is limited by the water present in situ. In this case, the water was generated through esterification reactions between the acetic acid and isopropoxide ligands. In order to obtain better control of the water generated in-situ, hence better control of the metal-oxo cluster core size, slight adjustments in the temperature and the amount of acetic acid achieved the desired results, as demonstrated by the metal-oxo core size of the titanium clusters increasing with temperature (150 °C), pressure and the amount of acetic acid.¹³⁰

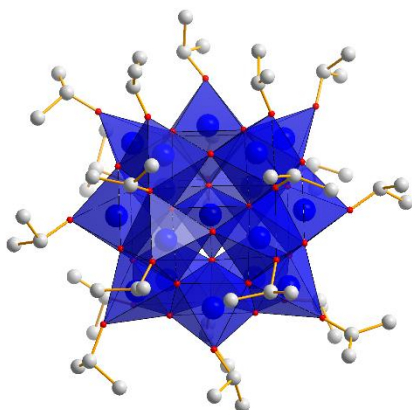


Figure 12. Polyhedral structural representation of the heptadecanuclear complex $[\text{Ti}_{17}\text{O}_{24}(\text{OPri})_{20}]$ (**1**). The Ti^{IV} polyhedra in royal blue, the O centres in red and C centres in grey. The hydrogen atoms been omitted for clarity.¹³⁰

(**1**) is a cluster comprising of 17 Ti^{IV} ions coordinated to both oxo and isopropoxo ligands, where the metal-oxo framework is very similar to the familiar Keggin structure (Figure 12). It contains a range of Ti coordination geometries, including: tetrahedral, octahedral and distorted trigonal bipyramidal geometries. These are complexed to oxo and isopropoxy ligands; including a number of multiply-bridging μ_2 -, μ_3 - and μ_4 -oxo bridges. By complexing bidentate ligands, it is possible to substitute a few of the alkoxide ligands that are more readily hydrolysed and as a result reduces precursor functionality, thus decreasing their reactivity towards hydrolysis. Typically, carboxylate moieties are a popular choice in controlling their reactivity.¹³⁰

This study illustrates that the esterification process is preferred when using solvothermal conditions as there is the greatest conversion of carboxylic acid molecules into isopropyl ester and water. Furthermore, in order to gain better control over the water generated in-situ, the temperature and the amount of acetic acid can be altered, thus allowing better management of the metal-oxo cluster core size; the higher the temperature and quantity of acetic acid, the larger the size of the metal-oxo cores of titanium clusters.

In 2010, the synthesis, crystallization and structure determination of three new POT clusters: $\text{Ti}_{14}\text{O}_{20}\text{H}(\text{OBU}^t)_{13}(\text{OAc})_4$ (**1**), $\text{Ti}_{18}\text{O}_{25}\text{OBU}^t_{12}\text{OAc}_{10}$ (**2**), and $\text{Ti}_{28}\text{O}_{40}\text{OBU}^t_{20}\text{OAc}_{12}$ (**3**) (Figure 13), were reported with the structural similarities. The largest POT synthesis and crystallisation was reported in this study, forming the first $\{\text{Ti}_{28}\}$ structure. During the synthesis, high temperatures and pressures were required, however, the overall POT growth is actually driven by the hydrolysis of titanium alkoxides which are released from the esterification reactions. Direct evidence to support this is demonstrated by the presence of tert-butyl acetate as a solvent of crystallization in the structure of (**1**). Throughout the reaction acetic acid is consumed and the titanium precursor is hydrolysed which in turn forms these larger clusters.¹³²

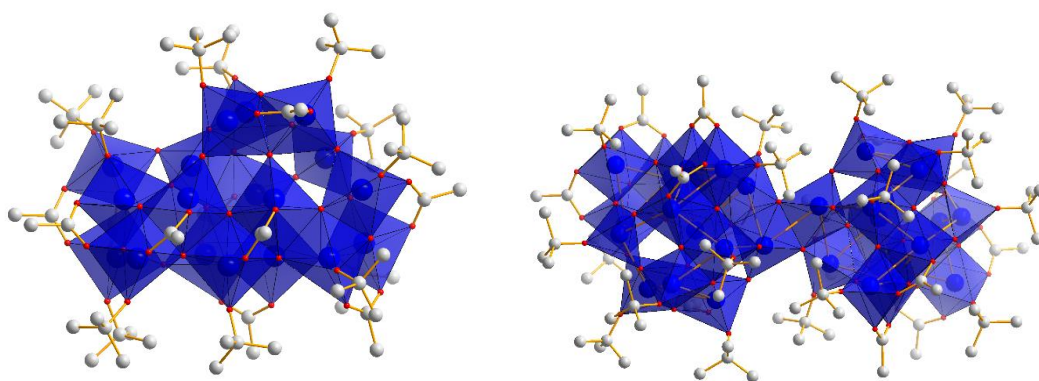


Figure 13. Polyhedral structural representation of the heptadecanuclear complex $[\text{Ti}_{14}\text{O}_{20}\text{H}(\text{OBU}^t)_{13}(\text{OAc})_4]$ (**1**) $[\text{Ti}_{18}\text{O}_{25}\text{OBU}^t_{12}\text{OAc}_{10}]$ (**2**) and $[\text{Ti}_{28}\text{O}_{40}\text{OBU}^t_{20}\text{OAc}_{12}]$ (**3**). The Ti^{IV} polyhedra in royal blue, the O centres in red and C centres in grey. The hydrogen atoms and counter anions have been omitted for clarity.¹³²

The bonding present in the metal oxide cores of these POT clusters shares features of the bulk pure-phase, however, there is undercoordination at the periphery as expected. Of the 14 Ti^{IV} present in structure (**1**), nine are six-coordinate and assume a distorted octahedral geometry, however, the remaining four are five-coordinate and assume a square pyramidal geometry. The remaining titanium atom is four-coordinate with a tetrahedral geometry. In comparison, structure (**2**) diverges

substantially from the previous two reported Ti_{18} structures but was extremely similar to one (**1**), differing only by the four titanium ions. Regarding the 18 Ti^{IV} ions present in (**2**), fifteen are six-coordinate assuming a distorted octahedral geometry and three are five-coordinate possessing a square-pyramidal geometries, respectively. Structure (**3**) is effectively two 14 Ti^{IV} clusters joined by two Ti^{IV} -oxo bridges. Of the 28 Ti^{IV} ions in this cluster, twenty are six-coordinate and the remaining eight are five-coordinate.¹³²

In addition to the polyoxometalate based compound discussed so far, other titanium-oxo clusters demonstrate great potential in various areas. Titanium-oxo clusters with the general formula $[Ti_nO_m(OR)_x(L)_y]$ exhibit a wide range of structural types which are characterized by the various ligand coordination modes, the coordination polyhedra connections, degree of condensation and the titanium atom coordination numbers, as reviewed by Rozes.¹³³ The carboxylate-substituted titanium oxo-clusters constitute a valuable class of titanium-oxo clusters, with their nuclearities ranging from 2, $[Ti_2O(O^iPr)_2(HO^iPr)_2(O_2CCl_3)_4]$ to 28, $[Ti_{28}O_{40}(O^tBu)_{20}(OOAc)_{12}]$.¹³² Due to the carboxylate-coordinated titanium oxo-alkoxy clusters high hydrolytic stability compared to pure titanium oxo-alkoxy clusters, approximately 20 monocarboxylates have been used for the synthesis of the titanium carboxylate systems $[Ti_nO_m(OR)_x(OOCR')_y]$. However, at the time there was no reported dicarboxylate crystal structure for these clusters, except for $[Ti_8O_8(OH)_4(O_2C-C_6H_4-CO_2)_6]$; a titanium-oxo-hydroxy cluster comprising of dicarboxylate linkers.¹³⁴

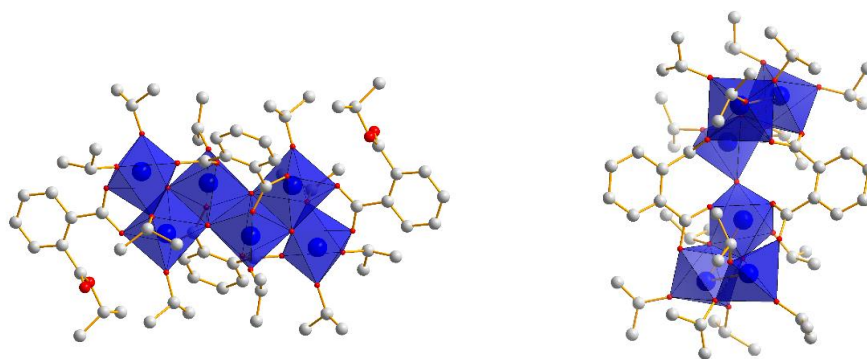


Figure 14. Polyhedral structural representation of the hexadecanuclear complex $[\text{Ti}_6\text{O}_4(\text{o-BDC})_2(\text{oBDCiPr})_2(\text{OiPr})_{10}]$ (**1**) and $[\text{Ti}_6\text{O}_3(\text{o-BDC})_2(\text{OiPr})_{14}]$ (**2**). The Ti^{IV} polyhedra in royal blue, the O centres in red and C centres in grey. The hydrogen atoms and counter anions have been omitted for clarity.¹²⁵

In 2012, two titanium-oxo-clusters $[\text{Ti}_6\text{O}_4(\text{o-BDC})_2(\text{oBDCiPr})_2(\text{OiPr})_{10}]$ (**1**) and $[\text{Ti}_6\text{O}_3(\text{o-BDC})_2(\text{OiPr})_{14}]$ (**2**) (BDC = benzene dicarboxylate) (Figure 14), were prepared via a single stage in situ solvothermal synthesis. This was achieved by successfully introducing a phthalic acid (benzene dicarboxylate acid, H_2BDC). Both $\{\text{Ti}_6\}$ oxo-clusters, (**1**) and (**2**), are constructed by two dual corner-missing cube subunit, $\{\text{Ti}_3\text{O}_3\}$. The two subunits are linked by double $\mu_3\text{-O}$ bridges for (**1**) and single $\mu_2\text{-O}$ bridge for (**2**), respectively. Nanostructural titanium dioxide materials, such as these, have been commonly utilised as photocatalysts for solar energy conversion and environmental applications, as a result of its low toxicity, abundance, high photostability, and high efficiency.¹²⁷

A particularly interesting area is the synthesis of inorganic-organic hybrids materials centred around the general molecular formula based on a $\{\text{Ti}_i(\mu\text{-O})_b\}$ ($i = 2, 3, 4$) core by modifying of hybrid interfaces.^{135,136,137} Schubert recommended a possible synthetic route involving the stepwise assembly of heavier titanium-oxo clusters. However, this is now preceded by the formation of pre-units, such as $[\text{Ti}_3\text{O}(\text{OR})_8(\text{O}_2\text{CR}')_2]$ or $[\text{Ti}_4\text{O}_2(\text{OR})_6(\text{O}_2\text{CR}')_6]$. Multinuclear Ti^{IV} μ -oxo-alkoxo-carboxylate complexes of the general formula $[\text{Ti}_a\text{O}_b(\text{OR})_c(\text{O}_2\text{CR}')_{4a-2b-c}]$ are of particular interest. An investigation into

multiple pathways of the 1:1 reactions of $[\text{Ti}(\text{O}^t\text{Bu})_4]$ with branched carboxylic acids $\text{R}'\text{COOH}$ ($\text{R}' = \text{C}(\text{Me})_2\text{Et}$, CH_2^tBu , ^tBu) meant further knowledge was gained on the structural conversion processes of multinuclear Ti^{IV} -oxo complexes. These reactions were carried out at room temperature and in argon atmosphere. This involved the conversion of previously formed metastable intermediate systems producing fundamentally stable and well-studied μ - Ti^{IV} -oxo complexes comprising of $\{\text{Ti}_6(\mu_3\text{-O})_6\}$ cores.¹³⁸ The synthetic procedure was kept consistent with the general synthesis scheme already discussed in previous reports, including using a mixture of toluene and *tert*-BuOH (1:1) as the solvent. From prior experience, this combination aids the stabilisation of intermediate structures.^{139,140} However, issues regarding understanding the formation mechanisms of polynuclear Ti^{IV} -oxo cluster with controlled structural core, $\{\text{Ti}_a(\mu_i\text{-O})_b\}$, is still unresolved. Nevertheless, an improved understanding of this process is crucial for synthesis of inorganic-organic hybrid materials to enable the development of precursors containing well-defined core structure.^{141,142}

A report in 2014 discussed the conversion process of $\{\text{Ti}_4\}$ complexes to $\{\text{Ti}_6\}$ clusters. The initial stage of the synthetic procedure produced two hexanuclear μ -oxo- Ti^{IV} clusters with molecular formulas; $[\text{Ti}_6\text{O}_6(\text{OtBu})_6(\text{O}_2\text{CC}(\text{Me})_2\text{Et})_6]\cdot\text{toluene}$ (**1**) and $[\text{Ti}_6\text{O}_6(\text{OtBu})_6(\text{O}_2\text{CCH}_2^t\text{Bu})_6]\cdot 1.5\text{toluene}$ (**2**) (Figure 15). The synthesized complexes are stable in air, however, are poorly soluble in organic solvents.

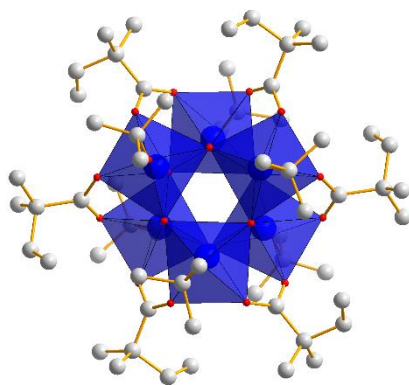


Figure 15. Polyhedral structural representation of the hexanuclear complex $[\text{Ti}_6\text{O}_6(\text{OtBu})_6(\text{O}_2\text{CC}(\text{Me})_2\text{Et})_6]\cdot\text{toluene}$ (**1**). The Ti^{IV} polyhedra in royal blue, the O centres in red and C centres in grey. The hydrogen atoms have been omitted for clarity.¹⁴³

Both structures consist of two Ti_3O_3 faces, bridged by six *syn-syn* carboxylate groups and six terminal alkoxide ligands to form the overall hexanuclear $\{\text{Ti}_6(\mu_3\text{-O})_6\}$ framework similar to that previously described for hexanuclear $\mu_3\text{-oxo-Ti}^{\text{IV}}$ clusters.^{139,140} The central part of their molecules consists of tetranuclear $\{\text{Ti}_4(\mu_3\text{-O})_4\}$ structural units stabilised by four carboxylate groups and four terminal tert-butoxide ligands.¹⁴⁴ A comparison of the $\{\text{Ti}_a(\mu_3\text{-O})_b\}$ cluster geometry could be made between the two structurally dissimilar products formed before and after the conversion. Both $\{\text{Ti}_6(\mu_3\text{-O})_6\}$ and $\{\text{Ti}_4(\mu_3\text{-O})_4\}$ core units are depicted as hexagonal or square-based cuboids with rectangular side faces. These are then linked by four carboxylate groups.¹³⁰

All titanium atoms are six coordinate and have an octahedral coordination sphere consisting of three oxo-anions, two carboxylates, and one O^tBu ligand. The titanium atoms occupying opposite sites on the side faces are connected by carboxylate bridges. Results of our investigations proved the conversion of hexanuclear cluster $[\text{Ti}_6\text{O}_6(\text{O}^t\text{Bu})_6(\text{O}_2\text{CR}')_6]$ into tetranuclear complex $[\text{Ti}_4\text{O}_4(\text{O}^t\text{Bu})_4(\text{O}_2\text{CR}')_4]$. This conversion could potentially be utilised as an additional pathway for the stepwise assembly of large clusters starting from smaller units, as demonstrated by Schubert.¹⁴⁵

Results from this study have allowed for the discovery and analysis of the conversion mechanism for multinuclear Ti^{IV} -oxo complexes, suggesting that controlling the synthesis of other materials with desired $\{\text{Ti}_a(\mu_3\text{-O})_b\}$ structural format is possible.

The unique structures and photocatalytic properties of Ti-oxide clusters has resulted in considerable attention being paid to their synthesis in the past decade. The choice of reaction conditions including the precursor, additive, solvent and temperature can be a critical factor in controlling the core size and composition during the solvothermal reaction of Ti^{IV} reagents with functional ligands.¹⁴⁶ The ligand exchange process involving pre-formed Ti oxide clusters is important in successfully obtaining functionalised oxo clusters. In addition, this method allows for assembly of new organic-inorganic hybrid materials without damage occurring to cores of the clusters. This technique is not suitable for other early transition metal-oxo complexes where passivating ligands are not present on the surfaces of the molecules. However, a similar or increased performance is expected if the complex is properly functionalized.¹⁴⁷

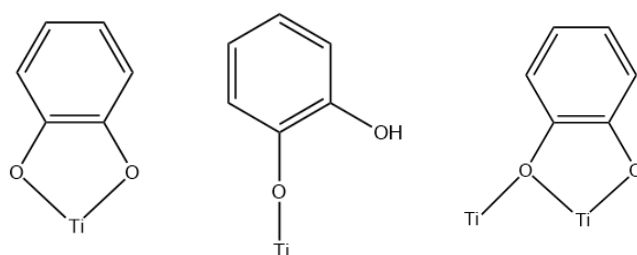


Figure 16. Binding modes of catechol ligands - Chelate-bidentate mode, Monodentate mode and chelate-bridging mode.¹⁴⁸

Sanchez et al. carefully studied the ligand-exchange reactions of $[\text{Ti}_{16}\text{O}_{16}(\text{OEt})_{32}]$ with alcohols.¹⁴⁹ The functionalized product of the $[\text{Ti}_{22}\text{O}_{32}(\text{O}i\text{C}_3\text{H}_7)_{23}\text{H}]^+$ cluster with 3,5-di-tert-butylcatechol (H_2DTBC). $[\text{Ti}_{17}\text{O}_{24}(\text{O}i\text{C}_3\text{H}_7)_{20}] \{\text{Ti}_{17}\}$ (Figure 17) is very important because it is one of the oldest Ti-oxide clusters and exhibits the classic Keggin structure. The ligand exchange of $\{\text{Ti}_{17}\}$ was first studied by Coppens et

al. who only obtained tetra-functionalised derivatives. $\{Ti_{17}\}$ was reacted with n equivalents of substituted catechols ($n =$ equivalents of added catechol; $n=1-8$) to perform the ligand exchange reaction. $\{Ti_{17}L_n\}$ complexes where $n = 1, 2,$ and 4 show that the catecholate ligand acts as a bidentate chelate and displaces one of the terminal isopropoxide ligands at the five-coordinated Ti_a . This results in an increase of the coordination number of Ti_a to six.¹⁴⁸

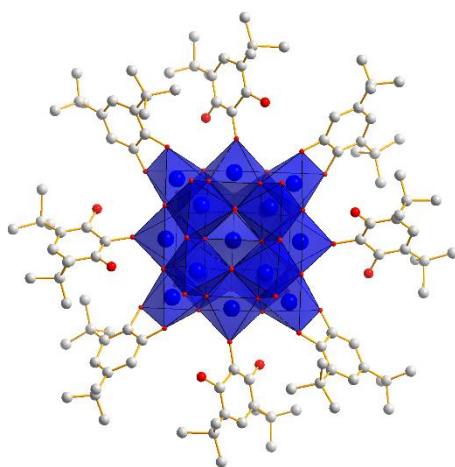


Figure 17. Polyhedral structural representation of the hexanuclear complex $[Ti_{17}O_{24}(OiC_3H_7)_{20}]$ (**1**). The Ti^{IV} polyhedra in royal blue, the O centres in red and C centres in grey. The isopropyl groups and counter anions have been omitted for clarity.¹⁵⁰

The current knowledge and methods discussed should provide an ideal starting point for the synthesis of other functionalised Ti oxide clusters. Also, it is hoped that the current findings may influence further applications of Ti_{17} and other Ti oxide clusters as building blocks in supramolecular chemistry, especially in the assembly of well-defined organic-inorganic hybrid materials.¹⁴⁸

3.3 Vanadium

The oxo-chemistry displayed by vanadium is more comparable to the Group 6 elements molybdenum and tungsten, of which numerous compounds with terminal oxo ligands are known.⁷¹ Vanadium can be found in a range of stable oxidation states and coordination geometries, and is thus a useful component in a range of systems.¹⁵¹ Controlled design of polyoxovanadates (POVs) has led to highly active materials for energy conversion, photocatalysis, molecular magnetism and materials science.¹⁵² V^V forms a significant range of pH-dependent polyoxoanions; in the more acidic region (pH ca. 3 – 6) the orange decavanadates, $[H_xV_{10}O_{28}]^{(6-x)-}$, with six-coordinate V ions predominate. Also, V^V can also be incorporated into Keggin-type structures by altering the pH.¹⁵³ In addition to fully oxidised V^V polyoxoanions, POVs can be based on mixed-valent V^V/V^{IV} and V^{IV}/V^{III} , fully reduced V^{IV} and highly reduced V^{III} species.¹⁵¹ They can demonstrate a range of intramolecular spin exchange phenomena, such as ferro/antiferro-magnetism and SMM behaviour.¹⁵⁴

Proper structural precedent did not exist for either vanadium alkoxides or vanadate esters before the 1990s.¹⁵⁵ In 1992, Pettersson et al. identified a new transient Keggin isopolyvanadate, $[H_{12}V_{13}O_{40}]^3$, comprising of a central tetrahedral $\{VO_4\}$ and four $\{V_3O_6H_3\}$ triad units.¹⁵⁶ Three similar structures have been previously reported for mono-capped and bicapped heteropolyoxovanadates (V), vanadophosphate with underlying α -Keggin structures, as well as a tricapped dodecavanadotrimanganate, also with an overall α -Keggin structure.¹⁵⁷ The isopolyvanadate, $[H_{12}V_{13}O_{40}]^3$, comprises several types of bridging oxygens, with some from the same trimetallic group while others are bridging different trimetallic groups.¹⁵⁴ When the cluster was examined, the recognised aqueous isopolyvanadates were discovered to be centred on corner-sharing $\{MO_4\}$ tetrahedra or on arrays of cubically packed, edge-sharing $\{MO_6\}$ octahedra, as illustrated in the decavanadate structure itself.^{158,86}

When employing the method of hydrothermal synthesis, the sequential substitution of bridging oxo-groups by alkoxide ligands allows for the preparation of a family of alkoxo polyoxovanadium

clusters with the hexavanadate core, $[V_6O_{19-3n}\{(OCH_2)_3CR\}_n]^*$ ($n = 2-4$).¹⁵⁹ Alkoxo-derivatives of POM structures have been indirectly prepared, notably V^V species based on the hexametalate and decavanadate cores with alkoxy-oxygens in surface bridging positions.¹⁵³ The V^V alkoxides are highly reactive, with several species forming in water and the alkoxide bridge forming from alcohols.¹⁵⁴

Despite the vast array of literature available on high-valent polyoxo(alkoxo) $V^{IV/V}$ clusters, owing to their useful redox, catalytic and magnetic properties, there is a surprising lack of information concerning low valent V^{III} or mixed $V^{III/IV}$ analogues. However, previous research leads chemists to believe that low-valent species may have significant promise as magnetic materials^{160,161} by exploiting the magnetic anisotropy of the V^{III} ion¹⁶² or using these clusters as powerful reducing agents.¹⁶³ The report published in 2006 by Ian Tidmarsh et al., details the solvothermal synthesis, structure and primary magnetic studies of the first fully reduced, high nuclearity V^{III} -based polyoxo(alkoxo)vanadium cage, a $\{V^{III}_{16}V^{IV}_2\}$ complex (Figure 18). V^{III} clusters, and perhaps most notably Mullers $\{V^{IV}\}_{15}$ clusters, have attracted significant attention due to their magnetic properties.^{164,165}

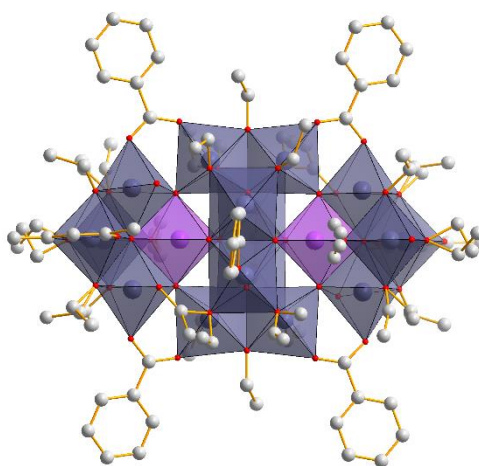


Figure 18. Polyhedral structural representation of the octadecanuclear complex $[V_{18}(O)_{12}(OH)_2(H_2O)_4(EtO)_{22}(O_2CPh)_6(acac)_2]$ (**1**). The V^{III}_{16} polyhedra in blue-grey and V^{IV}_2 polyhedra in light purple, the O centres in red and C centres in grey. The hydrogen atoms and counter anions have been omitted for clarity.¹⁶⁶

The reported synthesis of the octadecametallic $V^{III}_{16}V^{IV}_2$ species involved the solvothermolysis reaction in the presence of EtOH between the monomeric $[V(acac)_3]$ and $[VO(acac)_2]$ precursors ($acac^-$ = acetylacetonate) with benzoic acid in a 4:1 ratio at 150 °C under an inert atmosphere. The molecular product, $[V_{18}(O)_{12}(OH)_2(H_2O)_4(EtO)_{22}(O_2CPh)_6(acac)_2]$ (**1**) (Figure 18), contains sixteen V^{III} ions, capped by two vanadyls and has a 1:1 ratio of V:O(H). This can be considered the first example of a highly reduced, $V^{III/IV}$ polyoxovanadium cage. The 1 : 1 V : O(H) ratio in the $\{V^{III}_{16}V^{IV}_2O_{12}(OH)_2(OH_2)_4\}$ inorganic core of (**1**) means that it can be classed as a highly reduced polyoxo(alkoxo)vanadate.¹⁶⁶

In 2009, further exploration into the $[V_6O_7(OCH_3)_{12}]^{n+/-}$ cluster series was reported. The synthesis and structural characterisation of the neutral mixed-valence methoxo-polyoxovanadium cluster $[V_6O_8(OCH_3)_{11}]$ was also investigated. The most notable characteristic of both clusters is their high redox activity, with cyclic voltammetry disclosing several thermodynamically stable V^{IV}/V^V mixed-valence redox isomers. The primary interest in these clusters is their quality as models in investigating spin-spin interactions between the unpaired d-electrons residing in the vanadium centres, via superexchange mediating ligands. The magnetic measurements conducted on the $[V^{IV}_6O_7(OCH_3)_{12}]^{2-}$ complex revealed net antiferromagnetic interactions between the metal d-electrons. The magnitude of superexchange interaction varies as a result of exchanging the single μ -bridging methoxo- ligand in the $[V_6O_7(OCH_3)_{12}]^n$ series for a μ -bridging oxo ligand in the $[V_6O_8(OCH_3)_{11}]^n$ series. This triggers a large divergence in their individual redox properties. However, at lower temperatures the antiferromagnetic interactions present are inhibited due to geometric spin frustration. This appeared to be the first example of analysing a polynuclear metal-oxo cluster electrochemical potential shift. This could be attributed to a disparity in spin-spin interactions between unpaired d-electrons.³³

The preparation of the neutral oxo-vanadium species, $[V_6O_8(OCH_3)_{11}]$ (**1**) (Figure 19), involved the reaction of $VO(O^tBu)_3$ and methanol while heating in a pressure vessel to produce a green fraction, $[V_6O_7(OCH_3)_{12}]$. On the other hand, the same product can also be synthesised by adding $VO(OCH_3)_3$ to

dry methanol in 1 mL portions and tetrabutylammonium hydroxide solution, contained in a pressure vessel.

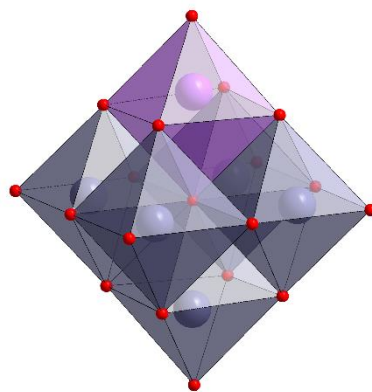


Figure 19. Polyhedral structural representation of the hexanuclear complex $[V_6O_8(OCH_3)_{12}]$ (**1**) and $[V_6O_7(OCH_3)_{12}]^{n+/-}$. The V^{IV}/V^V polyhedra in blue-grey/light purple, the O centres in red and C centres in grey. The hydrogen atoms and counter anions have been omitted for clarity.³³

Prior to this, the novel alkoxo-polyoxovanadium clusters reported were of the general composition $[V_6O_7(OR)_{12}]$ ($R = -CH_3, -C_2H_5$). Originally, these were derived from the highly symmetrical Lindqvist structure $[M_6O_{19}]^{n-}$ via substitution of the twelve μ -oxo ligands by monodentate bridging alkoxo ligands. Complex (**1**) comprises of a Lindqvist-based hexanuclear polyoxovanadate core, $[M_6O_{19}]^{n-}$, where eleven out of the twelve μ -bridging oxo ligands are substituted by monodentate methoxo ligands.¹⁶⁷ The $[V_6O_8(OCH_3)_{11}]^+$ (**1**) cation was one of the few cationic polyoxometalate derivatives known to date.^{168,169} The mixed-valence cluster comprises two V^{IV} and four V^V ions. Thus, with respect to d-electron content, it is isoelectronic to the dicationic cluster $[V^{IV}_2V^V_4O_7(OCH_3)_{12}]^{2+}$ of the dodecamethoxo-cluster series. The d-electron of the V^{IV} nuclei can, therefore, be extensively delocalized in the highly symmetrical $\{V_6O_{19}\}$ hexavanadate core.¹⁷⁰

In 1995, Zubieta et al. successfully synthesised an array of hexavanadate products containing trisalkoxo μ -bridging moieties.¹⁷¹ This led to the discovery of a rich class of V^{IV}/V^V mixed-valence complexes with remarkably exciting electronic and magnetic properties.^{172,33} The magnetic measurements performed on the highly reduced cluster species; $[V^{IV}_5V^VO_7(OCH_3)_{12}]^-$ and $[V^{IV}_6O_7(OCH_3)_{12}]^{2-}$ showed net antiferromagnetic exchange interactions between the metal centres, however, at lower temperatures these interactions were suppressed. At the time, this was also attributed to geometric spin frustration. Furthermore, when considering the function of transition metal-oxo clusters as redox centres in ubiquitous metalloproteins they are capable of conquering complex chemical transformations in nature. The findings in this study indicate their versatility may rely on their significant redox potential sensitivity regarding structural and/or chemical modifications.¹⁷³ Typically, this factor strongly influences the magnetic exchange interactions between the unpaired d-electrons. The variation in super exchange interaction magnitudes is a result of from a single μ -methoxo-ligand in the $[V_6O_7(OCH_3)_{12}]^{n+/-}$ series being formally exchanged for a μ -bridging oxo ligand in the $[V_6O_8(OCH_3)_{11}]^{n+/-}$ series. This resulted in an unexpectedly large discrepancy in their respective redox properties. At the time, this was thought to be the first example where a difference in spin-spin interactions was the only viable reason behind an electrochemical potential shift in the cluster.³³

Despite no magnetic data being currently available to support conclusions made for the undecamethoxo-cluster series, very strong antiferromagnetic exchange in polyoxovanadates(IV) mediated by μ -bridging oxo ligands are observed compared to μ -bridging alkoxo ligands.¹⁷⁴ The magnetic behaviour displayed has previously been observed in other spin frustrated transition metal-oxo clusters.¹⁷⁵ However, curiously this behaviour is not observed in Lindqvist-type polyalkoxo-hexavanadate(IV) complexes consisting of trisalkoxo nor those comprising of a combination of trisalkoxo and μ -bridging hydroxo ligands. These clusters typically display antiferromagnetic behaviour throughout the entire temperature range.¹⁷⁶

Polyoxovanadate alkoxide clusters are an emerging class of compounds that possess the requisite physical and electronic properties to constitute an ideal class of redox active reagents. This unique subset of POMs feature vanadyl ions in a Lindqvist arrangement, $[M_6O_{19}]^{n-}$; a classic POM structure generally observed for elements such as molybdenum, tungsten, niobium, and tantalum. When this structure was first reported, it was not possible to isolate the corresponding vanadium structure, $[V_6O_{19}]^{8-}$, unless the bridging oxygen atoms were substituted for alkoxides. This resulted in a reduced overall charge on the molecule and stabilised the low-valent vanadium centres within the cluster core. Subsequently, a mixed-valent POV alkoxide cluster was formed which is soluble in organic solvents in any oxidation state.¹⁷⁰

The extensive electronic delocalization between vanadium ions has resulted in the alkoxide-bridged hexavanadate cluster displaying excellent redox behaviour due to the presence of mixed oxidation states (V^{IV}/V^V). The electrochemical profile of hexavanadate POV-alkoxides have made this group of clusters the emphasis of a wide range of studies, demonstrating their exceptional magnetic properties and its catalytic significance in photoinduced water oxidation. However, deliberate tuning of the electrochemical profiles of these clusters via systematic modifications remains underexplored. Although there has been progress regarding changing the electronic properties of bridging ligand moieties, particularly the generation of a diverse group of trisalkoxy-derived POV-alkoxides. Efforts since have demonstrated that mixed-valency can be retained in the cluster after the addition of three amino groups, producing $[V_6O_{10}(NH_2C(CH_2O)_3)_3]$ (Figure 20). Unfortunately, bulky ligand modifications decreases the electrochemical reversibility in the redox profiles of the complexes.³³

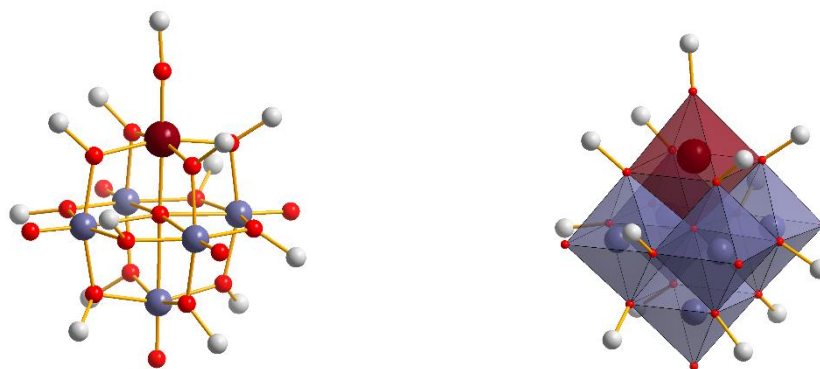


Figure 20. Polyhedral structural representation of the hexanuclear complex $[V_6O_{10}(NH_2C(CH_2O)_3)_3]$. The V^{IV}/V^V polyhedra in blue-grey, the O centres in red and C centres in grey. The hydrogen atoms and counter anions have been omitted for clarity.¹⁷⁰

Designing clusters with multiple functionalities is an attractive area to explore. For instance, developing vanadium complexes involving lanthanide ions could potentially pave the way for combining luminescent characteristics and even single-molecule magnetism with quantum bit-friendly properties of vanadium ions. All these complexes include $\{VO_6\}$ octahedral units, which to the best of our knowledge, have not yet been considered as potential qubits at room temperatures. In the first step of this research, diamagnetic lanthanides in complexes with paramagnetic vanadium ions were addressed.¹⁷⁷

Introducing oxygen donor-ligands into POM-based structures compensates for the charge, which is true for the largest subclass of POM derivatives, namely alkoxo-polyoxometalates. This is often achieved via formal substitution of peripheral ligands, typically bridging oxo groups, therefore, stabilising the structure.¹⁷⁸ Zubieta et al. successfully synthesised a range of such classical alkoxo-POM clusters with the general composition $[V_n^{IV}V_{6-n}^VO_7(OR)_{12}]_{(4-n)}$ which comprising of a hexavanadate $\{V_6O_{19}\}$ unit and incorporates trisalkoxo μ -bridging moieties. The structure types discovered were previously known for vanadium due to V^V small ionic radius in addition to the high charge of the theoretical hexavanadate anion.¹⁷¹ These systems were originally derived from the Lindqvist structure,

$[M_6O_{19}]^{n-}$, by substitution of all twelve μ -bridging oxo ligands with monodentate alkoxo ligands. Previously these had only been synthesised by employing methoxo ligands. These clusters are unique and were of great interest due to their neutrality which was an unusual characteristic for such clusters to possess.¹⁷⁹

The solvothermal synthesis of the μ -alkoxo-hexa(oxovanadium) cluster $[V_6O_7(OR)_{12}]$ ($R = -CH_3, -C_2H_5$) represent a synthetic limitation in terms being self-assembly processes which are dissimilar to rational synthesis (Figure 21). Regulating reaction conditions, such as solvent, concentration, temperature, pressure, reaction time and others, allows control over the products it yields, however, this is often poor and seldom straightforward. Therefore, efforts were made to explore more successful methods by developing current procedures on. The synthesis of $[V_6O_7(OCH_3)_{12}]$ (**1**) was previously attempted¹⁶⁷ before an alternative route for the synthesis of (**1**) was realised via its singly reduced species. The latter is obtained in good yield and high purity by the solvothermal reaction of $VO(O^tBu)_3$ and tetrabutylammonium borohydride in methanol. Complex (**1**) is simply obtained via oxidation of $N(n-C_4H_9)_4[V_6O_7(OCH_3)_{12}]$ with iodine.³³

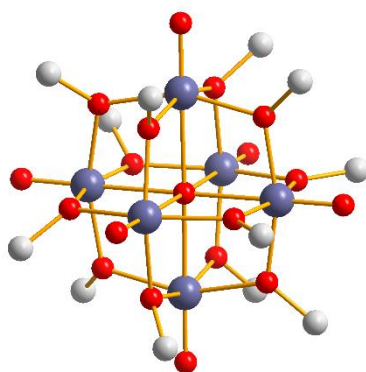


Figure 21. Polyhedral structural representation of the hexanuclear complex $[V_6O_7(OCH_3)_{12}]$ (**1**) and $[V_6O_7(OC_2H_5)_{12}]$ (**3**). The V^{IV}/V^V polyhedra in blue-grey, the O centres in red and C centres in grey. The hydrogen atoms and counter anions have been omitted for clarity.³³

The $[V_6O_7(OCH_3)_{12}]$ cluster has demonstrated great stability and rich ion chemistry, as well as exciting magnetic and electrochemical properties which indicates great potential in applications, such as catalysis and surface science. The vast array of mixed-valence states can be achieved by their fulfillment of the required symmetry and ability to accept up to 6 electrons without needing to participate in metal bonding. The IVCT is linked to the movement imposed on the μ -oxo centres by the ethyl groups' order-to-disorder transition. The species displaying both partial and full delocalisation of d-electrons, depends on the ratio of V^{IV}/V^V , the nature of the μ -alkoxo ligands and the collection temperature.³³

The results presented here are by no means conclusive for the Dodecatheon- and dodecaethoxo-oxo-hexa(oxovanadium) cluster series. However, the presented compounds in this intensely investigated field of research are unique systems comprising a novel, highly symmetrical hexanuclear framework, in which a large number of thermodynamically stable mixed-valence states can be realised. This provides promising potential in terms of the opportunities in utilising the numerous mixed-valence states. In more recent times, V^{IV} complexes have been actively investigated as potential candidates for molecular spin quantum bit operating at room temperatures.³³ Other vanadium-based complexes have also attracted special attention during the past decade due to their long decoherence times, both at cryogenic and room temperatures. The V^{IV} ion has an electron spin $S = 1/2$ and a nuclear spin $I = 7/2$ for stable isotope ^{51}V of nearly 100% natural abundance. These properties determine the intrinsically longer electron spin relaxation times compared to high-spin ($S > 1/2$) ions.¹⁷⁷ These characteristics are a prerequisite for use in data storage or nano spintronics technologies.¹⁸⁰ The magnetic measurements provide potential insight on electron-transfer mechanisms, such as ground-state delocalization and electron hopping, as well as the interaction of the unpaired d-electrons in such systems.³³

3.4 Chromium

Chromium cations, both individually and within clusters, display a variety of formal oxidation states, ranging from -IV to +VI. However, only those present in +II to +VI are accessible in water. Nevertheless, the most stable oxidation state is Cr^{III}, present in an array of stable inorganic complexes.¹⁸¹ The chemical and configurational stability of octahedral Cr^{III} led to their utilisation of the ions in the groundbreaking work of Alfred Werner.¹⁸²

During the twentieth century, specific properties were responsible for cobalt cluster reaction mechanism use in studies.¹⁸³ Prior research indicates that Keggin ions comprising of elements from across the periodic table are not always constructed from the most obvious units of the edge-sharing trimers. Instead, these are assembled from heterometal fragments composed of either the central tetrahedral metal and one or more octahedral metals. Alternatively a metal cation that stabilises the cluster on the outside, which is then connected to one or more octahedral metals. An interesting aspect explored in metal-oxo chemistry is open-shell transition metal clusters (i.e. Cr^{III}, Fe^{II/III}, Ni^{II}, Co^{II/III}, Mn^{II/III/IV}, Cu^{I/II}). However, these are not readily isolated as un-ligated metal-oxo clusters.¹⁸⁴

The discovery of SMMs has prompted substantial interest in paramagnetic cage structures. In the year 2000, the a novel dodecanuclear cluster was reported. This study was investigating the possibility of new synthetic routes to produce high nuclearity cage structures, leading to the discovery that heating smaller cages to high temperatures under an inert atmosphere creates larger cages, via oligomerisation.^{185,186} This dodecanuclear cluster was synthesised by the reaction between Cr(NO₃)₃·9H₂O and K(O₂CCHMe₂) in H₂O at ca. 80 °C, affording [Cr₃O(O₂CCHMe₂)₆(H₂O)₃](NO₃) (**1**). It was also found that upon heating the resulting product to 400 °C under a stream of nitrogen for 5 minutes produced a dark green solid, which when recrystallized in PrⁱOH-CH₂Cl₂ forms green crystals. The observed crude product displayed a cage with stoichiometry [Cr₁₂O₈(OH)₄(O₂CCHMe₂)₁₆(HO₂CCHMe₂)₄] (**2**) (Figure 22).¹⁸⁴

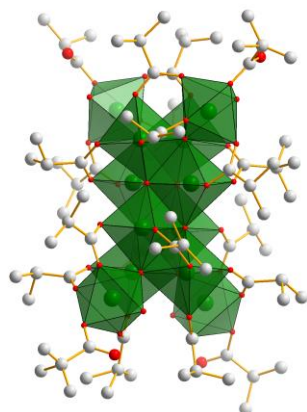


Figure 22. Polyhedral structural representation of the dodecanuclear complex $[\text{Cr}_{12}\text{O}_8(\text{OH})_4(\text{O}_2\text{CCHMe}_2)_{16}(\text{HO}_2\text{CCHMe}_2)_4]$ (**2**). The Cr^{III} polyhedra in green, the O centres in red and C centres in grey. The hydrogen atoms and counter anions have been omitted for clarity.¹⁸⁴

This structure consists of three face-sharing Cr_4O_4 heterocubanes; two terminal cubanes are capped by further chromium centres which are attached to the external μ_4 -oxides, assuming an approximate tetrahedral geometry. The cubane moiety at the centre of the structure is held together exclusively through four μ_4 -oxides. Subsequently, these four-coordinate oxygens do not have the expected tetrahedral geometry, but an arrangement commonly referred to as a 'saw-horse' geometry. This is due to the central Cr_8O_8 moiety being considered to be a fragment of the NaCl structure. When considering the various chromium sites present, it is possible to classify these into three categories in terms of the different groups attached to each metal. In the central cubane, each of the chromium sites are bound to four μ_4 -oxides and two oxygen donors from carboxylate bridges. Those surrounding the triple cubane are each bound to three μ_4 -oxides and three O-atoms from carboxylates. Finally, each of the sites capping the tricubane are bound to a μ_4 -oxide, as well as three oxygens from bridging carboxylates and two terminal groups.¹⁸⁴

A recent research interest includes polynuclear metal complexes with ring structures which have been intensively studied both structurally and spectroscopically. There is a growing attraction in

these systems is due to their high symmetry and aesthetic molecular frameworks, as well as their unique magnetic properties. The family of cyclic structures is continuously growing, including polymetal compounds such as $[\text{Fe}_{10}(\text{OCH}_3)_2\text{O}(\text{O}_2\text{CCH}_2\text{Cl})_{10}]^{187}$ and $[\text{Fe}_{18}(\text{OH})_6(\text{OCH}_3)_{24}(\text{O}_2\text{CCH}_3)_{12}(\text{XDK})_6]^{188}$. Compared to the analogous iron and manganese clusters, examples of structurally characterised chromium aggregates bridged by carboxylates ligands are very limited. In 1990, the cyclic octanuclear Cr^{III} structure, supported by fluoride and pivalate bridging ligands, was reported by Gerbeleu et al.¹⁸⁹ The neutral complex, with the formula $[\text{Cr}_8\text{F}_8(\text{O}_2\text{CCMe}_3)_{16}]$, comprises of eight chromium ions in an effectively planar arrangement. This cluster was synthesised via a reaction between CrF_3 and pivalic acid.¹⁹⁰

The weak antiferromagnetic interaction between the paramagnetic Cr^{III} ions has drawn significant attention to the complex. Although the results regarding magnetism were inconclusive, the theoretical modelling of the measured susceptibility data suggests that adjoining Cr^{3+} ions where $S = 3/2$ display fluctuating antiferromagnetic exchange interactions. This indicates that further research into both this cluster and those of a similar nature could lead to progression with Cr clusters in terms of their magnetic properties.¹⁹⁰

In prior studies, controlling hydrolysis has previously been described in terms of using of chelating organic ligands comprising of amino, carboxylato and frequently, alkoxo functionalities to obtain polymetal aggregates of both Fe^{III} and Al^{III} . Achieving this involved the use of bridging oxygen atoms derived from the solvent, which in this case was water, along with further oxygen bridges generally supplied by groups on the ligand.^{191,192} Despite oxide bridges being common in Fe^{III} cluster chemistry, hydroxide bridges often dominate Al^{III} complexation, therefore, there was interest in investigating if this chemistry was also common to Cr^{III} . Presently, there are very limited number of studies in the literature regarding larger hydroxo-bridged Cr^{III} aggregates, with known higher nuclearity complexes predominantly assuming acyclic or cubane-based arrangement where the hydroxo bridges are reinforced by carboxylate co-ligands.^{193,194} Previous speciation research suggests

that hydrolytic cluster formation similar to those of both Fe^{III} and Al^{III} should be possible. However, crystallisation of these species may prove difficult due to the Cr^{III} ion being fairly inert and the propensity to form the stable mononuclear octahedral complexes.¹⁸³

Dinuclear hydroxo-bridged complexes magnetic interactions have been comprehensively analyzed and conclusions indicate that the magnitude of the antiferromagnetic interaction is dependent upon the Cr-O(H) bond lengths. Nevertheless, a review published in 2005 reports on the successful synthesis and isolation of novel tetranuclear and hexanuclear hydroxo-bridged Cr^{III} species, stabilised by the organic ligands, hpdta⁵⁻. The synthesis of the two compounds varied slightly. The reaction pathway for compound **(1)**, (enH₂)[Cr₄(l-OH)₄(hpdta)₂].12H₂O (Figure 23), involved stirring H₅hpdta and 1,2-diaminoethane in water, as well as the inorganic salt, CrCl₃.6H₂O. The synthesis pathway for compound **2**, [Ba(OH₂)₅{Cr₄(l-OH)₄(hpdta)₂}.13H₂O, involved the reaction of H₅hpdta, CrCl₃.6H₂O BaCl₂.2H₂O and 1,2-diaminoethane in water while stirring, along with aqueous 1,2-diaminoethane. Both routes formed purple crystal of the two complexes.

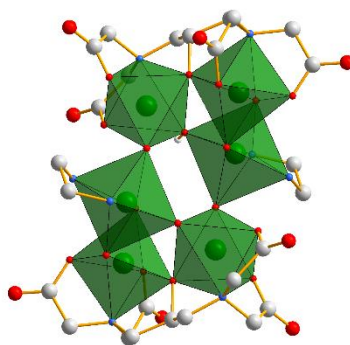


Figure 23. Polyhedral structural representation of the hexanuclear complex (enH₂)[Cr₄(l-OH)₄(hpdta)₂].12H₂O (**1**). The Cr^{III} polyhedra in green, the O centres in red, C centres in grey and N centres in blue. The hydrogen atoms and counter anions have been omitted for clarity.¹⁹⁵

Polymetallic clusters of chromium remain comparatively rare and small in nuclearity; the largest reported Cr^{III} clusters are constructed of only twelve metal ions. In comparison, Mn, Fe, Ni, Co and Cu clusters have occasionally comprised of more than eighty metal ions.^{48,196} Homometallic chromium chemistry is fascinating because all clusters contain bridging carboxylates and the majority have either cubes or wheel-based topologies. Many of the more successful synthetic routes involved heating the basic Cr carboxylates directly [Cr₃O(O₂CR)₆(H₂O)₃]⁺. On the other hand, others involved heating the Cr^{III} salt in the presence of a given carboxylic acid. For example, reacting CrF₃ and pivalic acid leads to a family of wheel-based clusters¹⁹⁷ as does the solvothermal heating of [Cr₃O(O₂CR)₆(H₂O)₃]⁺ in alcohol.¹⁹⁸

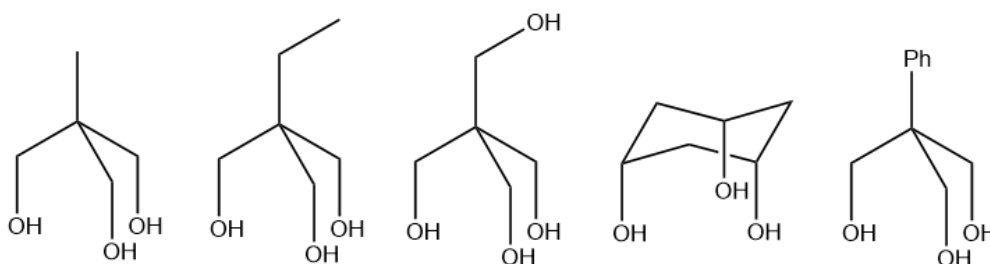


Figure 24. Schematic representation of the tripodal alcohol ligands used in the discussed synthesis of [Cr₂(H₂tmp)₂Cl₄]₂·2MeOH(1·2MeOH) (**1**), [Cr₈O₂(thme)₂(Hthme)₄Cl₆]₂·2MeOH(2·2MeOH) (**2**) and [Cr₈O₂(Hpeol)₂(H₂peol)₄Cl₆]₃·3MeOH(3·3MeOH) (**3**).¹⁹⁹

In 2006, the first attempts in synthesising three polymetallic Cr^{III} clusters were reported, including a novel dinuclear cluster and two octametallate clusters. The arrangement is centered around the decametallate ion, {M₁₀O₂₈}²⁶⁻ and contains no bridging carboxylate ligands. The dimeric complex [Cr₂(H₂tmp)₂Cl₄]₂·2MeOH (1·2MeOH) (**1**) is generated under reflux. An analogous reaction, but under solvothermal conditions produces the octametallate species [Cr₈O₂(thme)₂(Hthme)₄Cl₆]₂·2MeOH(2·2MeOH) (**2**) and [Cr₈O₂(Hpeol)₂(H₂peol)₄Cl₆]₃·3MeOH(3·3MeOH)

(3) (Figure 25). Similar synthetic routes were followed for both, employing the tripodal ligand 1,1,1-tris(hydroxymethyl)ethane (H₃thme) and its analogues (Figure 24).¹⁹⁶

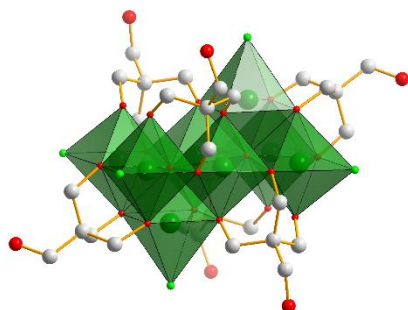


Figure 25. Polyhedral structural representation of the octanuclear complex [Cr₈O₂(thme)₂(Hthme)₄Cl₆]·2MeOH(2·2MeOH) (2) and [Cr₈O₂(Hpeol)₂(H₂peol)₄Cl₆]·3MeOH(3·3MeOH) (3). The Cr^{III} polyhedra in green, the O centres in red and C centres in grey. The hydrogen atoms and counter anions have been omitted for clarity.¹⁹⁹

The reactions between CrCl₂ and the tripodal ligands H₃thme, H₃ttmp, and H₄peol have produced new di- and octanuclear Cr^{III} clusters which may have been the first large series of Cr^{III} clusters to be synthesised and reported. Slight modifications to the reaction sequences and conditions used in this study may result in an array of diverse metal clusters displaying novel magnetic properties. There is promising evidence found in this study where magneto-structural correlations for [Cr₂(OR)₂]⁴⁺ and [Cr₂O₂]²⁺ complexes were discovered which may aid identification and characterisation of future polynuclear Cr^{III} clusters. For many years, Cr^{III} cluster formation has remained an elusive achievement due to its hydrolytic instability. In 2016, Nyman et al. presented an exceptional mechanism for synthesising and isolating a new mixed-metal chromium species, [Zn(H₂O)₃]ZnO₄Cr₁₂(OH)₂₄(H₂O)₁₂(NO₃)₈·xH₂O (δ-ZnCr₁₂) (Figure 26). The cationic cluster, [ZnO₄Al_{5.1}Cr_{6.9}(OH)₂₄(H₂O)₁₂Zn(H₂O)₃]⁸⁺ (Zn(CrAl)₁₂), is readily isolated in single-crystal form as

a nitrate salt. This cluster growth and crystallisation technique, using only monomer and dimer precursors to the Keggin-type ion, avoids the formation of complete metal-oxo clusters. It also allows for self-assembly and crystallisation to occur at the reaction solution surface by the evaporation of HNO₃-H₂O azeotrope, where excess nitrate was suppressing cluster formation prior to this.⁸⁴

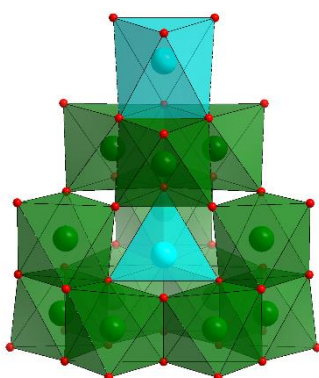


Figure 26. Polyhedral structural representation of the dodecanuclear complex $[\{\text{Zn}(\text{H}_2\text{O})_3\}\text{ZnO}_4\text{Cr}_{12}(\text{OH})_{24}(\text{H}_2\text{O})_{12}](\text{NO}_3)_8 \cdot x\text{H}_2\text{O}$ (**1**). The Cr^{III} polyhedra in green, the Zn centres in light blue, the O centres in red, C centres in grey and N centres in blue. The hydrogen atoms and counter anions have been omitted for clarity.²⁰⁰

The structure of (**1**) is comparable to the composition of the recently isolated Al/Cr cluster; however, it remains unknown if the assembly and isolation of this complex was promoted by Al³⁺ cations. The structure is constructed from heterometallic fragments stabilising the cluster from the outside. These fragments may be linked to one or more octahedral metal centres. Despite the structural similarities between this and other Keggin polycations, the synthesis is notably different. This particular metal complex was isolated via dehydration of a Cr/Zn nitrate solution, leaving a crude solid which was then re-crystallised. The central Zn ion facilitates the condensation reaction, regardless of pH, making it comparable to the role of Bi³⁺ in the Fe complex, despite the substantial variance in both radii and aqueous solubility between the two cations.⁸⁴

Overall, this synthetic route allows for the crystallisation and isolation of hydrolytically unstable clusters without the use of stabilising organic ligands. These metal-oxo complexes are useful in both mechanistic studies and applications. For example, they act as building blocks for both natural and synthetic metal-oxides,^{201,202} as well as functioning as catalysts^{203,204} and separating agents in energy applications.²⁰⁵ Only a limited number of stable metals oxo-hydroxo clusters have been successfully isolated without the use of supporting ligands, such as V^V, Nb^V, Ta^V and W^{VI}.^{85,206,86} However, these synthetic obstacles were overcome for this Cr^{III} complex. Firstly, using the oxidative dissolution of zinc to induce pH-driven hydrolysis and secondly, using metal nitrate concentrations 103 times higher than conventional syntheses, therefore, suppressing complex assembly. Lastly, this was achieved by utilising azeotropic evaporation of HNO₃-H₂O to drive assembly and crystallisation.⁸⁴ In order to advance the use of these discrete clusters in applications such as technology,^{92,93} medicine¹⁰⁵ and other vital applications, it is crucial to determine how the isolation of any transition metal-oxo clusters can be achieved without the use of ligands. This is an important area to explore as ligands could potentially be responsible for limiting a clusters chemistry.

3.5 Manganese

Research into manganese clusters is continually growing due to their exciting magnetic and electronic properties. This is a result of the multiple oxidation states available to create mixed-valence complexes and the accessible magnetic phenomena in these species. The Mn^{III} ion is particularly noteworthy in terms of molecular magnetism due to its high spin number ($S = 2$) and negative anisotropy parameter resulting from its Jahn–Teller distortion. This characteristic renders them a perfect candidate for SMM assembly.²⁰⁷ Over the years, numerous SMMs and their magnetic properties have been reported and studied,¹⁹ however, it is difficult to control both the magnetic exchange and the magnetic anisotropy of cluster molecules.

Early synthetic strategies for polynuclear SMMs comprising of 3d-transition metals involves combining a reagent containing the desired metal, often simple inorganic salts with primary organic ligands.²⁰⁸ This is a widely used synthetic route when preparing high-oxidation state manganese clusters. This pathway typically entails the comproportionation reaction of a Mn^{II}/Mn^{VII} ion source with a chelating or bridging ligand. Originally, this was the technique used in the synthesis of {Mn^{III}₈Mn^{IV}₄} complex (**1**),¹⁹ a molecule partially responsible for initiating the research of SMMs.

By modifying of the comproportionation process, this lead to the reductive aggregation route in manganese chemistry. This method differs by excluding an Mn^{II} source and using more than one solvent, therefore, meaning methanol also acts as both the reducing agent for Mn^{IV} and as a potential source of bridging MeO-groups.¹⁹ On the other hand, despite the other methods of synthesis proving successful, the spontaneous self-assembly approach is the long-term method used in the formation of high-valent manganese clusters, as with numerous other metal-oxo complexes. The ancillary oxygen and in this case, nitrogen donors are crucial in the formation and stabilisation of manganese-oxo clusters.²⁰⁹

As an alternative to oxo ligands, alkoxide ligands provide a powerful tool for assembling metal clusters,^{210,211,23} as demonstrated by recent work on alkoxoiron(III) complexes.²¹² Manganese chemistry with alkoxide ligands was a comparatively unexplored field in chemistry, therefore, the synthesis of Mn^{II} complexes, specifically [Mn₄(OMe)₄(L)₄(MeOH)₄] (L = dibenzoylmethane (dbm)) and [Mn₄(OEt)₄(dpm)₄(EtOH)₂],²³ with cuboidal [Mn₄(OR)₄]⁴⁺ cores, was relatively unusual. An unfortunate drawback to the use of alkoxide groups is their high sensitivity to oxidation when in contact with air, resulting from the hard-donor character of alkoxide ligands.²¹³

In 1998, the synthesis and characterisation of the high-spin heptanuclear alkoxo-manganese cluster, [Mn₇(OMe)₁₂(dbm)₆],CHCl₃,14MeOH, was reported, with a layered structure remarkably similar to that of a lithiophorite fragment (a manganese oxide mineral). The heptanuclear molecule discussed here was synthesised by dissolving MnCl₂ in anhydrous methanol and added dropwise to a

mixture of NaOMe and Hdbm in anhydrous methanol, with vigorous stirring. The precipitate was dissolved in chloroform followed by layering with anhydrous methanol to form cubic crystals. The structure consists of non-ionic centrosymmetric $[\text{Mn}_7(\text{OMe})_{12}(\text{dbm})_6]$ units, with an almost planar $\{\text{Mn}_6\}$ cluster core linked by μ_2 -OMe and μ_3 -OMe ligands. The remaining coordination sites are filled by the chelating dbm anions.²¹⁴ Employing alkoxide ligands is a useful method for high-nuclearity manganese cluster assembly in relation to the simultaneous aggregation and oxidation of Mn^{II} ions in forming $\text{Mn}^{\text{II/III}}$ polynuclear complexes.²¹⁵

The $\{\text{Mn}_{25}\}$ SMM complex reported in 2004 was the largest mixed-valent $\text{Mn}^{\text{II}}/\text{Mn}^{\text{III}}/\text{Mn}^{\text{IV}}$ cluster to date with an unusual five-layer structure, and at the time held the record ground-state spin for a molecular cluster of $S = 51/2$. The synthesis involved the reaction of $\text{MnCl}_2 \cdot 4\text{H}_2\text{O}$, pyridine-2,6-dimethanol and NaN_3 in a mixture of MeOH and MeCN, treated with NMe_4OH . The resulting solution slowly crystallised over time, forming the high nuclearity product, $[\text{Mn}_{25}\text{O}_{18}(\text{OH})_2(\text{N}_3)_{12}(\text{pdm})_6(\text{pdmH})_6](\text{Cl})_2 \cdot 12\text{MeCN}$ (Figure 27). The core structure of **(1)** comprises of five parallel layers, consisting of three different compositions with an ABCBA arrangement. The twelve μ_4 - O^{2-} , six μ_3 - O^{2-} , and two μ_3 -OH-ions hold the core together, in addition to the chelating and bridging ligands, $\text{pdm}^{2-}/\text{pdmH}^+$, and terminal and bridging N_3 -groups present.²¹⁶

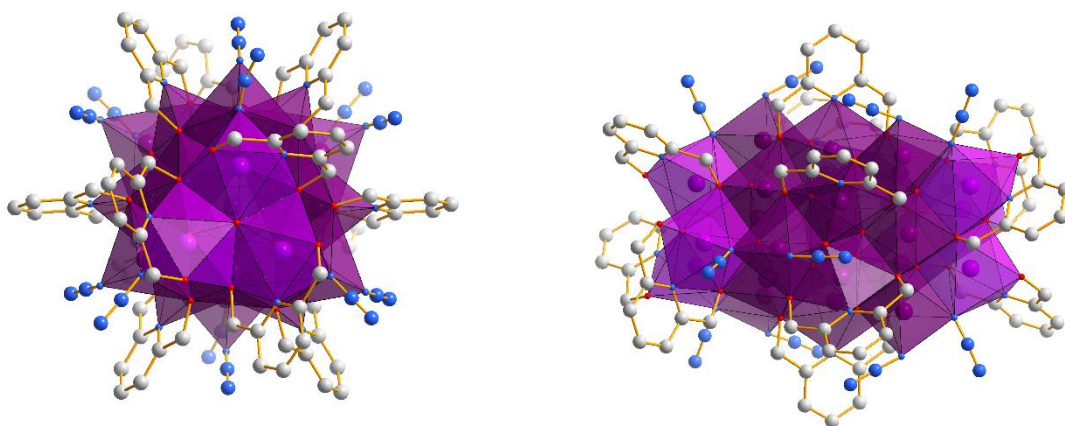


Figure 27. Polyhedral structural representation of the hexanuclear complex $[\text{Mn}_{25}\text{O}_{18}(\text{OH})_2(\text{N}_3)_{12}(\text{pdm})_6(\text{pdmH})_6](\text{Cl})_2 \cdot 12\text{MeCN}$ (**1**). The $\text{Mn}^{\text{II}}/\text{Mn}^{\text{III}}/\text{Mn}^{\text{IV}}$ polyhedra in purple, the O centres in red, C centres in grey and N centres in blue. The hydrogen atoms and counter anions have been omitted for clarity.²¹⁶

The first layer, labelled Layer A, forms a Mn^{III}_3 triangular unit with a capping 13-OH ions. Layer B has an Mn^{III}_6 triangular arrangement comprising of three corner-sharing Mn^{III}_3 triangles. Finally, Layer C has an Anderson-type structure observed in previous Mn complexes, consisting of a Mn^{III}_6 hexagon with a central Mn^{IV} ion. The individual layers are themselves held together and also connected to their neighboring layers by a mixture of oxide, alkoxide, and/or azide bridges. The outer shell of the complex is occupied by pdm^{2-} , pdmH^- , and terminal azide ligands, stabilizing the cluster as a whole. Furthermore, throughout the structure two types of Mn^{III} ions are present, the first observed in Layer B where almost all assume an octahedral geometry with JT axially elongated $\text{Mn}^{\text{III}}\text{-O}$ bonds. On the other hand, those present in Layer C are seven-coordinate, verging on a pentagonal bipyramidal geometry and also comprising of axially elongated $\text{Mn}^{\text{III}}\text{-O}$ bonds. The Mn_{25} cation lies on an inversion center and has a barrel-like cage structure.²¹⁶

The giant $\{\text{Mn}_{84}\}$ cluster reported in 2004, represented a crossover of the bottom-up and top-down approaches to nanoscale magnetic materials. A reaction between

$[\text{Mn}_{12}\text{O}_{12}(\text{O}_2\text{CMe})_{16}(\text{H}_2\text{O})_4] \cdot 4 \text{H}_2\text{O} \cdot 2 \text{MeCO}_2\text{H}$ (**2**) and $(\text{N}^t\text{Bu}_4)(\text{MnO}_4)$ in MeOH with a small quantity of acetic acid, followed by filtration and layering of the filtrate with chloroform. This produced the compound $[\text{Mn}_{84}\text{O}_{72}(\text{O}_2\text{CMe})_{78}(\text{OMe})_{24}(\text{MeOH})_{12}(\text{H}_2\text{O})_{42}(\text{OH})_6] \cdot x \text{H}_2\text{O} \cdot y \text{CHCl}_3$ (**1**·*x* H₂O·*y* CHCl₃). This torus structure crystallizes as nanotubular stacks.²¹⁷

Recent research trends in molecular magnetism primarily involve efforts in three materials categories: multifunctional magnetic materials, nanostructured magnetic materials and molecular nanomagnets.²¹⁸ Continuous development of molecular magnets has facilitated the precise adjustment and modification of a clusters magnetic properties by introducing or altering established coordination chemistry procedures. Moreover, further possibilities include the combination of magnetic properties with other mechanical, electrical and/or optical properties.^{219,220}

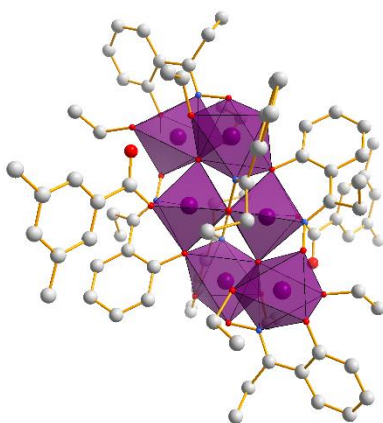


Figure 28. Polyhedral structural representation of the hexanuclear complex $[\text{Mn}^{\text{III}}_6\text{O}_2(\text{sao})_6(\text{O}_2\text{CPh})_2(\text{EtOH})_4]$. The Mn^{III} polyhedra in purple, the O centres in red and C centres in grey. The hydrogen atoms and counter anions have been omitted for clarity.²²¹

The report published in 2007 illustrates the purposeful structural deformation of the hexametallc complex, $[\text{Mn}^{\text{III}}_6\text{O}_2(\text{sao})_6(\text{O}_2\text{CPh})_2(\text{EtOH})_4]$ (saoH_2 = salicylaldehyde oxime or 2-hydroxybenzaldehyde oxime core) (Figure 28). The modifications to the overall complex, including

changing from a bridging to a monodentate ligand to a carboxylate. This alters the prevailing antiferromagnetic exchange interactions between metal centres to ferromagnetic exchange between the two antiferromagnetically coupled $\{\text{Mn}^{\text{III}}_3\}$ triangles present in this cluster. This is recognized by a $S = 4$ spin ground state.²²² Previously, the saO²-bridging ligands were deliberately substituted for their bulkier derivative Et-sao₂-(Et-saoH₂)₂-hydroxyphenylpropanone oxime), resulting in the analogous species $[\text{Mn}^{\text{III}}_6\text{O}_2(\text{Et-sao})_6(\text{O}_2\text{CPh})_2(\text{EtOH})_6]$. Here, the substantial structural alteration occurs to the core of the complex subsequently instigating severe twisting of the Mn-N-O-Mn moieties.²²¹

In summary, this study highlighted that the deliberate structural distortion of the $\{\text{Mn}_6\}$ molecule alters the dominant magnetic exchange from antiferromagnetic to ferromagnetic and therefore, changing the molecules spin ground state to $S = 12$. The relaxation studies performed on both the powder and crystal form revealed the clusters SMM behaviour with a record value of the effective energy barrier to magnetization reversal (U_{eff}). This was also the first to break the $\{\text{Mn}_{12}\}$ series record. These promising results indicate that smart and targeted structural distortion is a potentially powerful new method in molecular design, for example, in achieving significantly higher blocking temperatures of metal-oxo clusters generally.²²¹

A breakthrough discovery was made in 2011 when a novel Keggin-based POM-type structure was synthesised and isolated, comprising exclusively of $\text{Mn}^{\text{III}}/\text{Mn}^{\text{IV}}$ ions together with organic capping ligands present in the outer coordination shell of the complex. This cluster is synthesised via a one-pot reaction of $\text{Mn}(\text{NO}_3)_2 \cdot 6\text{H}_2\text{O}$ with 2,6-bis[N-(2-hydroxyethyl)iminomethyl]-4-methylphenol (H_3bemp) in methanol, yielding a tridecanuclear cluster with the formula $[\text{Mn}^{\text{III}}_{12}\text{Mn}^{\text{IV}}\text{O}_6(\text{OH})_2(\text{OMe})_4(\text{bemp})_6](\text{NO}_3)_4 \cdot 10\text{MeOH} \cdot 6\text{H}_2\text{O} (1(\text{NO}_3)_4)$ (Figure 29). Exchange of counterions was found to be possible, substituting the nitrate ion with hexafluorophosphate. The interesting magnetic properties and redox behaviour displayed by the three mixed-valence $\{\text{Mn}_{13}\}$ Keggin cluster was examined and reported.⁸⁷

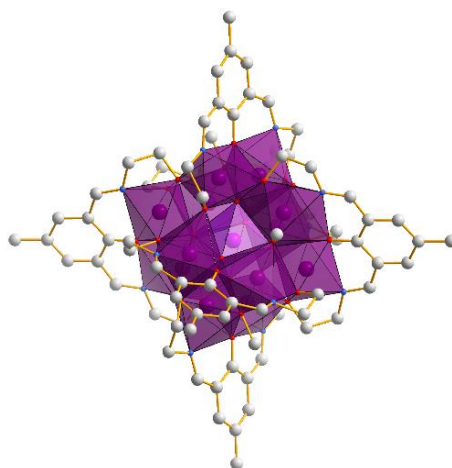


Figure 29. Polyhedral structural representation of the tridecanuclear complex $[\text{Mn}^{\text{III}}_{12}\text{Mn}^{\text{IV}}\text{O}_6(\text{OH})_2(\text{OMe})_4(\text{bemp})_6](\text{NO}_3)_4 \cdot 10\text{MeOH} \cdot 6\text{H}_2\text{O}$ ($1(\text{NO}_3)_4$). The $\text{Mn}^{\text{III}}/\text{Mn}^{\text{IV}}$ polyhedra in purple, the O centres in red and C centres in grey. The hydrogen atoms and counter anions have been omitted for clarity.⁸⁷

The distorted α -Keggin-type structure comprises of surfaces composed of non-basic terminal M=O bonds, as well as alkoxo- and phenoxo- bridging ligands. The core consists of three layers, the first being a heptanuclear disc comprising of a $\{\text{Mn}^{\text{III}}_6\}$ hexagonal unit comprising of both hydroxo and methoxo ligands displaying Jahn–Teller compression with a central templating Mn^{IV} ion. This forms oxo bridges to all twelve Mn^{III} centres and the remaining two coordination sites are occupied by an oxo and a phenoxo group. The other two identical $\{\text{Mn}^{\text{III}}_3\}$ triangular caps lie flat above and below the disc. The central Mn^{IV} assumes an octahedral geometry, coordinating to six μ_4 -oxide ions, each linking the Mn^{IV} ion to two Mn^{III} ions from the hexagonal ring. Two hydroxide and four methoxide anions bridge the seven-coordinate Mn^{III} unit. The outside of the complex is decorated with six 2,6-bis[*N*-(2-hydroxyethyl)iminomethyl]-4-methylphenol (bemp^{3-}) ligands, each coordinating four Mn^{III} ions. Moreover, all Mn^{III} centres in the trinuclear capping units all display Jahn–Teller elongation along the plane of the triangle.⁸⁷

The family of mixed-valence $\{\text{Mn}_{13}\}$ Keggin-based clusters synthesised displayed switchable redox behaviour without changing the overall structural integrity. Three oxidation states of the cluster were successfully isolated, with all clusters exhibiting similar SMM behaviour. This is a first regarding homometallic Keggin-based complexes. In terms of research concerning exclusive late first-row transition metal POM-based clusters, the investigation carried out above provides a starting point for potential future work in developing similar metal-oxo clusters with other late transition metals. This could lead to the development of unique clusters which these display analogous properties. One example includes substituting other first-row transition metals such as Fe and Co ions into this type of reaction and there is even the possibility of using mixtures of different metals.⁸⁷

From synthetic studies previously conducted, it has been realised that manganese in the 3^+ and 4^+ oxidation states in polynuclear clusters are primarily stabilised with bridging oxide (O^{2-}) groups. Organic capping ligands which decorate the outside of the complex and the presence of suitable chelating ligands play a crucial role in the formation of stable clusters with varying nuclearity as this process is usually determined by thermodynamic stability of the final product.²²³ The interest is also due to its ability to form mixed-valence complexes which lead to useful magnetic properties and redox behaviour. The use of alcohol-containing chelates has been a successful method, beginning with the deprotonation of the alcohol to provide bridging alkoxide groups which promote the growth of high nuclearity products.^{224,225}

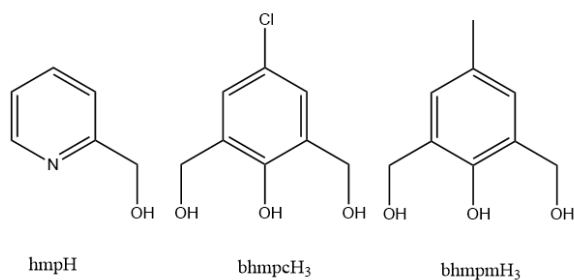


Figure 30. Schematic representation of the 2-(hydroxymethyl) pyridine (hmpH), 2,6-bis(hydroxymethyl)phenol (bhmpH₃) and 2,6-bis(hydroxymethyl)-4-chlorophenol (bhmcph₃) ligands employed in the synthesis of [Mn^{II}₂Mn^{III}₂(bhmcph₃)₂(hmp)₄Cl₂(MeOH)₂] (**1**).²²⁶

While exploring ligand possibilities to successfully yield polynuclear 3d-metal clusters with large spin values, 2-(hydroxymethyl)pyridine (hmpH) and 2,6-bis(hydroxymethyl)phenol (bhmpH₃), including the derivative, 2,6-bis(hydroxymethyl)-4-chlorophenol (bhmcph₃) (Figure 30). This has illustrated their versatility as both chelating and bridging groups²¹⁵ and in their SMM behaviour.^{227,228} Reacting with Mn^{II} salt, MnCl₂·4H₂O, with both hmpH and bhmcph₃ resulted in a new mixed-valence tetranuclear manganese complex, [Mn^{II}₂Mn^{III}₂(bhmcph₃)₂(hmp)₄Cl₂(MeOH)₂] (**1**) (Figure 31) being obtained. The core contains a mixed-valence [Mn^{II}₂Mn^{III}₂O₆] unit, comprising of both Mn^{II} and Mn^{III} ions, where the central metal ions are assembled in a double-cuboidal arrangement. The central six-coordinate Mn^{III} ion bonded to one nitrogen atom from a hmp⁻ ligand as well as five oxygen atoms from a bhmcph₃²⁻ and three from the hmp⁻ ligands. Meanwhile, the Mn^{II} ions, which are also six-coordinate and assume an octahedral geometry, are bonded to one oxygen atom from a methanol molecule as well as nitrogen and oxygen atoms from the hmp⁻ and bhmcph₃²⁻ ligands.²²⁹

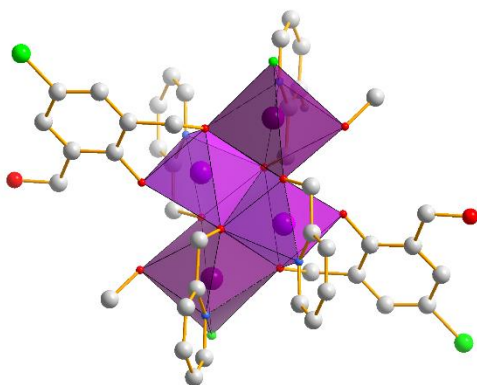


Figure 31. Polyhedral structural representation of the hexanuclear complex $[\text{Mn}_2^{\text{II}}\text{Mn}_2^{\text{III}}(\text{bhmcpH})_2(\text{hmp})_4\text{Cl}_2(\text{MeOH})_2]$ (**1**). The $\text{Mn}^{\text{II}}/\text{Mn}^{\text{III}}$ polyhedra in light/dark purple, the O centres in red and C centres in grey. The hydrogen atoms and counter anions have been omitted for clarity.²²⁶

This study indicated that this mixed-valence tetranuclear manganese cluster displays ferromagnetic interactions between the Mn^{II} and Mn^{III} ions present as demonstrated by the temperature dependence of the magnetic susceptibilities. With research into the magnetic and electronic properties of manganese clusters ever increasing, this study suggests promising future potential for clusters displaying the desirable magnetic characteristics that enable them to function as SMMs. It also illustrates that the use of alcohol containing chelates could be a successful strategy in synthesising and isolating future complexes because of their ability to form alkoxide ligands on deprotonation which make excellent bridging moieties. These could be employed in clusters comprising of manganese, as well as other transition metals in order to hopefully afford high nuclearity products. The ligands illustrated in Figure 29 have all demonstrated their versatility as both chelating and bridging ligands in successfully yielding polynuclear 3d-clusters with large S values and SMM characteristics.

In 2020, an octanuclear manganese complex, $[\text{Mn}^{\text{III}}_8(\mu_4\text{-O})_4(\text{L})_4(\text{OME})_4(\text{OAc})_2(\text{OCH}_2\text{CH}_2\text{NH}_3)_4]$ (**1**) ($\text{H}_2\text{L} = 3\text{-(dimethoxymethyl)-2-hydroxybenzoic acid}$) (Figure 32) was synthesized via the reaction of $\text{Mn}(\text{OAc})_2 \cdot 4\text{H}_2\text{O}$ with $\text{H}_2\text{L}'$ ($\text{H}_2\text{L}' = 3\text{-formylsalicylic acid}$), 2-aminoethanol and triethylamine in methanol followed by recrystallisation from acetonitrile. This example was the first case where an octanuclear Mn^{III} complex has a maximum spin ground state of $S = 16$. The cluster comprises a $[\text{Mn}^{\text{III}}_8(\mu_4\text{-O})_4(\mu_2\text{-O})_8]$ core considered to be a face-shared defective pentacubane, appearing as extended cubane structure. The core consists of eight Mn ions bridged by four $\mu_4\text{-O}$ as a result of oxide ions, another four $\mu_2\text{-O}$ atoms derived from the 2-aminoethanol moiety and the final four derived from the methoxide anion. Jahn–Teller distortion is present in four of the central Mn^{III} ions residing in the Mn_4O_4 cubane core coordination sphere, which can be further categorised into central and peripheral ions. There are different sources of oxygen atoms in the complex, including the 2-aminoethanol moiety, the methoxide anion and the acetate anion. The peripheral ions inhabit the peripheral sites coordination sphere with the sources of oxygen atoms including the 2-aminoethanol moiety, the methoxide anion and the acetate anion.²²²

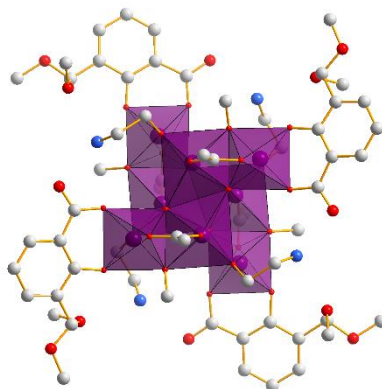


Figure 32. Polyhedral structural representation of the octanuclear complex $[\text{Mn}^{\text{III}}_8(\mu_4\text{-O})_4(\text{L})_4(\text{OME})_4(\text{OAc})_2(\text{OCH}_2\text{CH}_2\text{NH}_3)_4]$ (**1**). The Mn^{III} polyhedra in purple, the O centres in red, C centres in grey and N centres in blue. The hydrogen atoms have been omitted for clarity.²²²

This study supports the fact that cubane structure and stacked triangles make excellent magnetic cores in polynuclear complexes with high spin ground states. A tetranuclear cubane core comprising of four metal ions bridged by oxo groups is a recognised structural motif when designing multinuclear magnetic clusters. Complexes containing such cubane cores typically display ferromagnetic interactions as a result of the unintentional magnetic orbital orthogonality. This is a promising for future manganese clusters with a cubane or stacked triangle core and indicates that this could an area for further research. The cubane core is validated by the magnetic analysis conducted in the current study, illustrating the displayed SMM behaviour of this complex because of the presence of effective ferromagnetic interactions. These cores tend to display ferromagnetic interactions as a result of the accidental orthogonality of the magnetic orbitals.²³⁰ Also, the perpendicular alignment of the Jahn–Teller axis through μ -O bridges present in this cluster was an indication that ferromagnetic interactions were expected.²³¹

Chemical research has been heavily concentrated on the design and synthesis of novel polynuclear manganese and iron clusters, driven by their importance in molecular magnetism, particularly those coordinated via oxygen and nitrogen. There is a primary focus on exposing high nuclearity assemblies with the appropriate topology as both metal complexes are recognised for exhibiting large ground spin (S) values and large D values. This, therefore, indicates the potential to function as SMMs.^{47,232} Ideal candidates for advancement of molecular magnetic materials include species with a d^4 ground state and a negative magnetic anisotropy, such as Mn^{III} . Another potential building block in order to achieve a large spin ground state the high-spin d^5 Fe^{III} ion with an $S = 5/2$ ground state. However, antiferromagnetically coupled clusters are usually formed.^{233,234} Nevertheless, due to the manifestation of the spin frustration effects, large ground spin states have been achieved in specific Fe_x topologies. These have displayed slow magnetic relaxation and magnetic hysteresis.^{235,236} Unfortunately, practical application of these nanomagnets has been prevented because major obstacle of the low blocking temperatures where the molecule performs as a nanomagnet. During the development of new nanomagnets, a key objective is to create ligands that

help to obtain to novel clusters, therefore, aid rationalising the geometry, nuclearity, and topologies of Mn and Fe clusters. Higher blocking temperatures could be achieved via expanding the range of SMMs varieties and in turn allow their utilization in useful applications.²³⁷

3.6 Iron

Over the years, a large number of Fe^{III}-oxo clusters with various nuclearities have been synthesised and continue to attract substantial research interest due to their potential in various biological and molecular magnetism applications. The formation of high nuclearity Fe^{III}/O²⁻ clusters is achieved via a high charge-to-size ratio of Fe^{III}, which facilitates the creation of O²⁻ bridges by promoting the deprotonation of H₂O.^{238,239,240} This can typically generate strong antiferromagnetic Fe^{III}₂ exchange coupling, however, for particular iron topologies this may create spin frustration effects due to competing exchange interactions. As a result, it is possible to attain high-spin ground states given the negative zero-field splitting present, therefore, induce a satisfactory magnetic anisotropy.^{241,242,243} Consequently, there is a growing desire to establish new synthetic routes leading to the formation of novel Fe^{III}/O clusters. Previously, using a plethora of chelating and bridging ligands has resulted in numerous Fe^{III}-oxo core topologies and has been successful in achieving nuclearities up to Fe₂₂.^{244,245}

In the field of molecular metal oxides, the most abundant assembly is the Keggin structure, comprising of a central tetrahedral {XO₄} unit surrounded by four trimeric edges sharing octahedral {M₃O₆(μ-O)₃} motifs.²⁴⁶ The difficulty in obtaining low valent Keggin structures is due to their inability to form stable terminal oxo bonds and μ-oxo bridges as a result of the excessive negative charge necessary has resulted in limited success in synthesising useful clusters. This archetypal arrangement is recognised in numerous synthetic and natural materials including polyoxocations,²⁴⁷ polyoxometalates,²⁴⁸ ferrihydrite and magnetite.²⁴⁹ A common example, as mentioned above, is the

{Fe₁₃} cluster consisting of Fe^{III} ions in tetrahedral and octahedral positions, which has been isolated from both organic and aqueous media.

The synthesis of Bi₆[FeO₄Fe₁₂O₁₂(OH)₁₂(O₂C(CCl₃)₁₂)·[O₂C(CCl₃)]·14H₂O involved a reaction between a mixture of Bi(NO₃)₃·5H₂O and Fe(NO₃)₃·9H₂O suspended in water while heated. This was then added to a boiling solution of trichloroacetic acid and NaHCO₃ in of water, obtaining red needles by slow evaporation. The product was obtained from water²⁵⁰ by utilising the Bi³⁺ cations which function as a templating agent for the whole structure and assist with stabilizing the excess negative charge. A similar technique was used to acquire the TFA analogue; Fe(NO₃)₃·9H₂O was added to water, heated and added to Bi(NO₃)₃·5H₂O before the mixture was boiled down. This was added to water containing trifluoroacetic acid and sodium bicarbonate with stirring, and red needle shaped crystals were formed by slow evaporation.

Lippard et al.²⁴⁶ reported the first late-transition-metal Fe^{III} Keggin ion with an open-shell electronic structure, [Fe₁₃O₄F₂₄(OMe)₁₂]⁵⁻. The structure consists of 13 high-spin Fe^{III} atoms arranged to create an ideal α-Keggin structure with 12 surrounding iron atoms coordinated to terminal fluoride ligands and a central tetrahedral {FeO₄} core. Charge neutrality requires an overall charge of 4⁻, therefore, a 4⁺ oxidation state for the central iron atom; this high valent Fe^{IV} atom is unlikely in this cluster. The overall charge of 5⁻ thus established requires an all ferric system, including the central iron atom. Fe^{II} ions are poor π-acceptors and do not form M=O bonds, therefore, are not found in the usual standard POM structures, however, in more recent times been found to form Keggin-based structures. In this case, water ligands can fill the terminal positions on the surface that are normally occupied by oxo groups in POMs.²⁴⁶

In 2015, the {Fe₁₃} cluster is a Keggin-based complex obtained by Sadeghi et al. is a metal-oxo structural motif in both natural and synthetic materials.²⁵¹ Even before the proposed structure of ferrihydrite, an iron Keggin cluster was presumed to be synthetically attainable—analogue to the Al₁₃-Keggin cluster [AlO₄Al₁₂(OH)₂₄(H₂O)₁₂]⁷⁺, which was first crystallized and structurally characterized

over 50 years ago.²⁵² The synthesis of the {Fe₁₃} cluster in water involves the reaction of Fe(NO₃)₃·9H₂O and Bi(NO₃)₃·5H₂O nitrate with trichloroacetic acid and sodium bicarbonate (base). When dissolved in water, these produce a solution of pH ~ 1.4. Upon heating, the crude product precipitates which is then dissolved in tetrahydrofuran (THF), yielding crystals of Bi₆[FeO₄Fe₁₂O₁₂(OH)₁₂(O₂C(CCl₃)₁₂)]·[O₂C(CCl₃)]₁₂·14H₂O (Bi₆Fe₁₃L₁₂) (Figure 33). This is a very highly charged polyoxoanion, therefore, highly charged Bi³⁺ counter cations and trichloroacetate (TCA) co-ion are required to assist charge-stabilization and crystallization of the discrete {Fe₁₃} Keggin ion from water. TCA also acts as the ligand cap for each octahedral iron.²⁰²

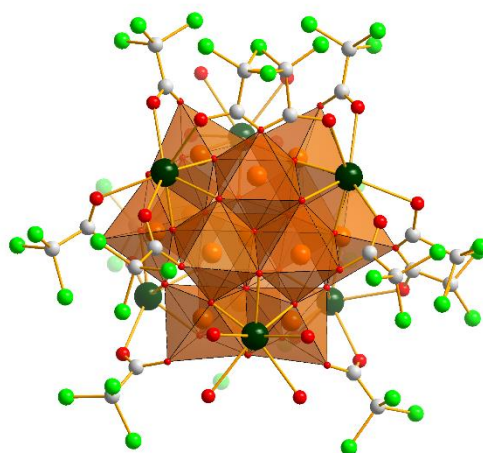


Figure 33. Polyhedral structural representation of the tridecanuclear complex Bi₆[FeO₄Fe₁₂O₁₂(OH)₁₂(O₂C(CCl₃)₁₂)]·[O₂C(CCl₃)]₁₂·14H₂O (**1**). The Fe^{III} polyhedra in orange, the O centres in red, C centres in grey, Cl centres in bright green and Bi in dark green. The hydrogen atoms and counter anions have been omitted for clarity.²⁰²

The {Fe₁₃} framework comprises of both bonded and fused iron-oxyhydroxide Keggin units where all 13 Fe ions and all six Bi ions are all trivalent. The core of (**1**) is an α -Keggin isomer comprising of twelve Fe³⁺ ions assuming an octahedral geometry and one central Fe³⁺ ions assuming a tetrahedral

geometry. The four octahedral triads are connected via corner-sharing, where the ligands present between the octahedra are oxo groups. However, the bridging ligands of the edge-sharing octahedra are hydroxyl groups.

The -17 charge present on this cluster signified the highest charge-density to have ever been observed for Keggin ions, including both polyoxocations or polyoxoanions. The most closely related species reported was the $[\text{FeO}_4\text{Fe}_{12}\text{F}_{24}(\text{OCH}_3)_{12}]^{5-}$ complex, however, the reaction was carried out in anhydrous conditions and the surface is entirely passivated with non-aqua ligands.²⁰² The presence of heavy chlorides indicates that the role of TCA is not necessarily to stabilize Fe_{13} but perhaps to aid in crystallization by providing suitable packing in lattice. Nevertheless, these can be easily displaced and substituted with other groups, as demonstrated by the use of THF in a previous example. The synthetic procedure used in synthesising $\{\text{Fe}_{13}\}$ cluster provides a long awaited link between iron monomers and ferrihydrite nanoparticles. This will hopefully provide a deeper understanding of this process in order to utilise techniques in other transition metal oxo-clusters.

Prior research has demonstrated that the synthesis of large Fe^{III} oxide species with analogous structural diversity to POMs is possible, however, the terminal oxo groups are replaced by mono/multidentate ligands. The largest POMs are typically composed of diamagnetic metal ions present in high oxidation states and often contain similar metal oxide cores to clusters constructed from high spin paramagnetic Fe^{III} ions. For example, prominent Fe^{III} clusters which most strongly resemble POM structures are the previously reported alpha-Keggin $\{\text{Fe}_{13}\}$ and the three-Keggin $\{\text{Fe}_{17}\}$ complexes, the latter surrounded by four additional metal capping ions. Moreover, the $\{\text{Fe}^{\text{III}}_{30}\}$ icosahedron has been heavily investigated, as this further illustrates that larger heterometallic oxide clusters comprising of late transition metals including paramagnetic iron is feasible. The successful synthesis of these species will offer a significant contribution to molecular magnetism, where there are few clusters with nuclearities higher than that of 20. This will also be significant in POM chemistry where it is possible for a larger order of magnitude to be achieved. The myriad of potentially

fascinating physical properties available from such species could theoretically minimise/reduce the gap between these two areas of chemistry.

An excellent example is the $\{\text{Fe}_{17}\}$ complex as this indicates a potentially successful synthesis route in creating such interesting species. Simply, anhydrous FeX_3 ($\text{X}=\text{Cl}, \text{Br}$) is dissolved in wet pyridine or an equivalent liquid base. The wet pyridine, seemingly satisfies five or more simultaneous functions: the solvent, the base, the source of water, the mono-dentate ligand encasing the metal oxide core, and the source of the charge balancing cation. The bulky organic cation is added in order to prevent rapid aggregation of molecules into forming smaller clusters with considerably more stable topologies and instead assist with separating the smaller building blocks, therefore, assisting the self-assembly of the larger nuclearity complex. The dissolution of anhydrous iron bromide in a mixture of pyridine and acetonitrile, in the presence of an organic amine, results in the formation of an $\{\text{Fe}_{34}\}$ metal oxo cluster. This is structurally characterised by alternate layers of tetrahedral and octahedral Fe^{III} ions connected by oxide and hydroxide ions. The outer shell of the complex is capped by a combination of pyridine molecules and bromide ions. In addition, the much studied $[\text{Fe}^{\text{III}}_{30}]$ icosidodecahedron,⁶ demonstrates that very large (heterometallic) molecular metal oxides containing paramagnetic metal ions can: (a) be synthesized, (b) retain POM-like architectures, and (c) possess fascinating physical properties—the high symmetry icosidodecahedron possessing geometric spin frustration.²⁵³

In 2019, the synthesis, structure and magnetic behaviour of $[\text{Fe}^{\text{III}}_{34}(\mu_4\text{-O})_4(\mu_3\text{-O})_{34}(\mu_2\text{-OH})_{12}\text{Br}_{12}(\text{py})_{18}]\text{Br}_2$ (**1**) (Figure 34) cluster was discussed. This cluster is formulated via an approach involving a small modification, such as the addition of either hexamethylenetetramine (HMTA) or morpholine, in the preparation of $[\text{Fe}_{17}]$. The metallic skeleton comprises of a $[\text{Fe}^{\text{III}}_4]$ tetrahedron encapsulated within a $[\text{Fe}^{\text{III}}_{18}]$ truncated tetrahedron, with the large faces capped by $[\text{Fe}^{\text{III}}_3]$ triangles. This is characterised by alternate layers of tetrahedral and octahedral Fe^{III} ions linked by oxide and hydroxide anions. The sixteen metal ions in the inner tetrahedron and outer triangles are all

tetrahedral and the eighteen Fe ions in the truncated tetrahedron are all octahedral. The presence of tetrahedral–octahedral–tetrahedral shells of metal ions is as found in the [Fe₁₃] and [Fe₁₇] complexes. The inner tetrahedron is connected to the [Fe^{III}₁₈] truncated tetrahedron via four μ_4 -O and six μ_3 -O ions. Each face-capping oxo-centred [Fe₃] triangle is connected to the [Fe^{III}₁₈] truncated tetrahedron via six μ_3 -O²⁻ ions. The remaining twelve μ_2 -OH⁻ ions link the metal ions situated on the triangular faces on the truncated tetrahedron.²⁵³

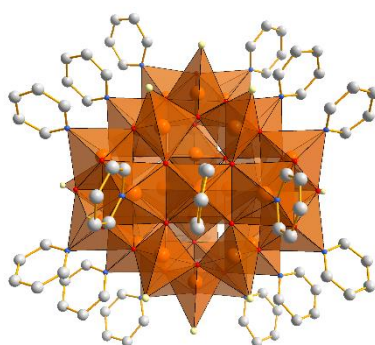


Figure 34. Polyhedral structural representation of the polynuclear complex [Fe^{III}₃₄(μ_4 -O)₄(μ_3 -O)₃₄(μ_2 -OH)₁₂Br₁₂(py)₁₈]Br₂. The Fe^{III} polyhedra in orange, the O centres in red, C centres in grey and N centres in blue. The hydrogen atoms and counter anions have been omitted for clarity.²⁵³

Magnetic measurements reveal relatively strong, competing antiferromagnetic exchange interactions between the Fe^{III} ions, with DFT calculations suggesting a direct correlation between the number of orbital interactions and the magnitude of the antiferromagnetic exchange. The simplicity of the synthetic procedure as well as the structural similarity of {Fe₃₄} to bulk iron oxides, such as magnetite and maghemite, suggests that a diverse family of novel Fe^{III} molecular metal oxide structures is a realistic future target. This, in turn, indicates an exciting route to the bottom-up formation of molecular metal oxide “nanoparticles” with a vast array of potential applications.²⁵³

Many of the clusters discussed here and in other studies usually employ two ligand types. For example, common instances include carboxylates and a chelate, however, the use of more than two has had limited exploration. Consequently, in the hope of discovering new Fe^{III}-oxo complexes, an investigation into combining carboxylates with two distinct chelates was carried out. In order to synthesise high-nuclearity Fe^{III} clusters, often a long-established synthetic procedure is employed as described here. This involves the reaction of [Fe₃O(O₂CR)₆L₃]⁺ (L = H₂O or similar) salts with possible chelating ligands. The metal salt core, [Fe₃O]⁷⁺, enables the preparation of higher nuclearity species. On the other hand, the chelating ligands facilitate both the growth of non-polymeric products and encourage the formation of valuable high nuclearity species. This is particularly true regarding alkoxide-containing chelates due to their exceptional bridging ability.

In this 2020 report, recent results communicating the syntheses, structures and magnetic properties of three new Fe^{III} oxo clusters are illustrated using the ligands picolinic acid (picH) and triethanolamine (teaH₃). The complexes [Fe₆O₂(OH)₂(O₂CR)₄(pic)₄(teaH)₂] (R = Me (**1**), Ph (**2**)) and [Fe₅O₂(O₂CBu^t)₄(pic)₃(teaH)₂] (**3**) (Figure 35) were obtained from the reaction of [Fe₃O(O₂CR)₆(H₂O)₃](NO₃) (R = Me, Ph, Bu^t) with picH and teaH₃ in a 1:2:1 ratio in MeCN. All metal centres are Fe^{III} with near-octahedral geometry.[63] When considering the structure of compound (**1**), the core consists of a planar [Fe₄(μ₃-O²⁻)₂]⁸⁺ unit on either side of which is attached to an [Fe(μ-OH)(μ-OR)₂] unit in a tripodal binding sense. Peripheral ligation is provided by two N,O,O-chelating teaH²⁻ groups also bridging to the butterfly unit, with the protonated alcohol arm unbound. In addition are four acetate groups ligated in their common *syn,syn* μ-bridging mode, as well as four N,O-chelating pic⁻ groups.

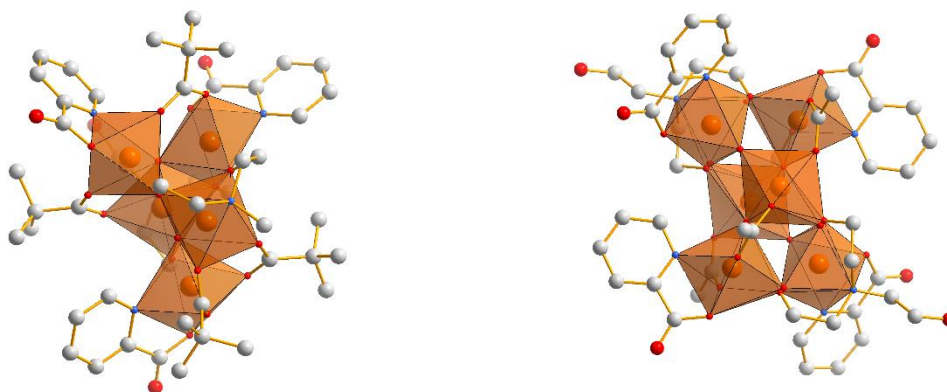


Figure 35. Polyhedral structural representation of the hexanuclear complex $[\text{Fe}_6\text{O}_2(\text{OH})_2(\text{O}_2\text{CR})_4(\text{pic})_4(\text{teaH})_2]$ ($\text{R} = \text{Me}$ (**1**), Ph (**2**)) and $[\text{Fe}_5\text{O}_2(\text{O}_2\text{CBu}^t)_4(\text{pic})_3(\text{teaH})_2]$ (**3**). The Fe^{III} polyhedra in orange, the O centres in red, C centres in grey and N centres in blue. The hydrogen atoms and counter anions have been omitted for clarity.²⁵⁴

Lacunary POM structures are widely recognized as a large division of multidentate inorganic ligands due to their exposed oxo ligands which are readily accessible for encapsulating to various transition metals to create multi-metal aggregates.²⁵⁵ Magnetic transition metal-containing POMs of this type are a key focus in the literature with numerous examples having been discussed in previous reviews.^{256,257} High spin Fe^{III} ions have five unpaired electrons with a large spin value of $S = 5/2$, therefore, typically display strong antiferromagnetic exchange interactions in the presence of oxo-bridges.^{47,258} Nevertheless, iron-based compounds may possess large ground-state spin values and display SMM behaviour.²⁵⁹

The ability of metal ions to bind to and release ligands under certain conditions as well as the capability of oxidising and reducing in other processes means they are ideal for use in biological systems. Haem ($\text{C}_{34}\text{H}_{32}\text{FeN}_4\text{O}_4$) (Figure 36a) is a metal complex comprising of a porphyrin bound to central iron ion (Figure 36b), which can bind or release molecular oxygen.²⁶⁰ The synthesis of haem is via a biochemical pathway which consists of a significant number of steps involving different enzymes

and substrates.²⁶¹ The basic tetrapyrrole unit comprises of four pyrrole groups connected in a cyclic motif via a methene bridge, forming the porphyrin ring macrocycle. The four nitrogens of each pyrrole bind to the central iron in the plane via the six d^2sp^3 hybrids of iron, serving as a tetradentate ligand system to the Fe^{II} .²⁶² This leaves three remaining d-orbitals available to accommodate the six Fe^{II} electrons. The haem Fe^{II} ion is capable of bonding to five or six coordinate ligands, with five coordinate complexes capable of binding small ligands such as oxygen, and partaking in catalysis.²⁶³

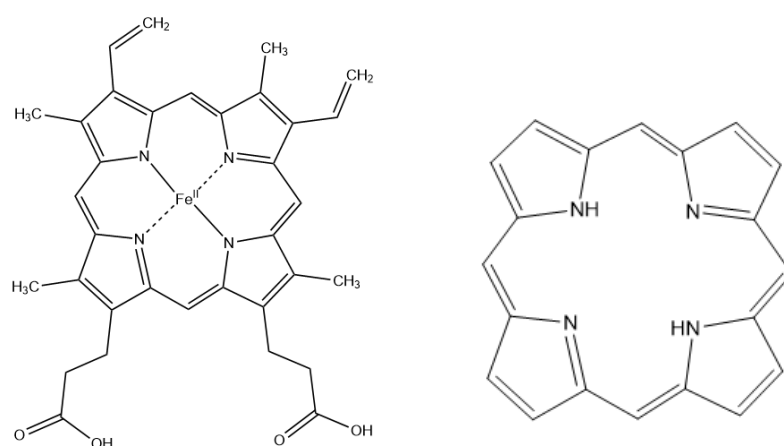


Figure 36. a) A structural representation of the haem group present in Haemoglobin, b) A structural representation of the porphyrin ring surrounding the central Fe^{II} .²⁶²

The system is highly conjugated, providing aromaticity and planarity to the system, however, distortions to the planar structure are common upon interaction with proteins. The ring can be structurally modified in various ways to create different haem types and both undergo conformational changes upon oxygenation and deoxygenation.²⁶⁴ Each individual protein subunit links to its neighbour via intermolecular interactions in order to form peptide chains.

Ferritin is another example of an interesting biological application of iron, a universal intracellular protein with a unique chemical structure capable of controlled storage and release of

iron. The structure consists of a spherical shell, namely apoferritin where Fe^{III} is concentrated in the iron-core as a bioavailable, crystalline iron-oxide mineral ferric-oxyhydroxy-phosphate complex. The complex consists of 24 peptide subunits that form two types of channels: the 3-fold channel and the nonpolar 4-fold channel. The ferritin protein nanocages self-assemble from the polypeptides into highly symmetrical cages, following the spontaneous folding of each into groups of 4 α -helices. However, there are also issues with this molecule due to the presence of paramagnetic metal centres causing significant difficulties with the distinguishing features of ferritin iron, as well as its solubility. Nevertheless, ferritin can also be utilised in materials science as a precursor in synthesising iron nanoparticles for carbon nanotube growth by chemical vapour deposition.²⁶⁵

3.7 Cobalt

Following an investigation into a $\{\text{Ni}_{10}\}$ cluster, a cobalt study considered the methods used in this Ni paper but using new materials with similar topologies and with different localized S or J values. These features created magnetic structures, with strong antiferromagnetic interactions between the edge pairs which define an inner octahedron centred around the μ_6 oxide, as well as weak antiferromagnetic coupling between four of the Ni^{II} located on the vertices that create the outer tetrahedron. This synthesis was first proposed by Anderson for relaxation in paramagnetic salts at low temperatures. Despite such isomorphous high-nuclearity structures being extremely rare, a limited number of examples comprising of Ni or Co are recognised. The research conducted involved the solvothermal reaction of Co^{II} -triol system, which is portrayed to be far more versatile than that of the Ni^{II} equivalent system when carried out under similar reaction conditions. The synthesis involved the reaction of $[\text{Co}(\text{dpm})_2(\text{H}_2\text{O})_2]$ (Hdpm=dipivaloylmethane), H_3tmp [1,1,1-tris(hydroxymethyl)propane, $\text{EtC}(\text{CH}_2\text{OH})_3$], and adamantyl carboxylic acid (AdCO_2H) in MeOH at 150 °C, yielding crystals of $[\text{Co}_{10}\text{O}(\text{dpm})_4(\text{tmp})_4(\text{AdCO}_2)_2(\text{AdCO}_2\text{H})_{0.5}(\text{MeOH})_{3.5}(\text{H}_2\text{O})_{1.5}]$.²⁶⁶

In terms of the overall structure of the $\{\text{Co}_{10}\}$ cluster, all metal ions are six coordinate with the core comprising of four edge-sharing $\{\text{Co}_4\text{O}_4\}$ cubane structures, centred around a μ_6 oxide. This which shows tremendous similarities to the $\{\text{Ni}_{10}\}$ cluster comprising of a supertetrahedral core, linked [4] via μ_6 oxide and surrounded by trisalkoxide ligands capping $\{\text{Ni}_6\}$ face. The metal ions form a tetrahedron with a fully deprotonated $(\text{tmp})^{3-}$ ligand, each $\{\text{Co}_6\}$ face and diketones binding the two vertices. Two carboxylate groups create bridges between two of the metal centres and the symmetrically equivalent metals and a further bridging carboxylate moiety which is disordered and mixed with solvent across 3 metal ions. The remaining metal atoms are capped by terminal solvent ligands. Hence, the $\{\text{Co}_{10}\text{O}(\text{L})_4(\text{diketonate})_4\}$ core of **(1)** is analogous to that of $\{\text{Ni}_{10}\}$. The final Co product is very sensitive to modifications in reaction conditions such as the ligand used or the solvent the procedure is carried out in. The symmetrical $\{\text{Co}_{10}\}$ cluster did display slight slow magnetic relaxation up to temperatures of 12 K, which is significantly higher than those previously reported for SMMs. The comparable behaviour in the Ni and Co clusters supports the association of unusual magnetic phenomena with the regular supertetrahedral $\{\text{M}_{10}\}$ structure. To conclude, Co is considerably less established than other first row ions, however, this straightforward reaction versatility demonstrates great future potential in terms of further development of Co^{II} cluster chemistry, and is attracting increasing attention.

All magnetic clusters, including supported, embedded and free-standing systems, are a key research focus,²⁶⁷ particularly regarding low-dimensional devices because these systems are essential in realizing their magnetic potential.²⁶⁸ Numerous aspects have major influence on the magnetism in low-dimensional systems, such as the symmetry of the cluster, the local coordination, and the interatomic distances. Theoretically, extensive research has been carried out on small cobalt clusters by various parties^{269,270} principally through ab initio schemes. The magnetic moment in these clusters primarily originates from the electron-hole pairs at the top of the 3d-electron levels and the number of holes depends on the number of exchanged 4s-electrons. Since the atomic environment is highly influential on magnetism, the average magnetic moment per atom of the clusters is expected to reflect

the cluster geometry. In Co clusters there is experimental evidence that particle sizes and structures are strongly dependent on the growth conditions such as pressure and temperature.²⁷¹ Reactions of hydrogen-saturated clusters with ammonia and water molecules, as well as photo-ionization experiments have been applied to obtain indications to the geometrical structures of Fe, Co, and Ni clusters.²⁷²

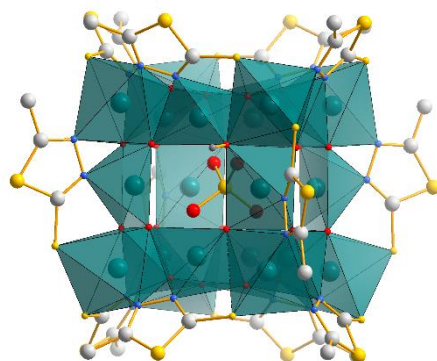


Figure 37. Polyhedral structural representation of the icosanuclear complex $[\text{Co}_{20}(\text{OH})_{24}(\text{MMT})_{12}(\text{SO}_4)](\text{NO}_3)_2 \cdot 6\text{H}_2\text{O}$. The Co^{II} polyhedra in teal, the O centres in red, C centres in grey, N centres in blue and S centres in gold. The hydrogen atoms have been omitted for clarity.²⁷³

Cobalt chemistry has been of great interest due to the noteworthy range of mixed-valence coordination clusters that are structurally and magnetically fascinating. Back in 2012, an eight-cobalt-capped α -Keggin cluster known as a polyoxoazocobaltite was reported. The cobalt complex, $[\text{Co}_{20}(\text{OH})_{24}(\text{MMT})_{12}(\text{SO}_4)](\text{NO}_3)_2 \cdot 6\text{H}_2\text{O}$ (Figure 36), was the first homometallic Co^{II} cluster possessing an alpha-Keggin structure to be characterised and reported (Figure 31). The α -Keggin core, $[\text{Co}_{12}(\text{OH})_{24}(\text{MMT})_{12}(\text{SO}_4)]^{14-}$, is encapsulated by the $[\text{Co}_{20}(\text{OH})_{24}(\text{MMT})_{12}(\text{SO}_4)]^{2+}$ unit. The twenty metal centres are six-coordinate, assuming a distorted octahedral geometry and eight Co^{II} atoms cap the overall structure. Interesting features of this cluster include the poly atom being the late transition metal Co^{II} , in addition to the organic terminal ligand becoming the primary part of the α -Keggin

structure, in contrast to conventional POMs. Exploration of this structure type is important because of its attractive magnetic and electrochemical properties, as well as its promising catalysis potential.²⁷³

The formation of metal-oxo triple bonds with early transition metals such as in VO^{2+} or MoO^{3+} ^{58,55} becomes increasingly difficult when progressing to late transition metals as the occupancy of p-anti-bonding metal d-orbitals increases. Furthermore, the metal-oxo bonds become weaker and more reactive, culminating in the rich chemistry of iron-oxo compounds. However, the stabilization of iron metal-oxo complexes and the others to the right of Group 8 in the periodic table has been achieved by coordinating oxygen to Lewis acids.²⁷⁴ There is only one compound considered to the left of the oxo wall; a Co^{IV} -oxo complex reported by the Nam group. However, the complex square-pyramidal geometry contains a $\text{Co}=\text{O}$ double bond, which results in an energetically accessible $d_{x^2-y^2}$ orbital.²⁷⁵

In 2019, the variation of the metal-oxo bond either side of the oxo wall, was examined by replacing iron with cobalt and analysing significant changes. The higher 4^+ oxidation state induces a larger orbital splitting, therefore, stabilising the low-spin configuration. In addition, the metal d-orbital energy may be lower than the oxygen orbital energy in cobalt-oxo complexes, therefore, Co^{IV} -oxo might be more appropriately defined as Co^{III} -oxyl species.¹² The benefit of cobalt having an expectable reactivity means the preparation of these complexes could be carried out in the gas phase. This allows the species in question to endure long enough for complete characterization by ion-spectroscopic methods and by ion–molecule reactions.²⁷⁶

Polynuclear transition metal coordination clusters continue to be a key research focus, especially during recent years due to their intriguing geometrical characteristics and fascinating physical properties like magnetism. This year, a range of novel octadecanuclear complexes of $[\text{M}_{18}(\text{OH})_6(\text{N,N-dimethyl-Asp})_{12}(\text{CO}_3)_2](\text{ClO}_4)_2(\text{C}_2\text{H}_5\text{OH})_2(\text{H}_2\text{O})_2$ were synthesised, however, this section will focus on clusters where $\text{M} = \text{Co}^{\text{II}}$ (**1**). The synthesis involved the serendipitous self-assembly of the Co precursor, $\text{Co}(\text{ClO}_4)_2 \cdot 6\text{H}_2\text{O}$, with a novel ligand, N,N-dimethyl-Aspartic acid (N,N-dimethyl-Asp), deposited via an in situ Michael addition reaction of 2-butenedioic acid under solvothermal reaction

conditions, in DMF and the presence of triethylamine. This form of self-assembly is a common bottom-up approach to developing coordination clusters which are difficult to obtain in routine synthetic procedures, as unexpected ligands are generated in-situ under superheated conditions.

3.8 Nickel

The design and construction of polynuclear nickel clusters are another area of interest because of their potential applications in catalysis, magnetism and photochemistry.²⁷⁷ For example, the Ni^{II} ion shows promise in SMM synthesis because of their significant single-ion anisotropy.²⁷⁸ The assembly of nickel oxo-clusters typically involves O- or N-donor containing ligands as structure-directing and stabilising agents.^{279,280} Generally, organic ligands such as carboxylate, alkoxide and pyridine are used,²⁸¹ however, POMs comprise of an O-enriched surface rendering them an excellent inorganic multidentate O-donor ligands and a great stabiliser for nickel-based clusters, as discussed below.²⁸²

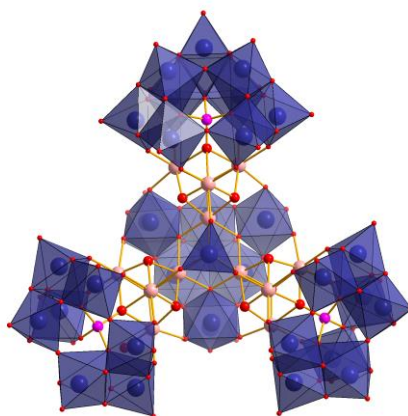


Figure 38. Polyhedral structural representation of the dodecanuclear complexes $[\text{Ni}_{12}(\text{OH})_9\text{WO}_4(\text{W}_7\text{O}_{26}(\text{OH}))(\text{PW}_9\text{O}_{34})_3]^{25-}$ (**1**). The Ni^{II} polyhedra in teal, the O centres in red, C centres in grey, W centres in indigo and P centres in pink. The hydrogen atoms and counter anions have been omitted for clarity.²⁸²

A brand new $[\text{Ni}_{12}(\text{OH})_9\text{WO}_4(\text{W}_7\text{O}_{26}(\text{OH}))(\text{PW}_9\text{O}_{34})_3]^{25-}$ $\{\text{Ni}_{12}\}$ cluster (Figure 38) based on tungsten POM ligands was reported in 2009. This study reported the reaction of nickel salts with the trivacant Keggin anion $[\text{PW}_9\text{O}_{34}]^{9-}$ $\{\text{WO}_4\}^{2-}$ which is one of the most commonly exploited POM-based ligands used in the construction of polynuclear metal oxo-clusters due to its strongly coordination to transition metal clusters.^{283,284} This complex comprises of a large $[\text{Ni}_{12}(\text{OH})_9\text{O}_{13}(\text{PW}_9\text{O}_{34})_3]^{38-}$ moiety packed between a single $\{\text{WO}_4\}$ tetrahedron and a $[\text{W}_7\text{O}_{26}(\text{OH})]^{11-}$ fragment. The central dodecanuclear nickel core $[\text{Ni}_{12}(\text{OH})_9\text{O}_{13}]^{11-}$ is formed by the condensation of three distorted $[\text{Ni}_4\text{O}(\text{OH})_3]$ cubane units and is presented as a unique three-petal structure surrounded by three $[\text{PW}_9\text{O}_{34}]^{9-}$ ligands. These are connected by a central $\mu_4\text{-O}$ and three $\mu_3\text{-O}$ bridging groups residing between adjacent $[\text{Ni}_4\text{O}(\text{OH})_3]$ units. Within each $\{\text{Ni}_4\}$ unit, all nickel atoms form a distorted octahedral coordination geometry and are linked via a single $\mu_4\text{-O}$ atom derived from a $\{\text{PO}_4\}$ group and three $\mu_3\text{-OH}$ bridges.²⁸²

Furthermore, an alpha-Keggin, eight-nickel-capped polyoxoazonickelate structure was also synthesised and reported in 2009, comprising of a Ni^{II} ion and central sulphur heteroatom (Figure 39). This is a tetragonal Keplerate-type cluster with tetrahedral high-symmetry with the molecular formula $[\text{Ni}_{20}(\text{OH})_{24}(\text{MMT})_{12}(\text{SO}_4)](\text{NO}_3)_{23} \cdot 6\text{H}_2\text{O}$ is the earliest example of an icosanuclear nickel cluster consisting of the open-shell alpha-Keggin ion $[\text{Ni}_{12}(\text{OH})_{24}(\text{MMT})_{12}(\text{SO}_4)]$.¹⁴ The classical alpha-Keggin core comprises of 12 six-coordinated Ni^{II} centres forming a cuboctahedron with eight triangular faces and six square faces, and the eight Ni^{II} caps create a unique hexahedron composed of 8 Ni^{II} ions. All 20 Ni^{II} centres are all six-coordinated and present in distorted octahedral coordination.²⁸⁵ The stabilisation of this structure is due to the protonation of the 24 bridging oxygens as well as complete capping of the structure with eight Ni^{II} cations. This reduces the electron density, therefore, lowering the overall negative charge on the structure.

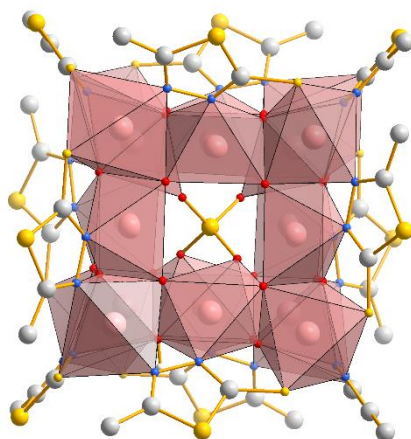


Figure 39. Polyhedral structural representation of the dodecanuclear complex $[\text{Ni}_{20}(\text{OH})_{24}(\text{MMT})_{12}(\text{SO}_4)](\text{NO}_3)_{23} \cdot 6\text{H}_2\text{O}$ (**1**). The Ni^{II} polyhedra in light pink, the O centres in red, C centres in grey and S centres in gold. The hydrogen atoms and counter anions have been omitted for clarity.²⁸⁵

3.9 Copper

The chemistry of high-nuclearity copper clusters have received considerable attention as a result of their potential application in the emerging field of nanomaterials.²⁸⁶ In 2004, a new pentadentate Schiff-base precursor, known as *N,N'*-(2-hydroxypropane-1,3-diyl)bis(acetylacetonimine) (H_3L), was employed in the synthesis of the discrete tetranuclear Cu^{II} cubane complex $\{[\text{Cu}^{\text{II}}(\text{HL})]_4\}$ (**1**). The synthetic route involved the reaction between $[\text{Cu}(\text{H}_2\text{O})_6](\text{ClO}_4)_2$ and H_3L with triethylamine in a mixture of $\text{CH}_2\text{Cl}_2/\text{MeOH}$. The cubane structure comprises of a tetranuclear core where all the Cu^{II} metal centres are connected via μ_3 -alkoxo oxygen atoms, forming the cubic arrangement of the metal and the oxygen atoms. The copper centres assume an approximately square-pyramidal geometry, consisting of six $\{\text{Cu}^{\text{II}}_2\text{L}\}^+$ units, where each Cu centre is linked via two μ_3 -OH groups. Furthermore, the N_2O_3 -donor Schiff base exhibits a trianionic pentadentate coordination mode, binding in a dianionic tridentate form through the terminal imine

nitrogen and enolized oxygen, as well as through the bridging anionic alkoxo group. The remaining hydroxy group and the imine nitrogen atom are pendant, non-coordinating sites suitable for cluster expansion through metal-driven self-assembly process.²⁸⁷

Additionally, an octanuclear Cu^{II} species was also reported with the molecular formula [Cu₈L₄(OH)₃](ClO₄) (Figure 40) and likewise, this cluster can be synthesised when [Cu(H₂O)₆](ClO₄)₂ reacts with [{Cu^{II}(HL)₄}] (1) in a 1:4 molar ratio in the presence of KOH. Previously, this complex had been isolated using a different synthetic route including binuclear precursor was present.²⁸⁸ The identical metal-driven self-assembly procedure carried out under different reaction conditions induces the formation of a new discrete tetradecanuclear mixed-valent copper cluster, [Cu^{II}₁₂Cu^I₂L₆(OH)₆](ClO₄)₂ (2), whereby the reaction involves an addition of four Cu^{II} ions.

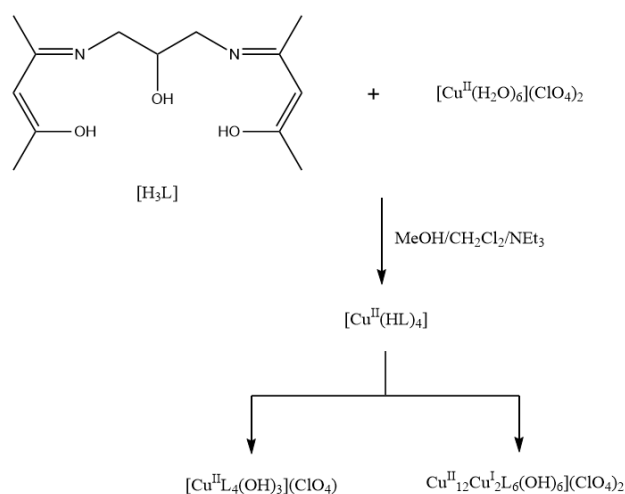


Figure 40. Schematic illustrating the reaction scheme in synthesising [{Cu^{II}(HL)₄}] (1) and [Cu^{II}₁₂Cu^I₂L₆(OH)₆](ClO₄)₂ (2)²⁸⁷

The cluster expansion process is associated with a significant change in the magnetic properties; the observed increase in the cMT value on reducing the temperature indicates intra-cluster ferromagnetic interaction.²⁸⁹ On the other hand, inter-cluster magnetic interaction contribution is thought to be negligible considering the large separation between the clusters. This complex comprises of a six $\{\text{Cu}_2\text{L}\}^+$ moieties with the overall planar geometry of the alkoxo oxygen atom, promoting strong antiferromagnetic interactions within the dimeric unit.²⁹⁰ In comparison, this tetradecanuclear complex illustrates strong antiferromagnetic behaviour with a singlet as a ground state.

In summary, the ferromagnetic cubane cluster (**1**) synthesised is particularly distinctive because the four pendant arms surrounding the molecule provides eight additional donor sites consisting of four imine nitrogen atoms and four hydroxy groups. These are available for binding to further metal ions which could increase the molecules potential as reactive precursor for producing high-nuclearity copper clusters via metal-driven self-assembly in the future. The use of similar ligands with the potential of binding to further metals could be utilised in other metal-oxo clusters to create higher nuclearity clusters overall. Furthermore, the isolation of discrete octanuclear Cu^{II} species as well as a tetradecanuclear mixed-valent complex with a propeller-shaped $\{\text{Cu}^{\text{II}}_{12}\text{Cu}^{\text{I}}_2\}$ core illustrates that the cubane complex can be used as a new precursor for the preparation of high-nuclearity clusters of nanometric size. Also, as mentioned previously, the cubane core comprising of metal ions bridged by oxo ligands is a key structural motif as these cluster tend to display ferromagnetic interactions due to unintentional magnetic orbital orthogonality. Therefore, this core is highly favoured when it comes to designing polynuclear cluster with magnetic properties.

Over half a century ago, the Danish chemist Bjerrum *et al.*²⁹⁴ communicated the aqueous coordination chemistry of Cu^{II} ions with simple alkyl amines and ammonia.^{291,292} Since, there has been considerable reason to revisit copper chemistry and in particular simple copper-amine systems under non-aqueous conditions. In 2005, two high nuclearity products were synthesised,

$[\text{Cu}_8(\text{OH})_{10}(\text{NH}_2(\text{CH}_2)_2\text{CH}_3)_{12}]^{6+}$ and $\{[\text{Cu}(\text{O}_2\text{CNH}(\text{CH}_2)_2\text{CH}_3)(\text{NH}_2(\text{CH}_2)_2\text{CH}_3)_3](\text{ClO}_4)\}_n$, from a simple mixture of the copper salt $\text{Cu}(\text{ClO}_4)_2 \cdot 6\text{H}_2\text{O}$ with 1–20 equivalents of n-propylamine in the presence of methanol. The structure of **(2)** notably does not contain multidentate ligands and its formation requires the self-assembly of at least 30 discrete components which includes twelve n-propylamine, ten hydroxide, eight Cu^{II} cations as well as counter anions.²⁹³ This is a record for copper-(hydr)oxo-clusters. The wing-tipped double cubane arrangement of **(2)** represents a new topology for multinuclear copper-(hydr)oxo clusters which shows promise if this can be recreated using other first-row transition metals.²⁹⁴

The use of reduced amine concentrations, compared to those previously mentioned, resulted in a new octanuclear copper-amine-hydroxide cluster, $[\text{Cu}_8(\text{OH})_{10}(\text{NH}_2(\text{CH}_2)_2\text{CH}_3)_{12}]^{6+}$ **(2)**, formed via self-assembly. The key factor in the formation of **(2)** appears to be the stabilisation specific to n-propylamine ligands. To date, the octanuclear complex was the largest copper hydroxide monodentate amine cluster reported. On the other hand, using an amine concentration greater than seven equivalents relative to the copper ion concentration results in the formation of a one-dimensional carbamate-bridged coordination polymer, $\{[\text{Cu}(\mu_2\text{-O}, \text{O}'\text{-O}_2\text{CNH}(\text{CH}_2)_2\text{CH}_3)(\text{NH}_2(\text{CH}_2)_2\text{CH}_3)_3](\text{ClO}_4)\}_n \{1\text{-ClO}_4\}_n$ **(3)**, which is proficient in fixing carbon dioxide from the air. Furthermore, the magnetic susceptibility findings indicate very weak antiferromagnetic coupling for the polymer-based molecule, whereas those for the octanuclear cluster exhibit marginally stronger net antiferromagnetic coupling interactions. This is illustrated for octanuclear cluster as the magnetic moment per Cu_8 steadily decreases which is indicative of net antiferromagnetic coupling, therefore, the data is generally in agreement with weak antiferromagnetic coupling, probably with low lying S levels being close in energy.²⁹⁴

One attractive target in the field of coordination induced metal-ligand aggregates is the successful preparation and isolation of paramagnetic polyhedral coordination cages of 3d-metal ions²⁹⁵ hydroxido and oxido bridged multicomponent assembly,²⁹⁶ and their utilisation in molecular

magnetism.²⁹⁷ Copper coordination cages formed from phenol-based dinucleating ligands²⁹⁸ are rare, with limited examples of dinuclear,²⁹⁹ tetranuclear,³⁰⁰ pentanuclear,³⁰¹ hexanuclear,³⁰² and cuboctahedral³⁰³ complexes reported. One example includes a hydroxido-bridged dinuclear Cu^{II} complex³⁰⁴ formed from a flexible ligand system based on H₃bpmp, (2,6-bis-[(3-hydroxy-propylimino)-methyl]-4-methyl-phenol). This bis-tridentate ligand H₃bpmp (Figure 41), comprises of two bidentate imine-phenol arms residing either side of a 4-methylphenol spacer and is synthesised from a mixture of 3-amino-1-propanol and 2,6-diformyl-4-methylphenol in MeOH.

Self-assembly has been employed for preparing numerous metal cage-based structures over the years^{305,208} with the appropriate arrangement of paramagnetic metal ions with coordinating ligands and bridging groups.³⁰⁶ The process can be encouraged by employing preformed dinuclear complexes with accessible donor or acceptor coordination sites on either the ligands or metal ions, such as small ancillary groups. The synthesis of {Cu₁₂} involves the reaction of the phenol-based ligand, H₃bpmp, with Cu²⁺ ions from the metal salt reagent in the presence of a hybrid base (NEt₃ and NaN₃), necessary for the in-situ generation of required hydroxido ions. This results in the creation of a novel NO₃⁻ capped and HO⁻ supported coordination cluster [Cu₆(μ₃-OH)₃(μ₃-Hbpmp)₃(μ₃-NO₃)₂(NO₃)₂(OH)₂·2H₂O·2MeOH (**1**) (Figure 42). When the elements are combined in the right proportions with MeOH, twelve Cu^{II} ions assemble in a cuboctahedral geometry, consisting of six square and eight triangular faces. Of the eight {Cu₃} triangular faces six of them are held in place via the six Hbpmp²⁻ ligands, leaving six free pendant propanol arms surrounding the central hexagonal plane. The careful selection of both the solvent and reaction conditions required in generating enough hydroxido groups are necessary for the self-assembly of the preformed dinuclear fragments and dictate the product formed.³⁰⁷

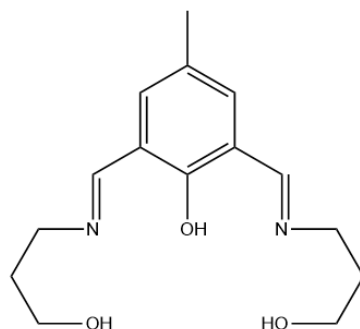


Figure 41. Schematic representation of the H₃bpmp ligand employed in the synthesis of [Cu₆(μ₃-OH)₃(μ₃-Hbpmp)₃(μ₃-NO₃)₂(NO₃)₂(OH)₂·2H₂O·2MeOH.³⁰⁷

This distinctive high-symmetry Cu^{II} cage comprises of face-capping hexadentate ligand units, bonded to six-coordinate metal-ions in an atypical dodecanuclear cubooctahedral arrangement. The {Cu₁₂} complex is mainly constructed from Hbpmp²⁻ ligands supported by in-situ generated hydroxido ions and templating NO³⁻ anions of the precursor metal ion salt. Capping a hydroxido {Cu₆} hexagon between two {Cu₃(μ₃-NO₃)⁵⁻} triangles create a hexagonal sandwiched and crosswise supported by six face capping forms of H₃bpmp²⁻, resulting in a novel Cu^{II} cage. The face-capping trinucleating binding mode is a result of the long imine-propanol arms present on the theoretically binucleating ligands. Overall, this dodecanuclear cage contains six doubly deprotonated Hbpmp²⁻ ligands and six hydroxido anions along with two NO³⁻ anions.³⁰⁷

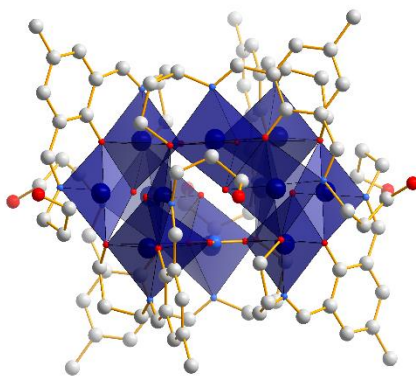


Figure 42. Polyhedral structural representation of the dodecanuclear complex $[\text{Cu}_6(\mu_3\text{-OH})_3(\mu_3\text{-Hbpm})_3(\mu_3\text{-NO}_3)]_2(\text{NO}_3)_2(\text{OH})_2 \cdot 2\text{H}_2\text{O} \cdot 2\text{MeOH}$. The Cu^{II} polyhedra in dark blue, the O centres in red, C centres in grey and S centres in gold. The hydrogen atoms and counter anions have been omitted for clarity.³⁰⁷

The design and synthesis of high-nuclearity coordination complexes of first-row magnetic transition metals has been intensely researched regarding molecular magnetism. Cage-type structures with tunable magnetic properties have been significant area of interest as these are important in developing unprecedented magnetic materials with a range of potential applications.³⁰⁸ This thermal behavior indicates the presence of dominant and strong antiferromagnetic interactions between the Cu^{2+} magnetic centers in the complex led to a diamagnetic ground state for the $[\text{Cu}_{12}]$ cage.

Molecules of high symmetry are another key research focus when considering molecular magnetism as this feature can be crucial. Keplerate describes a class of highly symmetrical polynuclear metal complexes where several metal ions reside on the vertices of a Platonic solid and the others on the vertices of an Archimedean solid.³⁰⁹ Keplerates were originally recognised by Müller³¹⁰ for polyoxometalates, however, a few complexes have been documented for 3d-metal oxo cage clusters.^{311,312} In 2015, the syntheses of a novel series of copper keplerates were reported. Two families of copper keplerates have been synthesised by combining two different copper starting

materials under diverse reaction conditions. The first group involves a {Cu₁₂} encapsulated in a cube of metals, and includes [Cu₂₀(μ₃-OH)₂₄(OH)₄(O₂CtBu)₈(NH₂iPr)₆(μ-NH₂iPr)][O₂CtBu]₄·[Cu₂₀(μ₃-OH)₂₄(O₂CtBu)₈(NH₂iPr)₈(m-NH₂iPr)][O₂CtBu]₈ (**2**).³⁰⁷ The {Cu₁₂} species is linked via twenty-four μ₃-OH ions and encapsulated by {M₈} cubes which is slightly distorted from the ideal polyhedral structure. Meanwhile, eight ^tBuCO²⁻ and monodentate NH₂iPr ligands and H₂O molecules complete the coordination sphere of the metal ions involved.³¹³

Despite the large nuclearity of these cages, the presence of $S = 1/2$ spin centres permit calculation of their magnetic properties and in this case indicates one antiferromagnetic nearest-neighbour coupling.^{314,315} The {Cu₂₀} cluster (**2**) is expected to have similar behaviour features antiferromagnetic interactions in corner- and edge-sharing triangles. The experimental magnetic properties resemble other keplerates,³¹³

3.10 Zinc

Dinucleating ligands have recently become a very active area of research regarding the field of coordination chemistry because these multidentate ligands are thought to be valuable components for high-nuclearity clusters. In recent times, designing the synthesis routes of oligonuclear metal complexes via utilisation of various multidentate ligands has been of great interest.^{316,317} In 1999, this study discovered employing a pentadentate Schiff-base ligand, such as bis(benzoylacetone)-1,3-diiminopropan-2-ol (H₃L) (Figure 43a), aids in the synthesis of tetranuclear or octanuclear Zn^{II} metal cores via a dinuclear Cu^{II} species (Figure 36).³¹⁸

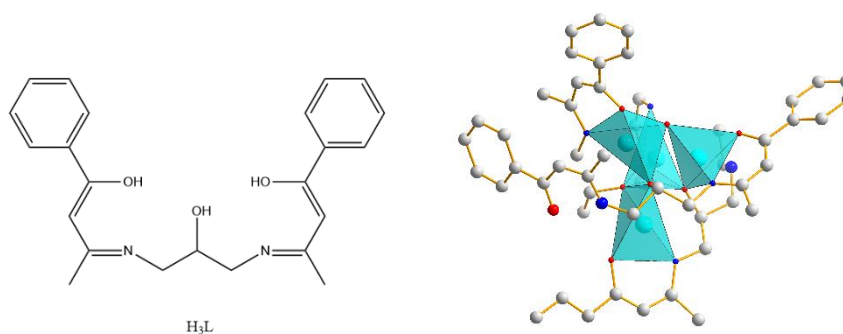


Figure 43. a) Schematic of the bis(benzoylacetone)-1,3-diiminopropan-2-ol ligand used in the synthesis. b) Polyhedral structural representation of the tetranuclear complex $[Zn_4(HL)_4]P_4CH_3CN(1P_4CH_3CN)$. The Zn^{II} polyhedra in light blue, the O centres in red, C centres in grey and S centres in gold. The hydrogen atoms and counter anions have been omitted for clarity.³¹⁹

This paper reported the preparation and structural characterization of the novel oligonuclear metal complexes, $[Zn_4(HL)_4]P_4CH_3CN(1P_4CH_3CN)$ (**1**) (Figure 43b), $[Zn_8(L)_4(OH)_4]P_2CH_3CN(2P_2CH_3CN)$ (**2**) and $[Zn_2Ni_2(L)_2(CH_3O)_2(CH_3OH)_2]$ (**3**), via a reaction of Zn^{II} chloride, H_3L and triethylamine carried out in the presence of acetonitrile at room temperature (Figure 44). This resulted in double deprotonations of the Schiff-base ligand to produce pale-yellow crystals of $1P_4CH_3CN$. Every Zn atom assumes a distorted trigonal-bipyramid coordination geometry with two alkoxo-oxygen atoms and one imino-nitrogen atom in the equatorial plane and one keto-oxygen atom and one alkoxo-oxygen atom at the axial positions. The remaining keto-oxygen and imino-nitrogen atoms are left uncoordinated to any metal atoms, therefore, were presumed to be accessible for further coordination. Thus high-nuclearity species formation was expected to occur by utilising this Schiff-base ligand further.³¹⁹

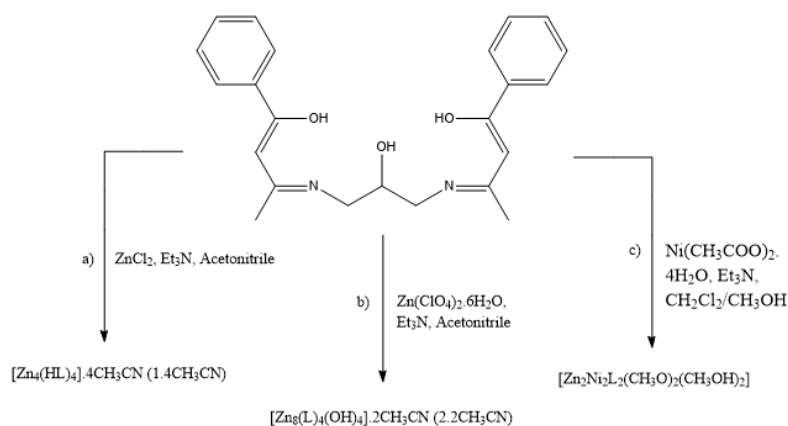


Figure 44. Schematic showing the reaction scheme in synthesising $[\text{Zn}_4(\text{HL})_4]\text{P}_4\text{CH}_3\text{CN}$ ($1\text{P}_4\text{CH}_3\text{CN}$) (**1**), $[\text{Zn}_8(\text{L})_4(\text{OH})_4]\text{P}_2\text{CH}_3\text{CN}$ ($2\text{P}_2\text{CH}_3\text{CN}$) (**2**) and $[\text{Zn}_2\text{Ni}_2(\text{L})_2(\text{CH}_3\text{O})_2(\text{CH}_3\text{OH})_2]$ (**3**).³¹⁹

Under more basic conditions when using $[\text{Zn}^{\text{II}}(\text{ClO}_4)_2 \cdot 6\text{H}_2\text{O}]$ as the metal source, a combination of $1\text{P}_4\text{CH}_3\text{CN}$ and $2\text{P}_2\text{CH}_3\text{CN}$ crystals were obtained. This formed an octanuclear structure comprising of two distorted hexahedra, connected by hydroxo ions. The Schiff-base ligand is triply deprotonated and bonded to each of zinc atoms via three donor atoms. Each Zn^{II} assumes a distorted trigonal bipyramid coordination geometry. The results from this study illustrate that it is possible to synthesise and isolate polynuclear Zn clusters successfully by employing a Schiff-base ligand with a rich coordination chemistry. Therefore, this allows for the preparation of a variety of oligonuclear metal complexes depending upon the degree of the deprotonation of the Schiff base.³¹⁹

Previous studies^{320,321} regarding $[\text{Zn}_4\text{O}]^{6+}$ core complexes comprising of Zn^{II} oxo-bonds, such as $[\text{Zn}_4(\mu_4\text{-O})(\text{O}_2\text{CNET}_2)_6]$ and similar complexes, has illustrated extraordinary impact on the reactivity of carbamate ligands. This results in both the carboxylic and amino elements of the ligands displaying intrinsic lability which is not typically observed in organic carbamates. There is a great interest in $[\text{Zn}_4(\mu_4\text{-O})(\text{O}_2\text{CNET}_2)_6]$ due to the cluster's fascinating chemistry regarding its electronic properties. The sensitivity of carbamates to hydrolysis is common knowledge, therefore, the lability of the C–N bond

provides tremendous support with the stability problems during the ZnO deposition process.³²² The overall aim of this investigation was the development of analogous (dialkylcarbamato)zinc complexes consisting of bulkier ⁱPr groups which effectively coat the surface of the (oxido)tetrazinc cluster. By increasing the alkyl group bulk, it was hoped to have several desirable effects, including providing better steric protection from hydrolysis of the interior carbamate linkages by ambient water, and to extend the core-to-core distance to weaken polar interactions between clusters. Moreover, there is evidence to suggest that increasing the size of the alkyl group increases the intrinsic thermal stability of the carbamate group.³²³

In zinc coordination chemistry, the tetrahedral $[Zn_4O]^{6+}$ core is a widespread motif, appearing in zinc carboxylates,^{324,325} carbamates^{326,327} and phosphates.³²⁸ When considering the carboxylato and carbamato series, bridging oxygens extend the tetrahedral core into an arrangement resembling the wurtzite-type ZnO.³²⁹ Therefore, the carbamato complex $[Zn_4(\mu_4-O)(O_2CNEt_2)_6]$ (**3**) is considered to be a derivative of the molecular model of crystalline ZnO.³³⁰ A paper published in 2008 reported the high-yielding and reproducible synthesis of the first homonuclear (diisopropylcarbamato)(μ_4 -oxo)zinc complex, $[Zn_4(\mu_4-O)(O_2CN^iPr_2)_6]$ (**1**), and its closely related dimer $[Zn_8(\mu_4-O)_2(O_2CN^iPr_2)_{12}]$ (**2**) (Figure 45).³³¹ Complex (**1**) and (**2**) were synthesised via an identical procedure involving the photolysis of $ZnEt_2$ and ⁱPrNH and CO_2 , followed by stoichiometric hydrolysis. The exclusive product of complex (**1**) was obtained via recrystallisations from CH_3CN and $(CH_3)_2CCN$, whereas recrystallisation from alkane solvents produced crystals of octanuclear Zn cluster (**2**). Furthermore, a new and more reliable reaction pathway involving $ZnEt_2$ was employed to obtain the known $[Zn_4(\mu_4-O)(O_2CNEt_2)_6]$ (**3**) and it may prove even more widely applicable. The dialkylzinc compound $ZnEt_2$ is still an effective starting material for the self-assembly of tetra- and octanuclear (carbamato)(μ -oxido)zinc clusters from HNR_2 , CO_2 and H_2O .³³¹

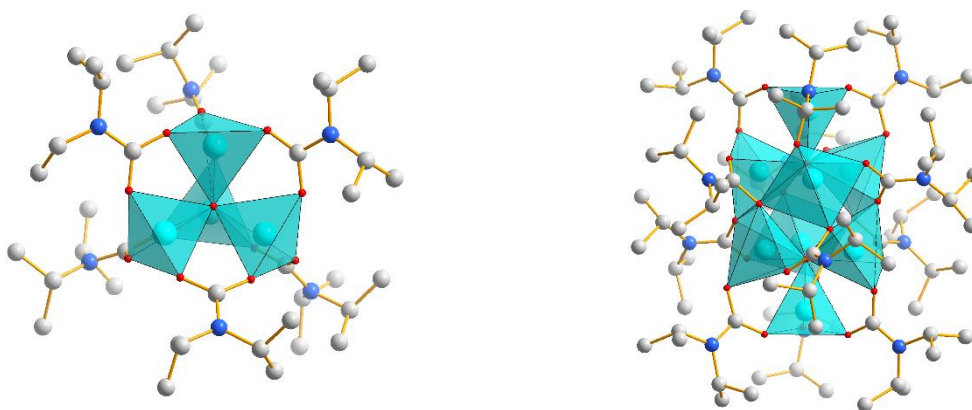


Figure 45. Polyhedral structural representation of the tetranuclear complex $[Zn_8(\mu_4-O)_2(O_2CN^iPr_2)_{12}]$ (**1**) and $[Zn_4(\mu_4-O)(O_2CNEt_2)_6]$ (**2**). The Zn^{II} polyhedra in light blue, the O centres in red, C centres in grey and S centres in gold. The hydrogen atoms and counter anions have been omitted for clarity.³³¹

Overall, a convenient route has been developed for the synthesis of (carbamato)zinc clusters. The subtle solvent effects discovered in this work may stimulate a re-examination of carbamate chemistry of other metals. In particular, the lability of the (carbamato)zinc complexes offers a route to mixed-metal clusters. The oxo-bridging in Zn clusters makes polynuclear Zn^{II} complexes attractive precursors for zinc oxide-based inorganic materials³³² including the construction of multinuclear Zn^{II} species using macrocyclic or salen-type ligands.^{333,334,335} An excellent option for this type of reaction are Schiff-base ligands due to the multiple hard O-donors present within a reasonably flexible environment, thus encouraging the assembly of larger of Zn^{II} ion clusters.³³⁶ The utilisation of these ligands in capturing multiple Zn^{II} and other metal ions has recently been reviewed³³⁷ and in order to directly obtain Zn_xO_y clusters, it is possible to functionalise the Schiff base ligand with O-containing donor substituents.

4 Second and third transition metal series

As discussed, examination of empirical properties of transition metal-oxo clusters reveals that early metal-oxo compounds exhibit high stability, are relatively inert and are characterized by very strong M-O bonds. Late transition metal oxo-complexes tend to be highly reactive oxidizing agents with much weaker M-O bonds.³³⁸ In fact, the bond strengths of early metal-oxo diatomics are approximately twice as strong as their late metal-oxo equivalents. It is thought that the differences in the metal-oxo bond character are responsible for the sharp contrast in bond energies and reactivities of early and late transition metal-oxo complexes.⁵⁹

Higher oxidation states are usually more stable for heavier transition metals compared to the lighter elements in the first transition series where the presence of lower oxidation states, especially 2^+ and 3^+ , is such a central part of the chemistry. On the other hand, this property is comparatively inconsequential for most heavier metal ions.³³⁹ Although the elements residing in the second and third transition series of any given group in the periodic table have chemical properties and characteristics analogous to those in the first series, they nevertheless display unambiguous variances from the lighter element of that group. In order to illustrate this fact further, the following element specific examples illustrate the differences. The first being that although cobalt adopts a substantial number of tetrahedral and octahedral geometries when present in its 2^+ oxidation state, as well as this being the characteristic state in ordinary aqueous chemistry. The 2^+ states of second and third series elements including rhodium and iridium are rare and relatively insignificant. Fairly valid, useful analogies have been noticed concerning the lighter element chemistry and the two heavier elements of the group. For instance, rhodium cluster chemistry, where rhodium is present in the 3^+ state, is typically comparable to that of cobalt complexes, with cobalt in a 3^+ state. Nevertheless, there are more consistent differences than similarities between the first-row elements of the transition metal series and the heavier elements further down each group. Consequently, the isolation and separation of terminal late transition metal-oxo (LTMO) species, beyond the oxo wall has been

limited. According to research, this has only been achieved with metals such as iridium and platinum where the ligand fields are not tetragonal.

Within a given group of the periodic table, the similar chemistry between the second and third transition series elements is a result of a process known as lanthanoid contraction. In brief, the 5d and 6s valence-shell orbitals of the third transition series elements are only weakly shielded by the 4f electrons from the increasing nuclear charge moving from left to right across a given period. Thus, producing a steady contraction in orbital size to occur throughout the lanthanoid series. Consequently, the atomic and ionic radii of the element immediately following the lanthanoid series, hafnium, are practically identical to the corresponding radii of that of the element directly above it, zirconium.

5 Conclusions and Future Directions

In summary, this report has provided an in-depth overview of the current state of the art in first-row transition metal oxo-clusters, delivering insight into their synthesis, structure and properties. This expands on more conventional and heavily studied metal-oxo clusters comprising of early, heavy transition metals (e.g. polyoxometalates) and gives deeper consideration to those occurring in the mid- to late- section of the periodic table, particularly involving elements from groups VIII-X. Previously, there has been limited discussion of later transition metal-oxo compounds due to their instability relative to electron deficient early metals that more readily form strong oxo-bonds. By providing a detailed review of the metal-oxo bond nature, the effects of the metal and its electronic configuration on the resulting structure and properties of a given oxo-cluster are discussed. Developing greater understanding of these concepts is vital in the future development of the field and can help to establish new synthetic methods in order to isolate new oxo-clusters, with unusual structures, compositions or properties.

While there is already a wide range of structural types available in metal-oxo chemistry and this is continuing to expand, there is still significant scope for further advancements in the field. Research into polynuclear early-transition metal-oxide species is a subject of huge interest at present. This mainly encompasses the sub-field of polyoxometalate chemistry; high nuclearity species formed from group V and VI metals. POMs unique electronic structure means the surfaces are almost exclusively comprised of terminal oxo ligands that stabilise the overall cluster (a fairly unique feature of this class of compounds). The forming of this passivating layer of stable terminal M=O groups on the surface of the cluster prevents the formation of the bulk metal oxide during synthesis. In contrast, clusters consisting of mid- to late-transition metals commonly require organic capping ligands in order to stabilise the structure. This is supported by the oxo wall concept, stating that clusters of metals past group VIII do not form passivating terminal oxo-groups and helps to explain the difficulty in synthesising polynuclear metal-oxo clusters based on metals such as manganese, cobalt or nickel.

Moreover, varying or modifying the ligands is a promising strategy in altering the properties of clusters to display more desirable characteristics.²³⁷ Synthesising either trapped or delocalized mixed-valence varieties may offer the opportunity to be able to tune the magnetochemistry of the cluster and also allow the introduction of valence fluctuation. This could be achieved by utilising suitable organic or inorganic ligands, mainly carboxylates, polyamines, and polyols. Therefore, the “growth” of the metal oxo cores can be controlled in such a way to obtain finite size clusters. The metal-oxygen cores of these clusters often exhibit closest-packing layered structures which are typical of bulk metal oxides. Exploiting this tendency to address the synthesis of high-nuclearity, preferably high-valent manganese clusters which may behave as single-molecule magnets.²¹⁴ This is important because it provides a new model for studying metal oxide chemistry and opens up possibilities of nanoclusters with novel properties, meaning they are relevant in fields such as catalysis, electrochemistry or molecular magnetism. In more recent years, new approaches to synthesising and stabilising novel mid- to late-transition metal clusters have been developed, enabling the formation of high nuclearity species. These offer considerable promise for isolating a range of unique molecular analogues of bulk metal oxides. Various examples are discussed above, such as the chromium cluster recently synthesised and successfully isolated by Nyman et al. This exclusive {Cr₁₂} δ -Keggin polycation was an early example of an unligated cluster which are important in both mechanistic studies and applications. Simple molecular oxo-hydroxo metal clusters, assembled in water without stabilizing organic ligands such as this, are also building blocks for both natural and synthetic metal oxides as well as precursors for environmental, energy and medical applications.

Throughout this review there has been an overall focus on metal-oxygen bonding and how this is a key factor influencing the electronic and magnetic properties in mid- to late-transition metal species, typically in Mn, Fe and Co, as well as on some occasions Ni. These metals in particular are of great importance because their clusters have all displayed some level of SMM character which indicates great future potential in advancing these properties, given further research. Tuning

polynuclear cluster properties is one possible method of enhancing SMM performance, such as targeted distortions of bridging ligands.

In the future, a favourable outcome would involve huge steps having been made towards the efficient and successful assembly of 3d mixed-valence transition metal-oxo clusters displaying a stable high-spin ground state via electron delocalisation at the metal centre.³⁴⁰ The ability to replicate or improve metal oxide properties can be very difficult, however, molecular clusters with well separated energy levels and characteristic electronic structures can be modified in order to display desirable features or properties.⁸⁷ This includes aspects such as valence tautomerism, multi-bistability with spin crossover and SMM behaviour which is achieved by tuning the frontier orbitals and modifying the electronic interactions between the metal centres.^{341,342} For example, mixed-valent POVs including V^V/V^{IV} and V^{IV}/V^{III} , fully oxidised V^V , fully reduced V^{IV} and highly reduced V^{III} species,¹⁵¹ all demonstrate a range of intramolecular spin exchange phenomena, such as ferro/antiferro-magnetism and SMM behaviour. Overall, the aim would be to synthesise and isolate clusters with controllable redox states, which when altered then modifies the compound's physical properties.⁸⁷

Furthermore, despite the first example of double exchange being discovered back in 1951 by Zener, there has seemingly been relatively limited research conducted in this area since. While a number of theoretical articles have described double-exchange stabilisation in mixed-valence complexes, there remains a limited number of experimental reports of high-spin molecules with double-exchange stabilising the high-spin state.

In conclusion, this review summarises the rich and diverse chemistry of polynuclear 3d-metal oxo coordination clusters. The importance of their electronic structure in the formation, stability and arrangement of these species is critically analysed as well as its influence on their properties. There has already been tremendous success in this field, however, with the enormous future potential of these systems, it is highly likely that the study of these molecular clusters will only continue to grow as new synthetic routes are discovered and different clusters are isolated with valuable properties. By

providing a framework for understanding the fundamental properties of first-row transition metal-oxo clusters, this review has aimed to provide details on state of the art clusters currently known and highlight the exciting future potential in this active research area.

6 References

- 1 M. Nyman, in *Encyclopedia of Earth Sciences Series*, 2018, **42**, 1242–1247.
- 2 M. Swart and M. Gruden, *Acc. Chem. Res.*, 2016, **49**, 2690–2697.
- 3 J. A. Alonso, *Chem. Rev.*, 2000, **100**, 637–677.
- 4 Y. Yang, H. Liu and P. Zhang, *Phys. Rev. B - Condens. Matter Mater.*, 2011, **84**, 205430.
- 5 K. Harpp, in *Encyclopedia of Earth Sciences Series*, 2018, 1201–1207.
- 6 J. Hou, Y. Wang, K. Eguchi, C. Nanjo, T. Takaoka, Y. Sainoo, R. Arafune, K. Awaga and T. Komeda, *Commun. Chem.* 2020, **3**, 1-11.
- 7 W. Nam, in *Accounts of Chemical Research*, 2007, **40**, 465.
- 8 J. Cho, J. Woo, J. Eun Han, M. Kubo, T. Ogura and W. Nam, *Chem. Sci.*, 2011, **2**, 2057–2062.
- 9 C. R. Waidmann, A. G. Dipasquale and J. M. Mayer, *Inorg. Chem.*, 2010, **49**, 2383–2391.
- 10 H. B. Gray, *Chem. Int.*, 2019, **41**, 16–19.
- 11 Q. Shi, Z. M. Zhang, Y. G. Li, Q. Wu, S. Yao and E. B. Wang, *Inorg. Chem. Commun.*, 2009, **12**, 293–295.
- 12 K. Ray, F. Heims and F. F. Pfaff, *Eur. J. Inorg. Chem.*, 2013, 3784–3807.
- 13 V. A. Larson, B. Battistella, K. Ray, N. Lehnert and W. Nam, *Nat. Rev. Chem.*, **4**, 404–419.
- 14 G. E. Uhlenbeck and S. Goudsmit, *Naturwissenschaften*, 1925, **13**, 953–954.
- 15 I. A. Akimov, V. L. Korenev, V. F. Sapega, L. Langer, S. V. Zaitsev, Y. A. Danilov, D. R. Yakovlev and M. Bayer, *Phys. Status Solidi Basic Res.*, 2014, **251**, 1663–1672.
- 16 R. M. Bozorth, *Rev. Mod. Phys.*, 1947, **19**, 29–86.
- 17 *J. Chem. Educ.*, 1995, **72**, A19.
- 18 E. Coronado and K. R. Dunbar, *Inorg. Chem.*, 2009, **48**, 3293–3295.
- 19 D. Maniaki, E. Pilichos and S. P. Perlepes, *Front. Chem.*, 2018, **6**, 461.
- 20 E. Coronado and D. Gatteschi, *J. Mater. Chem.*, 2006, **16**, 2513–2515.
- 21 C. Benelli and D. Gatteschi, *Angew. Chem. Int. Ed.*, 2015, **55**, 1959.
- 22 R. Sessoli, D. Gatteschi, A. Caneschi and M. A. Novak, *Nature*, 1993, **365**, 141–143.
- 23 L. E. Pence, A. Caneschi and S. J. Lippard, *Inorg. Chem.*, 1996, **35**, 3069–3072.
- 24 S. Hill, S. Datta, J. Liu, R. Inglis, C. J. Milios, P. L. Feng, J. J. Henderson, E. Del Barco, E. K. Brechin and D. N. Hendrickson, *Dalt. Trans.*, 2010, **39**, 4693–4707.
- 25 D. Garanin and E. Chudnovsky, *Phys. Rev. B - Condens. Matter Mater. Phys.*, 1997, **56**, 11102–11118.
- 26 M. N. Leuenberger and D. Loss, *Nature*, 2001, **410**, 789–793.
- 27 H. B. Heersche, Z. De Groot, J. A. Folk, H. S. J. Van Der Zant, C. Romeike, M. R. Wegewijs, L. Zobbi, D. Barreca, E. Tondello and A. Cornia, *Phys. Rev. Lett.*, 2006, **96**, 206801.

- 28 C. A. R. Sa de Melo, *Phys. Today*, 2002, **55**, 54-56.
- 29 C. Creutz and H. Taube, *J. Am. Chem. Soc.*, 1973, **95**, 1086–1094.
- 30 D. M. D’Alessandro and F. R. Keene, *Chem. Soc. Rev.*, 2006, **35**, 424–440.
- 31 P. Day, N. S. Hush and R. J. H. Clark, *Philos. Trans. R. Soc. A Math. Phys. Eng. Sci.*, 2008, **366**, 5–14.
- 32 M. B. Robin and P. Day, *Adv. Inorg. Chem. Radiochem.*, 1968, **10**, 247–422.
- 33 C. Daniel and H. Hartl, *J. Am. Chem. Soc.*, 2005, **127**, 13978–13987.
- 34 C. Zener, *Phys. Rev.*, 1951, **82**, 403–405.
- 35 P. W. Anderson, *Phys. Rev.*, 1959, **115**, 2–13.
- 36 A. Palii, B. Tsukerblat, S. Klokishner, K. R. Dunbar, J. M. Clemente-Juan and E. Coronado, *Chem. Soc. Rev.*, 2011, **40**, 3130–3156.
- 37 M. P. Shores and J. R. Long, *J. Am. Chem. Soc.*, 2002, **124**, 3512–3513.
- 38 K. Pradhan and P. Jena, *Appl. Phys. Lett.*, 2014, **105**, 163112.
- 39 V. Barone, A. Bencini, I. Ciofini, C. A. Daul and F. Totti, *J. Am. Chem. Soc.*, 1998, **120**, 8357–8365.
- 40 D. Aravena, D. Venegas-Yazigi and E. Ruiz, *Sci. Rep.*, 2016, **6**, 1-7.
- 41 G. Blondin and J. J. Girerd, *Chem. Rev.*, 1990, **90**, 1359–1376.
- 42 M. Drillon, G. Pourroy and J. Darriet, *Chem. Phys.*, 1984, **88**, 27–37.
- 43 J. J. Borrás-Almenar, E. Coronado, S. M. Ostrovsky, A. V. Palii and B. S. Tsukerblat, *Chem. Phys.*, 1999, **240**, 149–161.
- 44 T. Beissel, F. Birkelbach, E. Bill, T. Glaser, F. Kesting, C. Krebs, T. Weyhermüller, K. Wieghardt, C. Butzlaff and A. X. Trautwein, *J. Am. Chem. Soc.*, 1996, **118**, 12376–12390.
- 45 B. Bechlars, D. M. D’Alessandro, D. M. Jenkins, A. T. Iavarone, S. D. Glover, C. P. Kubiak and J. R. Long, *Nat. Chem.*, 2010, **2**, 362–368.
- 46 F. K. Malinowski, F. Martins, T. B. Smith, S. D. Bartlett, A. C. Doherty, P. D. Nissen, S. Fallahi, G. C. Gardner, M. J. Manfra, C. M. Marcus and F. Kuemmeth, *Nat. Commun.*, 2019, **10**, 1196.
- 47 G. Christou, D. Gatteschi, D. N. Hendrickson and R. Sessoli, *MRS Bull.*, 2000, **25**, 66–71.
- 48 D. Collison, M. Murrie, V. S. Oganessian, S. Piligkos, N. R. J. Poolton, G. Rajaraman, G. M. Smith, A. J. Thomson, G. A. Timko, W. Wernsdorfer, R. E. P. Winpenny and E. J. L. McInnes, *Inorg. Chem.*, 2003, **42**, 5293–5303.
- 49 J. M. Frost, K. L. M. Harriman and M. Murugesu, *Chem. Sci.*, 2016, **7**, 2470–2491.
- 50 J. Long, *Front. Chem.*, 2019, **7**, 63.
- 51 A. K. Boudalis, B. Donnadiou, V. Nastopoulos, J. M. Clemente-Juan, A. Mari, Y. Sanakis, J. P. Tuchagues and S. P. Perlepes, *Angew. Chemie - Int. Ed.*, 2004, **43**, 2266–2270.
- 52 C. Benelli, M. Murrie, S. Parsons and R. E. P. Winpenny, *J. Chem. Soc. - Dalt. Trans.*, 1999, 4125–4126.
- 53 R. Bagai and G. Christou, *Chem. Soc. Rev.*, 2009, **38**, 1011–1026.

- 54 R. E. P. Winpenny, *J. Chem. Soc. Dalton Trans.*, 2002, **2**, 1–10.
- 55 J. R. Winkler and H. B. Gray, *Struct. Bond.*, 2011, **142**, 17–28.
- 56 J. Selbin, *Coord. Chem. Rev.*, 1966, **1**, 293–314.
- 57 C. Furlani, *Zeitschrift für Phys. Chemie*, 1957, **10**, 291–305.
- 58 C. J. Ballhausen and H. B. Gray, *Inorg. Chem.*, 1962, **1**, 111–122.
- 59 E. A. Carter and W. A. Goddard, *J. Phys. Chem.*, 1988, **92**, 2109–2115.
- 60 K. P. O’Halloran, C. Zhao, N. S. Ando, A. J. Schultz, T. F. Koetzle, P. M. B. Piccoli, B. Hedman, K. O. Hodgson, E. Bobyr, M. L. Kirk, S. Knottenbelt, E. C. Depperman, B. Stein, T. M. Anderson, R. Cao, Y. V. Geletii, K. I. Hardcastle, D. G. Musaev, W. A. Neiwert, X. Fang, K. Morokuma, S. Wu, P. Kögerler and C. L. Hill, *Inorg. Chem.*, 2012, **51**, 7025–7031.
- 61 C. A. Daul, *Journal of Physics: Conference Series*, 2013, **428**, 1.
- 62 R. F. Bryan, *Acta Crystallogr. Sect. B Struct. Sci.*, 1994, **50**, 630–630.
- 63 E. C. Constable, *Metals and Ligand Reactivity*, Wiley VCH, 1996.
- 64 S. Alvarez, *Angew. Chemie*, 2014, **126**, 4608–4609.
- 65 J. K. Burdett, *Chemical bonds: a dialog*, Wiley, Chichester, 1997.
- 66 C. J. Ballhausen and M. A. Weiner, *J. Electrochem. Soc.*, 1963, **110**, 97C.
- 67 R. Mason, *Acta Crystallogr. Sect. B.*, 1972, **28**, 658–658.
- 68 G.J.W., *J. Mol. Struct.*, 1972, **11**, 162–163.
- 69 G. Frenking and N. Fröhlich, *Chem. Rev.*, 2000, **100**, 717–774.
- 70 Y. Shimoyama and T. Kojima, *Inorg. Chem.*, 2019, **58**, 9517–9542.
- 71 C. Limberg, *Angew. Chemie - Int. Ed.*, 2009, **48**, 2270–2273.
- 72 R. Cao, T. M. Anderson, P. M. B. Piccoli, A. J. Schultz, T. F. Koetzle, Y. V. Geletii, E. Slonkina, B. Hedman, K. O. Hodgson, K. I. Hardcastle, X. Fang, M. L. Kirk, S. Knottenbelt, P. Kögerler, D. G. Musaev, K. Morokuma, M. Takahashi and C. L. Hill, *J. Am. Chem. Soc.*, 2007, **129**, 11118–11133.
- 73 R. J. Eisenhart, L. J. Clouston and C. C. Lu, *Acc. Chem. Res.* 2015, **48**, 2885–2894.
- 74 W. Stumm, *Adv. Colloid Interface Sci.*, 1991, **35**, 198.
- 75 P. R. Sharp, *J. Chem. Soc. Dalton Trans.*, 2000, 2647–2657.
- 76 A. K. Rappé and W. A. Goddard, *J. Am. Chem. Soc.*, 1980, **102**, 5114–5115.
- 77 T. A. Betley, Q. Wu, T. Van Voorhis and D. G. Nocera, *Inorg. Chem.*, 2008, **47**, 1849–1861.
- 78 V. P. Oliveira, E. Kraka and F. B. C. Machado, *Inorg. Chem.*, 2019, **58**, 14777–14789.
- 79 D. Munz, *Chem. Sci.*, 2018, **9**, 1155–1167.
- 80 E. Poverenov, I. Efremenko, A. I. Frenkel, Y. Ben-David, L. J. W. Shimon, G. Leituss, L. Konstantinovski, J. M. L. Martin and D. Milstein, *Nature*, 2008, **455**, 1093–1096.
- 81 T. M. Anderson, W. A. Neiwert, M. L. Kirk, P. M. B. Piccoli, A. J. Schultz, T. F. Koetzle, D. G.

- Musaev, K. Morokuma, R. Cao and C. L. Hill, *Science*, 2004, **306**, 2074–2077.
- 82 D. Lockwood, *Chem. Eng. News Arch.*, 2012, **90**, 9.
- 83 E. Spaltenstein, R. R. Conry, S. C. Critchlow and J. M. Mayer, *J. Am. Chem. Soc.*, 1989, **111**, 8741–8742.
- 84 W. Wang, L. B. Fullmer, N. A. G. Bandeira, S. Goberna-Ferrón, L. N. Zakharov, C. Bo, D. A. Keszler and M. Nyman, *Chem*, 2016, **1**, 887–901.
- 85 W. H. Casey, *Chem. Rev.*, 2006, **106**, 1–16.
- 86 M. T. Pope, *Angew. Chemie*, 1984, **96**, 730.
- 87 G. N. Newton, S. Yamashita, K. Hasumi, J. Matsuno, N. Yoshida, M. Nihei, T. Shiga, M. Nakano, H. Nojiri, W. Wernsdorfer and H. Oshio, *Angew. Chemie - Int. Ed.*, 2011, **50**, 5716–5720.
- 88 A. M. Ako, I. J. Hewitt, V. Mereacre, R. Clérac, W. Wernsdorfer, C. E. Anson and A. K. Powell, *Angew. Chemie - Int. Ed.*, 2006, **45**, 4926–4929.
- 89 N. V. Izarova, A. Kondinski, N. Vankova, T. Heine, P. Jäger, F. Schinle, O. Hampe and U. Kortz, *Chem. - A Eur. J.*, 2014, **20**, 8556–8560.
- 90 J. H. Son, D. H. Park, D. A. Keszler and W. H. Casey, *Chem. - A Eur. J.*, 2015, **21**, 6727–6731.
- 91 J. T. Rhule, C. L. Hill, D. A. Judd and R. F. Schinazi, *Chem. Rev.*, 1998, **98**, 327–357.
- 92 C. Busche, L. Vilà-Nadal, J. Yan, H. N. Miras, D. L. Long, V. P. Georgiev, A. Asenov, R. H. Pedersen, N. Gadegaard, M. M. Mirza, D. J. Paul, J. M. Poblet and L. Cronin, *Nature*, 2014, **515**, 545–549.
- 93 A. Llordés, G. Garcia, J. Gazquez and D. J. Milliron, *Nature*, 2013, **500**, 323–326.
- 94 A. Roucoux, J. Schulz and H. Patin, *Chem. Rev.*, 2002, **102**, 3757–3778.
- 95 N. T. K. Thanh, N. Maclean and S. Mahiddine, *Chem. Rev.*, 2014, **114**, 7610–7630.
- 96 L. R. Baker, G. Kennedy, J. M. Krier, M. Van Spronsen, R. M. Onorato and G. A. Somorjai, *Catal. Letters*, 2012, **142**, 1286–1294.
- 97 X. López, J. J. Carbó, C. Bo and J. M. Poblet, *Chem. Soc. Rev.*, 2012, **41**, 7537–7571.
- 98 R. H. Holm, *Chem. Rev.*, 1987, **87**, 1401–1449.
- 99 A. Müller, E. Krickemeyer, J. Meyer, H. Bögge, F. Peters, W. Plass, E. Diemann, S. Dillinger, F. Nonnenbruch, M. Randerath and C. Menke, *Angew. Chemie Int. Ed. English.*, 1995, **34**, 2122–2124.
- 100 A. Müller, E. Beckmann, H. Bögge, M. Schmidtman and A. Dress, *Angew. Chemie - Int. Ed.*, 2002, **41**, 1162–1167.
- 101 S. Liu, Z. Tang, E. Wang and S. Dong, *Electrochem. commun.*, 2000, **2**, 800–804.
- 102 M. Ammam, *J. Mater. Chem. A.*, 2013, **1**, 6291–6312.
- 103 M. T. Pope and A. Müller, *Angew. Chemie Int. Ed. English.*, 1991, **30**, 34–48.
- 104 J. Lin, Z. Ding, Y. Hou and X. Wang, *Sci. Rep.*, 2013, **3**, 1056–1061.
- 105 Y. Liu, A. Z. Fire, S. Boyd and R. A. Olshen, *Estimating Clonality.*, 2014, 1–20.
- 106 S. S. Wang and G. Y. Yang, *Chem. Rev.*, 2015, **115**, 4893–4962.

- 107 K. Eguchi, T. Seiyama, N. Yamazoe, S. Katsuki and H. Taketa, *J. Catal.*, 1988, **111**, 336–344.
- 108 A. Kondinski and T. N. Parac-Vogt, *Front. Chem.* 2018, **6**, 346.
- 109 M. T. Pope, *Inorg. Chem.*, 1972, **11**, 1973–1974.
- 110 N. I. Gumerova and A. Rompel, *Nat. Rev. Chem.*, 2018, **2**, 112.
- 111 K. Nomiya and M. Miwa, *Polyhedron.*, 1984, **3**, 341–346.
- 112 M. E. Weeks, *J. Chem. Educ.*, 1933, **10**, 223–227.
- 113 A. E. Williams-Jones and O. V. Vasyukova, *Econ. Geol.*, 2018, **113**, 973–988.
- 114 C. Van Cleave and D. C. Crans, *Inorganics.*, 2019, **7**, 111.
- 115 R. Anwander, *Angew. Chemie - Int. Ed.*, 1998, **37**, 599–602.
- 116 D. S. Zhang, B. Q. Ma, T. Z. Jin, G. Song, C. H. Yan and T. C. W. Mak, *New J. Chem.*, 2000, **24**, 61–62.
- 117 Y. M. Byun and S. Ögüt, *J. Chem. Phys.*, 2019, **151**, 134305.
- 118 S. Stevenson, M. A. Mackey, M. A. Stuart, J. P. Phillips, M. L. Easterling, C. J. Chancellor, M. M. Olmstead and A. L. Balch, *J. Am. Chem. Soc.*, 2008, **130**, 11844–11845.
- 119 J. M. Gonzales, R. A. King and H. F. Schaefer, *J. Chem. Phys.*, 2000, **113**, 567–572.
- 120 D. L. Freeman and J. D. Doll, *Annu. Rev. Phys. Chem.*, 1996, **47**, 43–80.
- 121 K. A. Moltved and K. P. Kepp, *J. Phys. Chem. C.*, 2019, **123**, 18432–18444.
- 122 J. D. Ayala, G. Vicentini and G. Bombieri, *J. Alloys Compd.*, 1995, **225**, 357–362.
- 123 E. P. Turevskaya, A. I. Belokon', Z. A. Starikova, A. I. Yanovsky, E. N. Kiruschenkov and N. Y. Turova, *Polyhedron.*, 2000, **19**, 705–711.
- 124 M. C. Bernini, N. Snejko, E. Gutierrez-Puebla and A. Monge, *CrystEngComm.*, 2011, **13**, 1797–1800.
- 125 Y. Y. Wu, W. Luo, Y. H. Wang, Y. Y. Pu, X. Zhang, L. S. You, Q. Y. Zhu and J. Dai, *Inorg. Chem.*, 2012, **51**, 8982–8988.
- 126 M. Czakler, C. Artner and U. Schubert, *New J. Chem.*, 2018, **42**, 12098–12103.
- 127 X. Chen and S. S. Mao, *Chem. Rev.*, 2007, **107**, 2891–2959.
- 128 G. Zhang, J. Hou, M. Li, C. H. Tung and Y. Wang, *Inorg. Chem.*, 2016, **55**, 4704–4709.
- 129 R. H. Wu, M. Guo, M. X. Yu and L. G. Zhu, *Dalt. Trans.*, 2017, **46**, 14348–14355.
- 130 N. Steunou, G. Kickelbick, K. Boubekeur and C. Sanchez, *J. Chem. Soc. - Dalt. Trans.*, 1999, 3653–3655.
- 131 C. F. Campana, Y. Chen, V. W. Day, W. G. Klemperer and R. A. Sparks, *J. Chem. Soc. - Dalt. Trans.* 1999, 1045–1124.
- 132 J. B. Benedict, R. Freindorf, E. Trzop, J. Cogswell and P. Coppens, *J. Am. Chem. Soc.*, 2010, **132**, 13669–13671.
- 133 C. Sanchez, L. Rozes, F. Ribot, C. Laberty-Robert, D. Grosso, C. Sassoie, C. Boissiere and L. Nicole, *Comptes Rendus Chim.*, 2010, **13**, 3–39.

- 134 M. Dan-Hardi, C. Serre, T. Frot, L. Rozes, G. Maurin, C. Sanchez and G. Férey, *J. Am. Chem. Soc.*, 2009, **131**, 10857–10859.
- 135 H. Schmidt, *Applied Organometallic Chemistry.*, 2001, **15**, 331–343.
- 136 I. Mijatovic, G. Kickelbick, M. Puchberger and U. Schubert, *New J. Chem.*, 2003, **27**, 3–5.
- 137 U. Schubert, *Chem. Soc. Rev.*, 2011, **40**, 575–582.
- 138 P. Piszczek, A. Radtke, T. Muzioł, M. Richert and J. Chojnacki, *Dalt. Trans.*, 2012, **41**, 8261–8269.
- 139 P. Piszczek, M. Richert, A. Grodzicki, T. Głowiak and A. Wojtczak, *Polyhedron.*, 2005, **24**, 663–670.
- 140 P. Piszczek, M. Richert and A. Wojtczak, *Polyhedron.*, 2008, **27**, 602–608.
- 141 L. Rozes and C. Sanchez, *Chem. Soc. Rev.*, 2011, **40**, 1006–1030.
- 142 P. Piszczek, M. Richert, A. Radtke, T. Muzioł and A. Wojtczak, *Polyhedron.*, 2009, **28**, 3872–3880.
- 143 A. Radtke, P. Piszczek, T. Muzioł and A. Wojtczak, *Inorg. Chem.*, 2014, **53**, 10803–10810.
- 144 X. Lei, M. Shang, A. Patil, E. E. Wolf and T. P. Fehlner, *Inorg. Chem.*, 1996, **35**, 3217–3222.
- 145 U. Schubert, *J. Mater. Chem.*, 2005, **15**, 3701–3715.
- 146 M. Inoue, in *Chemical Processing of Ceramics, Second Edition*, CRC Press, Boca Raton, 2005.
- 147 R. A. Sperling and W. J. Parak, *Philos. Trans. R. Soc. A Math. Phys. Eng. Sci.*, 2010, **368**, 1333–1383.
- 148 C. Liu, J. Hu, F. Zhu, J. Zhan, L. Du, C. H. Tung and Y. Wang, *Chem. - A Eur. J.*, 2019, **25**, 14843–14849.
- 149 G. Fornasieri, L. Rozes, S. Le Calvé, B. Alonso, D. Massiot, M. N. Rager, M. Evain, K. Boubekeur and C. Sanchez, *J. Am. Chem. Soc.*, 2005, **127**, 4869–4878.
- 150 M. B. Badia, V. G. Maurino, T. Pavlovic, C. L. Arias, M. A. Pagani, C. S. Andreo, M. Saigo, M. F. Drincovich and M. C. Gerrard Wheeler, *Plant J.*, 2019, **101**, 652–665.
- 151 M. Stuckart and K. Y. Monakhov, *Encyclopedia of Inorganic and Bioinorganic Chemistry*, 2018, 1–19.
- 152 K. Kastner, J. Forster, H. Ida, G. N. Newton, H. Oshio and C. Streb, *Chem. - A Eur. J.*, 2015, **21**, 7686–7689.
- 153 U. Kortz, *Eur. J. Inorg. Chem.*, 2009, 5056–5276.
- 154 W. Guan, L. K. Yan, Z. M. Su, E. B. Wang and X. H. Wang, *Int. J. Quantum Chem.*, 2006, **106**, 1860–1864.
- 155 D. C. Crans, *Pure and Applied Chemistry.*, 2005, **77**, 1497–1527.
- 156 L. Pettersson, I. Andersson and O. W. Howarth, *Inorg. Chem.*, 1992, **31**, 4032–4033.
- 157 H. Ichida, K. Nagai, Y. Sasaki and M. T. Pope, *J. Am. Chem. Soc.*, 1989, **111**, 586–591.
- 158 J. W. Emsley and J. Feeney, *Prog. Nucl. Magn. Reson. Spectrosc.*, 2007, **50**, 179–198.
- 159 M. I. Khan, Q. Chen, D. P. Goshorn and J. Zubieta, *Inorg. Chem.*, 1993, **32**, 672–680.

- 160 H. Weihe and H. U. Güdel, *J. Am. Chem. Soc.*, 1998, **120**, 2870–2879.
- 161 S. L. Castro, Z. Sun, C. M. Grant, J. C. Bollinger, D. N. Hendrickson and G. Christou, *J. Am. Chem. Soc.*, 1998, **120**, 2365–2375.
- 162 P. L. W. Tregenna-Piggott, H. Weihe, J. Bendix, A.-L. Barra and H.-U. Güdel, *Inorg. Chem.*, 1999, **38**, 5928–5929.
- 163 M. Sadakane and E. Steckhan, *Chem. Rev.*, 1998, **98**, 219–237.
- 164 D. Gatteschi, L. Pardi, A. L. Barra, A. Müller and J. Döring, *Nature*, 1991, **354**, 463–465.
- 165 K. Hegetschweiler, B. Morgenstern, J. Zubieta, P. J. Hagrman, N. Lima, R. Sessoli and F. Totti, *Angew. Chemie - Int. Ed.*, 2004, **43**, 3436–3439.
- 166 I. S. Tidmarsh, R. H. Laye, P. R. Brearley, M. Shanmugam, E. C. Sañudo, L. Sorace, A. Caneschi and E. J. L. McInnes, *Chem. Commun.*, 2006, 2560–2562.
- 167 J. Spandl, C. Daniel, I. Brüdgam and H. Hartl, *Angew. Chemie - Int. Ed.*, 2003, **42**, 1163–1166.
- 168 J. K. Li, X. Q. Huang, S. Yang, H. W. Ma, Y. N. Chi and C. W. Hu, *Inorg. Chem.*, 2015, **54**, 1454–1461.
- 169 M. P. Santoni, G. La Ganga, V. Mollica Nardo, M. Natali, F. Puntoriero, F. Scandola and S. Campagna, *J. Am. Chem. Soc.*, 2014, **136**, 8189–8192.
- 170 L. E. VanGelder, W. W. Brennessel and E. M. Matson, *Dalt. Trans.*, 2018, **47**, 3698–3704.
- 171 M. I. Khan and J. Zubieta, *Progress in Inorganic Chemistry*, 2007, **43**, 1–149.
- 172 Q. Chen and J. Zubieta, *Inorg. Chem.*, 1990, **29**, 1456–1458.
- 173 M. Søndergaard, *Encyclopedia of Inland Waters*, 2009, 852–859.
- 174 G. B. Karet, Z. Sun, D. D. Heinrich, J. K. McCusker, K. Folting, W. E. Streib, J. C. Huffman, D. N. Hendrickson and G. Christou, *Inorg. Chem.*, 1996, **35**, 6450–6460.
- 175 S. B. Yu, R. H. Holm and G. C. Papaefthymiou, *Inorg. Chem.*, 1991, **30**, 3476–3485.
- 176 Q. Chen, D. P. Goshorn, C. P. Scholes, X. L. Tan and J. Zubieta, *J. Am. Chem. Soc.*, 1992, **114**, 4667–4681.
- 177 I. V. Kurganskii, E. S. Bazhina, A. A. Korlyukov, K. A. Babeshkin, N. N. Efimov, M. A. Kiskin, S. L. Veber, A. A. Sidorov, I. L. Eremenko and M. V. Fedin, *Molecules.*, 2019, **24**, 4582.
- 178 P. Gouzerh and A. Proust, *Chem. Rev.*, 1998, **98**, 77–111.
- 179 F. Dong, S. Heinbuch, Y. Xie, E. R. Bernstein, J. J. Rocca, Z. C. Wang, X. L. Ding and S. G. He, *J. Am. Chem. Soc.*, 2009, **131**, 1057–1066.
- 180 J. Hermenau, M. Ternes, M. Steinbrecher, R. Wiesendanger and J. Wiebe, *Nano Lett.*, 2018, **18**, 1978–1983.
- 181 J. H. Cary, H. I. Maibach, D. Burrows and J. J. Hostynek, *Kanerva's Occupational Dermatology*, 2019, 647–660.
- 182 E. C. Constable and C. E. Housecroft, *Chem. Soc. Rev.*, 2013, **42**, 1429–1439.
- 183 K. H. Theopold, *Encyclopedia of Inorganic Chemistry*, 2nd ed., R. B. King ed., Wiley: New York, 2005.

- 184 S. Parsons, A. A. Smith and R. E. P. Winpenny, *Chem. Commun.*, 2000, 579–580.
- 185 E. K. Brechin, S. G. Harris, S. Parsons and R. E. P. Winpenny, *Chem. Commun.*, 1996, 1439–1440.
- 186 I. M. Atkinson, C. Benelli, M. Murrie, S. Parsons and R. E. P. Winpenny, *Chem. Commun.*, 1999, **7**, 285–286.
- 187 K. L. Taft, S. J. Lippard, C. D. Delfs, D. Gatteschi, G. C. Papaefthymiou and S. Foner, *J. Am. Chem. Soc.*, 1994, **116**, 823–832.
- 188 S. P. Watton, P. Fuhrmann, L. E. Pence, A. Caneschi, A. Cornia, G. L. Abbati and S. J. Lippard, *Angew. Chemie (International Ed. English)*, 1997, **36**, 2774–2776.
- 189 J. Overgaard, B. B. Iversen, S. P. Paliy, G. A. Timco, N. V. Gerbeleu and F. K. Larsen, *Chem. - A Eur. J.*, 2002, **8**, 2775–2786.
- 190 M. Eshel, A. Bino, I. Felner, D. C. Johnston, M. Luban and L. L. Miller, *Inorg. Chem.*, 2000, **39**, 1376–1380.
- 191 W. Schmitt, P. A. Jordan, R. K. Henderson, G. R. Moore, C. E. Anson and A. K. Powell, *Coord. Chem. Rev.*, 2002, **228**, 115–126.
- 192 W. Schmitt, M. Murugesu, J. C. Goodwin, J. P. Hill, A. Mandel, R. Bhalla, C. E. Anson, S. L. Heath and A. K. Powell, *Polyhedron.*, 2001, **20**, 1687–1697.
- 193 A. C. Royer, R. D. Rogers, D. L. Arrington, S. C. Street and J. B. Vincent, *Polyhedron.*, 2002, **21**, 155–165.
- 194 M. Murrie, S. Parsons, R. E. P. Winpenny, F. E. Mabbs, E. J. L. McInnes, C. C. Wilson and G. M. Smith, *Chem. Commun.*, 1999, **7**, 643–644.
- 195 S. B. Mukkamala, R. Clérac, C. E. Anson and A. K. Powell, *Polyhedron.*, 2006, **25**, 530–538.
- 196 E. K. Brechin, *Chem. Commun.*, 2005, 5141–5153.
- 197 E. J. L. McInnes, S. Piligkos, G. A. Timco and R. E. P. Winpenny, *Coord. Chem. Rev.*, 2005, **249**, 2577–2590.
- 198 R. H. Laye and E. J. L. McInnes, *Eur. J. Inorg. Chem.*, 2004, 2811–2818.
- 199 C. E. Talbot-Eeckelaers, G. Rajaraman, J. Cano, G. Aromí, E. Ruiz and E. K. Brechin, *Eur. J. Inorg. Chem.*, 2006, 3382–3392.
- 200 W. Wang, M. Amiri, K. Kozma, J. Lu, L. N. Zakharov and M. Nyman, *Eur. J. Inorg. Chem.*, 2018, **2018**, 4638–4642.
- 201 J. Baumgartner, A. Dey, P. H. H. Bomans, C. Le Coadou, P. Fratzl, N. A. J. M. Sommerdijk and D. Faivre, *Nat. Mater.*, 2013, **12**, 310–314.
- 202 O. Sadeghi, L. N. Zakharov and M. Nyman, *Science.*, 2015, **347**, 1359–1362.
- 203 D. Barats, G. Leitus, R. Popovitz-Biro, L. J. W. Shimon and R. Neumann, *Angew. Chemie - Int. Ed.*, 2008, **47**, 9908–9912.
- 204 Q. Yin, J. M. Tan, C. Besson, Y. V. Geletii, D. G. Musaev, A. E. Kuznetsov, Z. Luo, K. I. Hardcastle and C. L. Hill, *Science (80-)*, 2010, **328**, 342–345.
- 205 E. M. Wylie, K. M. Peruski, J. L. Weidman, W. A. Phillip and P. C. Burns, *ACS Appl. Mater. Interfaces.*, 2014, **6**, 473–479.

- 206 M. Nyman and P. C. Burns, *Chem. Soc. Rev.*, 2012, **41**, 7354–7367.
- 207 E. C. Yang, S. Y. Huang, W. Wernsdorfer, L. X. Hong, M. Damjanovic, L. Niekamp and G. H. Lee, *RSC Adv.*, 2019, **9**, 37740–37746.
- 208 T. R. Cook, Y. R. Zheng and P. J. Stang, *Chem. Rev.*, 2013, **113**, 734–777.
- 209 D. Bansal, A. Mondal, N. Lakshminarasimhan and R. Gupta, *Dalt. Trans.*, 2019, **48**, 7918–7927.
- 210 K. L. Taft, L. E. Pence, S. J. Lippard, A. Caneschi, C. D. Delfs and G. C. Papaefthymiou, *J. Am. Chem. Soc.*, 1993, **115**, 11753–11766.
- 211 A. Caneschi, A. Cornia, A. C. Fabretti, S. Foner, D. Gatteschi, R. Grandi and L. Schenetti, *Chem. - A Eur. J.*, 1996, **2**, 1379–1387.
- 212 G. L. Abbati, A. Cornia, A. C. Fabretti, W. Malavasi, L. Schenetti, A. Caneschi and D. Gatteschi, *Inorg. Chem.*, 1997, **36**, 6443–6446.
- 213 P. Abbasi, K. Quinn, D. I. Alexandropoulos, M. Damjanović, W. Wernsdorfer, A. Escuer, J. Mayans, M. Pilkington and T. C. Stamatatos, *J. Am. Chem. Soc.*, 2017, **139**, 15644–15647.
- 214 G. L. Abbati, A. Cornia, A. C. Fabretti, A. Caneschi and D. Gatteschi, *Inorg. Chem.*, 1998, **37**, 3759–3766.
- 215 N. C. Harden, M. A. Bolcar, W. Wernsdorfer, K. A. Abboud, W. E. Streib and G. Christou, *Inorg. Chem.*, 2003, **42**, 7067–7076.
- 216 M. Murugesu, M. Habrych, W. Wernsdorfer, K. A. Abboud and G. Christou, *J. Am. Chem. Soc.*, 2004, **126**, 4766–4767.
- 217 A. J. Tasiopoulos, A. Vinslava, W. Wernsdorfer, K. A. Abboud and G. Christou, *Angew. Chemie - Int. Ed.*, 2004, **43**, 2117–2121.
- 218 B. Yao, M. K. Singh, Y. F. Deng, Y. N. Wang, K. R. Dunbar and Y. Z. Zhang, *Inorg. Chem.*, 2020, **59**, 8505–8513.
- 219 P. Bhatt, A. Kumar, C. Ritter and S. M. Yusuf, *J. Phys. Chem. C.*, 2020, **124**, 19228–19239.
- 220 J. N. Boyn, J. N. Boyn, J. Xie, J. S. Anderson, D. A. Mazziotti and D. A. Mazziotti, *J. Phys. Chem. Lett.*, 2020, **11**, 4584–4590.
- 221 C. J. Milios, A. Vinslava, W. Wernsdorfer, S. Moggach, S. Parsons, S. P. Perlepes, G. Christou and E. K. Brechin, *J. Am. Chem. Soc.*, 2007, **129**, 2754–2755.
- 222 T. Shiga, H. Nojiri and H. Oshio, *Inorg. Chem.*, 2020, **59**, 4163–4166.
- 223 L. K. Thompson, O. Waldmann and Z. Xu, *Coord. Chem. Rev.*, 2005, **249**, 2677–2690.
- 224 M. Murugesu, A. Mishra, W. Wernsdorfer, K. A. Abboud and G. Christou, *Polyhedron.*, 2006, **25**, 613–625.
- 225 J. C. Goodwill, R. Sessoli, D. Gatteschi, W. Wernsdorfer, A. K. Powell and S. L. Heath, *J. Chem. Soc. Dalt. Trans.*, 2000, 1835–1840.
- 226 C. Y. Shao, L. L. Zhu and P. P. Yang, *Zeitschrift fur Anorg. und Allg. Chemie*, 2012, **638**, 1307–1310.
- 227 C. Boskovic, W. Wernsdorfer, K. Folting, J. C. Huffman, D. N. Hendrickson and G. Christou, *Inorg. Chem.*, 2002, **41**, 5107–5118.

- 228 T. C. Stamatatos, K. A. Abboud, W. Wernsdorfer and G. Christou, *Angew. Chemie - Int. Ed.*, 2007, **46**, 884–888.
- 229 D. B. Huo, J. D. Leng, J. Wang, Z. Z. Wang, W. M. Lu, X. S. Hong, A. J. Zhou and Y. Y. Lin, *J. Coord. Chem.*, 2017, **70**, 936–948.
- 230 H. Oshio and M. Nakano, *Chem. - A Eur. J.*, 2005, **11**, 5178–5185.
- 231 N. Berg, T. Rajeshkumar, S. M. Taylor, E. K. Brechin, G. Rajaraman and L. F. Jones, *Chem. - A Eur. J.*, 2012, **18**, 5906–5918.
- 232 D. Gatteschi and R. Sessoli, *J. Magn. Magn. Mater.*, 2004, **272–276**, 1030–1036.
- 233 C. Cañada-Vilalta, T. A. O'Brien, M. Pink, E. R. Davidson and G. Christou, *Inorg. Chem.*, 2003, **42**, 7819–7829.
- 234 T. Glaser, T. Lügger and R. D. Hoffmann, *Eur. J. Inorg. Chem.*, 2004, 2356–2362.
- 235 A. L. Barra, L. C. Brunel, D. Gatteschi, L. Pardi and R. Sessoli, *Acc. Chem. Res.*, 1998, **31**, 460–466.
- 236 L. F. Jones, E. K. Brechin, D. Collison, J. Raftery and S. J. Teat, *Inorg. Chem.*, 2003, **42**, 6971–6973.
- 237 M. D. Godbole, O. Roubeau, A. M. Mills, H. Kooijman, A. L. Spek and E. Bouwman, *Inorg. Chem.*, 2006, **45**, 6713–6722.
- 238 D. Foguet-Albiol, K. A. Abboud and G. Christou, *Chem. Commun.*, 2005, 4282–4284.
- 239 T. Taguchi, M. S. Thompson, K. A. Abboud and G. Christou, *Dalt. Trans.*, 2010, **39**, 9131–9139.
- 240 I. A. Gass, C. J. Milios, M. Evangelisti, S. L. Heath, D. Collison, S. Parsons and E. K. Brechin, *Polyhedron.*, 2007, **26**, 1835–1837.
- 241 D. Gatteschi, R. Sessoli and A. Cornia, *Chem. Commun.*, 2000, 725–732.
- 242 A. K. Powell, S. L. Heath, D. Gatteschi, L. Pardi, R. Sessoli, G. Spina, F. Del Giallo and F. Pieralli, *J. Am. Chem. Soc.*, 1995, **117**, 2491–2502.
- 243 C. Cañada-Vilalta, T. A. O'Brien, E. K. Brechin, M. Pink, E. R. Davidson and G. Christou, *Inorg. Chem.*, 2004, **43**, 5505–5521.
- 244 O. Botezat, J. Van Leusen, P. Kögerler and S. G. Baca, *Inorg. Chem.*, 2018, **57**, 7904–7913.
- 245 K. Graham, F. J. Douglas, J. S. Mathieson, S. A. Moggach, J. Schnack and M. Murrie, *Dalt. Trans.*, 2011, **40**, 12271–12276.
- 246 A. Bino, M. Ardon, D. Lee, B. Spingler and S. J. Lippard, *J. Am. Chem. Soc.*, 2002, **124**, 4578–4579.
- 247 G. Johansson, L.-O. Gullman, A. Kjekshus and R. Söderquist, *Acta Chem. Scand.*, 1960, **14**, 771–773.
- 248 J. F. Keggin, *Nature.*, 1933, **132**, 351.
- 249 W. B. Kamb, *Acta Crystallogr.*, 1960, **13**, 15–24.
- 250 B. Li, J. W. Zhao, S. T. Zheng and G. Y. Yang, *Inorg. Chem. Commun.*, 2009, **12**, 69–71.
- 251 *Proc. R. Soc. London. Ser. A, Contain. Pap. a Math. Phys. Character.*, 1934, **144**, 75–100.

- 252 G. Johansson, G. Lundgren, L. G. Sillén and R. Söderquist, *Acta Chem. Scand.*, 1960, **14**, 769–771.
- 253 A. E. Dearle, D. J. Cutler, H. W. L. Fraser, S. Sanz, E. Lee, S. Dey, I. F. Diaz-Ortega, G. S. Nichol, H. Nojiri, M. Evangelisti, G. Rajaraman, J. Schnack, L. Cronin and E. K. Brechin, *Angew. Chemie - Int. Ed.*, 2019, **58**, 16903–16906.
- 254 A. P. Singh, R. P. Joshi, K. A. Abboud, J. E. Peralta and G. Christou, *Polyhedron.*, 2020, **176**, 114182.
- 255 A. Haider, M. Ibrahim, B. S. Bassil, A. M. Carey, A. N. Viet, X. Xing, W. W. Ayass, J. F. Miñambres, R. Liu, G. Zhang, B. Keita, V. Mereacre, A. K. Powell, K. Balinski, A. T. N'Diaye, K. Küpper, H. Y. Chen, U. Stimming and U. Kortz, *Inorg. Chem.*, 2016, **55**, 2755–2764.
- 256 S. T. Zheng and G. Y. Yang, *Chem. Soc. Rev.*, 2012, **41**, 7623–7646.
- 257 D. M. Kurtz, *Chem. Rev.*, 1990, **90**, 585–606.
- 258 B. Botar, Y. V. Geletii, P. Kögerler, D. G. Musaev, K. Morokuma, I. A. Weinstock and C. L. Hill, *J. Am. Chem. Soc.*, 2006, **128**, 11268–11277.
- 259 J. D. Compain, P. Mialane, A. Dolbecq, I. M. Mbomekallé, J. Marrot, F. Sécheresse, E. Rivière, G. Rogez and W. Wernsdorfer, *Angew. Chemie - Int. Ed.*, 2009, **48**, 3077–3081.
- 260 M. S. Liao, M. J. Huang and J. D. Watts, *J. Phys. Chem. A.*, 2010, **114**, 9554–9569.
- 261 A. S. Ogun, N. V. Joy and M. Valentine, *StatPearls.*, 2020, 1-3.
- 262 M. Shepherd, A. E. Medlock and H. A. Dailey, *Encyclopedia of Biological Chemistry: Second Edition*, Academic Press, 2013, 544–549.
- 263 D. Buongiorno and G. D. Straganz, *Coord. Chem. Rev.*, 2013, **257**, 541–563.
- 264 N. Shivran, S. C. Gadekar and V. G. Anand, *Chem. - An Asian J.*, 2017, **12**, 6–20.
- 265 M. Worwood, *Blood Rev.*, 1990, **4**, 259–269.
- 266 L. Lisnard, F. Tuna, A. Candini, M. Affronte, R. E. P. Winpenny and E. J. L. McInnes, *Angew. Chemie - Int. Ed.*, 2008, **120**, 9841–9845.
- 267 P. J. Hagrman, D. Hagrman and J. Zubietta, *Angew. Chemie - Int. Ed.*, 1999, **38**, 2638–2684.
- 268 J. L. Rodríguez-López, F. Aguilera-Granja, K. Michaelian and A. Vega, in *Journal of Alloys and Compounds*, 2004, **369**, 93–96.
- 269 Z. Q. Li, Y. Hashi and Y. Kawazoe, *J. Magn. Magn. Mater.*, 1997, **167**, 123–128.
- 270 Y. Jinlong, X. Chuanyun, X. Shangda and W. Kelin, *Phys. Rev. B*, 1993, **48**, 12155–12163.
- 271 O. Kitakami, H. Sato, Y. Shimada, F. Sato and M. Tanaka, *Phys. Rev. B - Condens. Matter Mater. Phys.*, 1997, **56**, 13849–13854.
- 272 E. K. Parks, B. J. Winter, T. D. Klots and S. J. Riley, *J. Chem. Phys.*, 1992, **96**, 8267–8274.
- 273 L. Dong, X. Li, J. Cao, W. Chu and R. Huang, *Dalt. Trans.*, 2013, **42**, 1342–1345.
- 274 S. Hong, F. F. Pfaff, E. Kwon, Y. Wang, M. S. Seo, E. Bill, K. Ray and W. Nam, *Angew. Chemie - Int. Ed.*, 2014, **53**, 10403–10407.
- 275 B. Wang, Y. M. Lee, W. Y. Tcho, S. Tussupbayev, S. T. Kim, Y. Kim, M. S. Seo, K. Bin Cho, Y. Dede, B. C. Keegan, T. Ogura, S. H. Kim, T. Ohta, M. H. Baik, K. Ray, J. Shearer and W. Nam,

- Nat. Commun.*, 2017, **8**, 14839.
- 276 E. Andris, R. Navrátil, J. Jašík, M. Srnec, M. Rodríguez, M. Costas and J. Roithová, *Angew. Chemie - Int. Ed.*, 2009, **58**, 9619–9624.
- 277 W. Wernsdorfer, T. C. Stamatatos and G. Christou, *Phys. Rev. Lett.*, 2008, **101**, 237204.
- 278 M. Moragues-Cánovas, É. Rivière, L. Ricard, C. Paulsen, W. Wernsdorfer, G. Rajaraman, E. K. Brechin and T. Mallah, *Adv. Mater.*, 2004, **16**, 1101–1105.
- 279 J. Y. Xu, X. Qiao, H. Bin Song, S. P. Yan, D. Z. Liao, S. Gao, Y. Journaux and J. Cano, *Chem. Commun.*, 2008, 6414–6416.
- 280 J. W. Zhao, C. M. Wang, J. Zhang, S. T. Zheng and G. Y. Yang, *Chem. - A Eur. J.*, 2008, **14**, 9223–9239.
- 281 A. Proust, R. Thouvenot and P. Gouzerh, *Chem. Commun.*, 2008, 1837–1852.
- 282 H. M. Zhang, Y. G. Li, Y. Lu, R. Clérac, Z. M. Zhang, Q. Wu, X. J. Feng and E. B. Wang, *Inorg. Chem.*, 2009, **48**, 10889–10891.
- 283 Q. Wu, Y. G. Li, Y. H. Wang, E. B. Wang, Z. M. Zhang and R. Clérac, *Inorg. Chem.*, 2009, **48**, 1606–1612.
- 284 U. Kortz, I. M. Mbomekalle, B. Keita, L. Nadjo and P. Berthet, *Inorg. Chem.*, 2002, **41**, 6412–6416.
- 285 L. Dong, R. Huang, Y. Wei and W. Chu, *Inorg. Chem.*, 2009, **48**, 7528–7530.
- 286 C. Cadiou, M. Murrie, C. Paulsen, V. Villar, W. Wernsdorfer and R. E. P. Winpenny, *Chem. Commun.*, 2001, **1**, 2666–2667.
- 287 A. Mukherjee, M. Nethaji and A. R. Chakravarty, *Angew. Chemie - Int. Ed.*, 2004, **43**, 87–90.
- 288 K. Geetha, M. Nethaji and A. R. Chakravarty, *Inorg. Chem.*, 1998, **37**, 2612–2612.
- 289 H. Oshio, Y. Saito and T. Ito, *Angew. Chemie (International Ed. English)*, 1997, **36**, 2673–2675.
- 290 A. Mukherjee, M. K. Saha, M. Nethaji and A. R. Chakravarty, *Polyhedron*, 2004, **23**, 2177–2182.
- 291 B. V. Agarwala, L. Ilcheva, J. Bjerrum, G. V. Romanov, V. P. Spiridonov, T. G. Strand and V. F. Sukhoverkhov, *Acta Chem. Scand.*, 1980, **34a**, 725–731.
- 292 W. H. Brock, K. A. Jensen, C. K. Jørgensen and G. B. Kauffman, *Polyhedron*, 1983, **2**, 1–7.
- 293 G. P. Stahly, *Cryst. Growth Des.*, 2007, **7**, 1007–1026.
- 294 F. Bramsen, A. D. Bond, C. J. McKenzie, R. G. Hazell, B. Moubaraki and K. S. Murray, *Chem. - A Eur. J.*, 2005, **11**, 825.
- 295 C. Bazzicalupi, A. Bianchi, C. Giorgi, P. Gratteri, P. Mariani and B. Valtancoli, *Inorg. Chem.*, 2013, **52**, 2125–2137.
- 296 A. Biswas, L. K. Das, M. G. B. Drew, C. Diaz and A. Ghosh, *Inorg. Chem.*, 2012, **51**, 10111–10121.
- 297 J. M. Clemente-Juan, E. Coronado and A. Gaita-Ariño, *Chem. Soc. Rev.*, 2012, **41**, 7464–7478.
- 298 S. Majumder, S. Sarkar, S. Sasmal, E. C. Sañudo and S. Mohanta, *Inorg. Chem.*, 2011, **50**, 7540–7554.

- 299 P. K. Nanda, V. Bertolasi, G. Aromí and D. Ray, *Polyhedron.*, 2009, **28**, 987–993.
- 300 M. Sarkar, R. Clérac, C. Mathonière, N. G. R. Hearn, V. Bertolasi and D. Ray, *Inorg. Chem.*, 2010, **49**, 6575–6585.
- 301 A. K. Ghosh, R. Clérac, C. Mathonière and D. Ray, *Polyhedron*, 2013, **54**, 196–200.
- 302 A. A. Mohamed, S. Ricci, A. Burini, R. Galassi, C. Santini, G. M. Chiarella, D. Y. Melgarejo and J. P. Fackler, *Inorg. Chem.*, 2011, **50**, 1014–1020.
- 303 Q. T. He, X. P. Li, Y. Liu, Z. Q. Yu, W. Wang and C. Y. Su, *Angew. Chemie - Int. Ed.*, 2009, **48**, 6156–6159.
- 304 A. Asokan, B. Varghese and P. T. Manoharan, *Inorg. Chem.*, 1999, **38**, 4393–4399.
- 305 A. V. Davis and K. N. Raymond, *J. Am. Chem. Soc.*, 2005, **127**, 7912–7919.
- 306 R. D. Hancock, H. Maumela and A. S. De Sousa, *Coord. Chem. Rev.*, 1996, **148**, 315–347.
- 307 A. K. Ghosh, M. Pait, R. Clérac, C. Mathonière, V. Bertolasi, A. Bauzá, A. Frontera, K. Pramanik and D. Ray, *Dalt. Trans.*, 2014, **43**, 4076–4085.
- 308 J. N. A. Zhao, L. Mi, J. Hu, H. Hou and Y. Fan, *J. Am. Chem. Soc.*, 2008, **130**, 15222–15223.
- 309 S. Alvarez, *Dalt. Trans.*, 2013, **42**, 8617–8636.
- 310 A. Müller, S. Sarkar, S. Q. N. Shah, H. Bögge, M. Schmidtmann, S. Sarkar, P. Kögerler, B. Hauptfleisch, A. X. Trautwein and V. Schünemann, *Angew. Chemie - Int. Ed.*, 1999, **38**, 3238–3241.
- 311 A. J. Blake, R. O. Gould, P. E. Y. Milne and R. E. P. Winpenny, *J. Chem. Soc. Chem. Commun.*, 1991, 1453–1455.
- 312 V. Baskar, K. Gopal, M. Helliwell, F. Tuna, W. Wernsdorfer and R. E. P. Winpenny, *Dalt. Trans.*, 2010, **39**, 4747–4750.
- 313 M. A. Palacios, E. Moreno Pineda, S. Sanz, R. Inglis, M. B. Pitak, S. J. Coles, M. Evangelisti, H. Nojiri, C. Heesing, E. K. Brechin, J. Schnack and R. E. P. Winpenny, *ChemPhysChem.*, 2016, **17**, 55–60.
- 314 J. Schnack, *Journal of Low Temperature Physics.*, 2006, **142**, 283–288.
- 315 J. Schnack and R. Schnalle, *Polyhedron.*, 2009, **28**, 1620–1623.
- 316 M. Mikuriya and S. Tashima, *Polyhedron.*, 1998, **17**, 207–209.
- 317 M. Mikuriya, *Bull. Japan Soc. Coord. Chem.*, 2008, **52**, 17–28.
- 318 Y. Nishida and S. Kida, *J. Chem. Soc. Dalt. Trans.*, 1986, 2633–2640.
- 319 M. Mikuriya and K. Minowa, *Inorg. Chem. Commun.*, 2000, **3**, 227–230.
- 320 C. S. McCowan, T. L. Groy and M. T. Caudle, *Inorg. Chem.*, 2002, **41**, 1120–1127.
- 321 C. S. McCowan and M. T. Caudle, *Dalt. Trans.*, 2005, 238–246.
- 322 D. Belli Dell'Amico, F. Calderazzo, L. Labella, F. Marchetti and G. Pampaloni, *Chem. Rev.*, **103**, 3857–3897.
- 323 U. P. Kreher, A. E. Rosamilia, C. L. Raston, J. L. Scott and C. R. Strauss, *Molecules*, 2004, **9**, 387–393.

- 324 O. Berkesi, I. Dreveni, J. A. Andor and P. L. Goggin, *Inorganica Chim. Acta*, 1991, **181**, 285–289.
- 325 W. Clegg, D. R. Harbron, C. D. Homan, P. A. Hunt, I. R. Little and B. P. Straughan, *Inorganica Chim. Acta*, 1991, **186**, 51–60.
- 326 A. Beiforte, F. Calderazzo, U. Englert and J. Strähle, *Inorg. Chem.*, 1991, **30**, 3778–3781.
- 327 D. B. Dell’Amico, F. Calderazzo, L. Labella and F. Marchetti, *Inorganica Chim. Acta*, 2003, **350**, 661–664.
- 328 R. Murugavel, M. Sathiyendiran and M. G. Walawalkar, *Inorg. Chem.*, 2001, **40**, 427–434.
- 329 S. C. Abrahams and J. L. Bernstein, *Acta Crystallogr. Sect. B Struct. Crystallogr. Cryst. Chem.*, 1969, **25**, 1233–1236.
- 330 M. Casarin, E. Tondello, F. Calderazzo, A. Vittadini, M. Bettinelli and A. Gulino, *J. Chem. Soc. Faraday Trans.*, 1993, **89**, 4363–4367.
- 331 P. F. Haywood, M. R. Hill, N. K. Roberts, D. C. Craig, J. J. Russell and R. N. Lamb, *Eur. J. Inorg. Chem.*, 2008, 2024–2032.
- 332 S. Polarz, C. L. Pueyo and M. Krumm, *Inorganica Chim. Acta*, **363**, 4148–4157.
- 333 M. Yamamura, H. Miyazaki, M. Iida, S. Akine and T. Nabeshima, *Inorg. Chem.*, 2011, **50**, 5315–5317.
- 334 R. M. Haak, A. Decortes, E. C. Escudero-Adán, M. M. Belmonte, E. Martin, J. Benet-Buchholz and A. W. Kleij, *Inorg. Chem.*, 2011, **50**, 7934–7936.
- 335 M. Martínez Belmonte, E. C. Escudero-Adán, E. Martin and A. W. Kleij, *Dalt. Trans.*, 2012, **41**, 5193–5200.
- 336 H. L. C. Feltham and S. Brooker, *Coord. Chem. Rev.*, 2009, **253**, 1458–1475.
- 337 L. You and E. V. Anslyn, *Supramol. Chem.*, John Wiley and Sons, Sussex UK, **1**, 135–160
- 338 D. L. Hildenbrand, *Chem. Phys. Lett.*, 1975, **34**, 352–354.
- 339 G. Pass and H. Sutcliffe, *Practical Inorganic Chemistry*, Chapman and Hall, 1974, 39–48.
- 340 D. L. Caulder and K. N. Raymond, *J. Chem. Soc. - Dalt. Trans.*, 1999, 1185–1200.
- 341 A. Scheurer, K. Gieb, M. S. Alam, F. W. Heinemann, R. W. Saalfrank, W. Kroener, K. Petukhov, M. Stocker and P. Müller, *Dalt. Trans.*, 2012, **41**, 3553–3561.
- 342 M. Nihei, H. Tahira, N. Takahashi, Y. Otake, Y. Yamamura, K. Saito and H. Oshio, *J. Am. Chem. Soc.*, 2010, **132**, 3553–3560.